IDŐJÁRÁS

QUARTERLY JOURNAL
OF THE HUNGARIAN METEOROLOGICAL SERVICE

CONTENTS

VOL. 120 * NO. 3 * JULY – SEPTEMBER 2016

IDŐJÁRÁS

Quarterly Journal of the Hungarian Meteorological Service

Editorial Office: Kitaibel P.u. 1, H-1024 Budapest, Hungary
P.O. Box 38, H-1525 Budapest, Hungary
E-mail: journal.idojaras@met.hu
Fax: (36-1) 346-4669

Indexed and abstracted in Science Citation Index Expanded™ and Journal Citation Reports/Science Edition
Covered in the abstract and citation database SCOPUS®

Subscription by mail:
IDŐJÁRÁS, P.O. Box 38, H-1525 Budapest, Hungary
E-mail: journal.idojaras@met.hu

IDŐJÁRÁS

Quarterly Journal of the Hungarian Meteorological Service
Vol. 120, No. 3, July – September, 2016, pp. 267–282

Overview of the tropospheric ozone problem: formation, measurements, trends, and impacts (Hungarian specialties)

Zita Ferenczi[1*] and **Kornélia Imre**[2]

[1]*Hungarian Meteorological Service,*
Gilice tér 39, H-1181 Budapest, Hungary

[2]*MTA-PE Air Chemistry Research Group,*
Egyetem út 10, H-8200, Veszprém, Hungary

[*]*Corresponding author E-mail: ferenczi.z@met.hu*

(Manuscript received in final form February 1, 2016)

Abstract—Ground-level or tropospheric ozone (O_3) is an oxidant air pollutant that has harmful effect on human health and vegetation, however, it is a short-lived greenhouse gas. Ozone is a secondary pollutant; which means that it is not directly emitted in the ambient air, but also produced from the photochemical oxidation of non-methane volatile organic compounds (NMVOCs), methane (CH_4), or carbon monoxide (CO) in the presence of nitrogen oxides (NO_x). It is destroyed both photochemically and through deposition to the surface. Summarizing the chemistry of ozone is complex and non-linear. Background concentrations of ground-level ozone in Europe do not show a significant downward trend, but in Hungary essential reduction (–0.28 μg/m^3) was observed at K-puszta station in the last decades. In the monthly distribution the amplitude decrease with increase in altitude, at K-puszta 45.1 μg/m^3, while at Nyírjes 36.6 μg/m^3 amplitudes were observed. Based on our data we found that the ozone gradient is about +1.4 μg/m^3/m. Breathing ozone can result in a number of negative health effects that are observed in relevant segments of the population. Ozone also is known as the air pollutant most damaging to agricultural crops and other plants. This article gives a general overview of the ozone problem focusing on the Hungarian specialties.

Key-words: air quality, ground level ozone measurements, AOT40, trends, vegetation

1. Introduction

In recent decades, ozone has been received increasing attention in the analysis of the regional and local air quality. In addition to being very important for sustaining life near the Earth's surface by absorbing hazardous UV radiation within the stratosphere, ozone is one of the most important greenhouse gases (*Paoletti* and *Cudlin,* 2012).

In the troposphere it is a strong oxidant air pollutant affecting human health and natural ecosystems, and reducing crop yields (*Wilkinson et al.,* 2012). Its concentration has doubled between the end of the 19th century and the 1980's. The annual average in the Northern Hemisphere has risen to 60–90 $\mu g/m^3$, and recently it increased with a further 10 $\mu g/m^3$ (*Wilson et al.,* 2012). In spite of the international agreements aimed to decrease the precursor gas emission, its concentration has been increasing (*Derwent et al.,* 2003, *Dentener et al.,* 2005). The reasons of the increase of ground level ozone concentration have not yet been understood well scientifically, but likely the sectors such as international shipping and air transport could be responsible for it, because the emissions of precursor gases from these activities are not regulated strictly enough (*Dentener et al.,* 2005). Since the sources of ozone are not confined to a smaller area but can be found worldwide, the problems related to ozone pollution has to be managed globally. Ground-level ozone episodes, when O_3 concentrations may reach at 400 $\mu g/m^3$ or more, occur in polluted regions under hot and sunny conditions. This has been ascribed to photochemical processes due to the occurrence on a large scale of favorable meteorological circumstances (*Guicherit* and *Van Dop,* 1977). The long-range transport of tropospheric ozone and its precursors have important impact on O_3 concentrations at regional and local scales. In the low to midlatitudes, O_3 transport from the polluted source regions like North/South America, Europe, and Asia generally accounts for more than 50% of ozone even in remote locations (*Sudo* and *Akimoto,* 2007).

The Council Directive on air pollution by ozone (92/72/EEC) defines several threshold levels, and it establishes a harmonized procedure for monitoring and exchanging data. It also arranges to provide the public with information when warning and information threshold levels are exceeded.

- Health protection threshold: days with an 8-hour average ozone concentration of more than 120 $\mu g/m^3$.
- Population information threshold: the hourly average ozone concentrations exceed 180 $\mu g/m^3$.
- Population warning threshold: the hourly average ozone concentrations exceed 360 $\mu g/m^3$.

Air pollution is a process that introduces diverse pollutants into the atmosphere that cause harm to humans, other living organisms, and the natural

environment (*Brauer et al.,* 2012; *Kim et al.,* 2013). The effects of O_3 found that exposure to ambient O_3 levels is linked to such respiratory ailments as asthma, inflammation, and premature aging of the lung, and to such chronic respiratory illnesses as emphysema and chronic bronchitis (*Delfino et al.,* 1998). More than two million deaths are estimated to occur globally each year as a direct consequence of air pollution through damage to the lungs and the respiratory system (*Shah et al.,* 2013). Among these deaths, around 2.1 and 0.47 million are caused by fine particulate matter (PM) and ozone, respectively (*Chuang et al.,* 2011; *Shah et al.,* 2013).

Besides positive CO_2 and nitrogen fertilization, many studies have show that ozone and its precursors are efficiently transported in the regional scale and consequently ozone tends to present relatively high background levels in rural areas. Over 90% of vegetation damage may be result of tropospheric ozone alone (*Adams et al.*, 1986). Previously, it was thought that tropospheric ozone is an urban problem, elevated O_3 concentrations are now recognized as extending far beyond city limits. Elevated concentrations in rural regions significantly affect crop yields, forest productivity, and natural ecosystems. Evaluations of the national economic impact of ozone on crop yield have indicated values of the order of US$ 2-4 billion in the United States and of 4 billion EUR in Europe (*Murphy et al.,* 1999, *Holland et al.*, 2002).

Ozone in the ground level is also expected to contribute to the devastation of building and material. In developed countries, where the control of emissions of air pollutants are relatively efficient, and the emission projections for the precursor gases indicate continuous decrease (*Kelly et al.,* 2010), the O_3 concentration will likely decline in the next decades. Although the climate change will complicate the picture the rate of decline will be slowed down. Due to the climate change heat waves may occur more often and could cause extremely high ozone concentrations for a short time. This fact could also demonstrate that while O_3 as a greenhouse gas affects the climate, the climate change will result weather conditions which may lead to the elevation of O_3 concentration in the ground level. It also shows that the climate change is one of the most complex problems, and this also proves the importance the international cooperation to solve the issue of air quality. Currently, in Europe the revised Gothenburg protocol specifies emission reduction commitments for precursors. In case of Hungary the emission reduction of volatile organic compounds (VOCs) was committed by 30 percent as NO_x by 42 percent, both of them are precursor gases of ozone.

1.1. Ozone formation and air quality

Ozone is found in two different areas of the atmosphere – the stratosphere and the troposphere. In the stratosphere, ozone provides a protective shield by filtering out the dangerous ultraviolet radiation from the sun. Here the ozone molecules

are formed by the photo-dissociation of molecular oxygen, and the atomic oxygen reacts with molecular oxygen to produce ozone.

Tropospheric ozone is not emitted directly in to the atmosphere, so it is described as a secondary air pollutant. It is an important atmospheric oxidant, smog component, and a short-lived greenhouse gas. In the troposphere, it is formed by photochemical reactions of nitrogen oxides with volatile organic compounds, methane, and/or carbon monoxide in the presence of sunlight. NO_x is primarily a product of fossil fuel combustion (63%), but secondarily it is a result of biomass burning (14%) (*IPCC,* 2001). Natural vegetation is a source of VOCs, which decompose into peroxy radicals, which react with NO to produce NO_2. In urban regions with high concentrations of NO_x, ozone production is generally VOC-limited, whereas in suburban or rural regions with low NO_x levels, ozone production is NO_x-limited. The different spatial distributions of NO_x and VOC production, as well as NO destruction of ozone, often result in the largest ozone concentrations downwind of urban centers, rather than in urban areas themselves (*Gregg et al.,* 2003). Transport of the chemical mixtures eventually results photodissociation and O_3 transformation at sites quite distant from original source of the precursor emissions. Increasing rate emissions of its precursors have caused ozone concentrations to experience a strong increase in highly populated continental regions during the last century (*Marenco et al.*, 1994). Tropospheric ozone concentrations can also be influenced by UV radiation. A rise in UV radiation intensity is expected to decrease tropospheric ozone in a clean environment, while increased UV in regions with precursors (NO_x, CO, CH_4) rich atmospheres will lead to increased tropospheric ozone concentrations. Mainly in summer months, when conditions of O_3 formation improve (high temperature, radiation, wind stagnation), O_3 levels typically rise even in remote background areas. Ozone is, therefore, no longer just an issue for air quality, but a complex environmental problem.

1.2. Ozone measurements and trends in Europe and Hungary

The analysis of European rural background ozone trends between 1996–2005 had carried out by *Wilson et al.* (2012). They processed data available from the EMEP and GAW monitoring stations and concluded that, on the European scale only slight increase in ozone levels (0.32–0.04 $\mu g/m^3$ per year) with a total range of 2.56 to 2.1 $\mu g/m^3$ per year can be determined. The greatest reduction is observed at K-puszta, Hungary (–4.11% per year). The first trend analysis using the tropospheric ozone measurements from K-puszta was published by *Haszpra et al.* (2003). In this paper, 0.64 $\mu g/m^3$ per year increasing ozone trend was determined for the time period of 1990–2002.

In Hungary, the Hungarian Meteorological Service is responsible for the rural ground-level ozone measurements. The institute maintains three background monitoring stations, where tropospheric ozone measurements are carried out

beside the observation of other pollutants. Since the stations are located in different geographical environments from plains to mountains, this effect is reflected in the measured data. *Fig. 1* shows the positions of the monitoring stations in Hungary.

Farkasfa background air pollution monitoring station is located in the western part of Hungary (46°54'37" N, 16°18'34" E, 312 m asl), at the area of the Őrség National Park. The station is surrounded by forest and no essential local source can be found nearby. The tropospheric ozone measurements started at this station in 1996. For many reasons, the ozone measurements were interrupted between 2005–2006, but in May of 2006, the operation of the station restarted.

K-puszta is the regional background air pollution monitoring station located in the central part of Hungary, on the Hungarian Great Plain (46°58' N, 19°33' E, 125 m asl). The station is located in a big forest clearing. In the wider region, agricultural fields, forest patches, pastures, and open bushy regions can be found. The prevailing wind blows from the west-to-north sector. The nearest town (Kecskemét, approximately 112 thousand inhabitants) is about 15 km to the southwest. The tropospheric ozone measurements started at this station in 1990. K-puszta monitoring station belongs to the European air quality monitoring (e.g., EMEP) and the Global Atmosphere Watch (GAW) networks. The station was also involved in the Tropospheric Ozone Research, a Sub-Project of EUROTRAC project (*Haszpra et al.,* 1997).

Nyírjes background air pollution monitoring station is located in the Mátra Mountains, in the northeast part of Hungary (47°52' N, 19°57' E, 702 m asl). The tropospheric ozone measurements started at this station in 1996.

Fig. 1. Location of the ground-level background ozone monitoring stations in Hungary

2. Results

2.1. Annual trend in background stations

This part concerns the background stations for the annual trend analysis over the 1996–2014 period. Atmospheric lifetimes of ozone precursors are long enough to allow them to be transported on long distance, but the range of the impact depends on meteorological and geographical conditions. Although the stations are located in background areas, the local topography and surroundings are different. These circumstances undoubtedly may influence the ozone concentration. *Fig. 2* shows the calculated ozone trends for the Hungarian monitoring stations. We assumed that the trends are linear calculated by deseasonalizing the ozone time series. Mann-Kendall analysis of Sen-Theil slopes was used for the calculations.

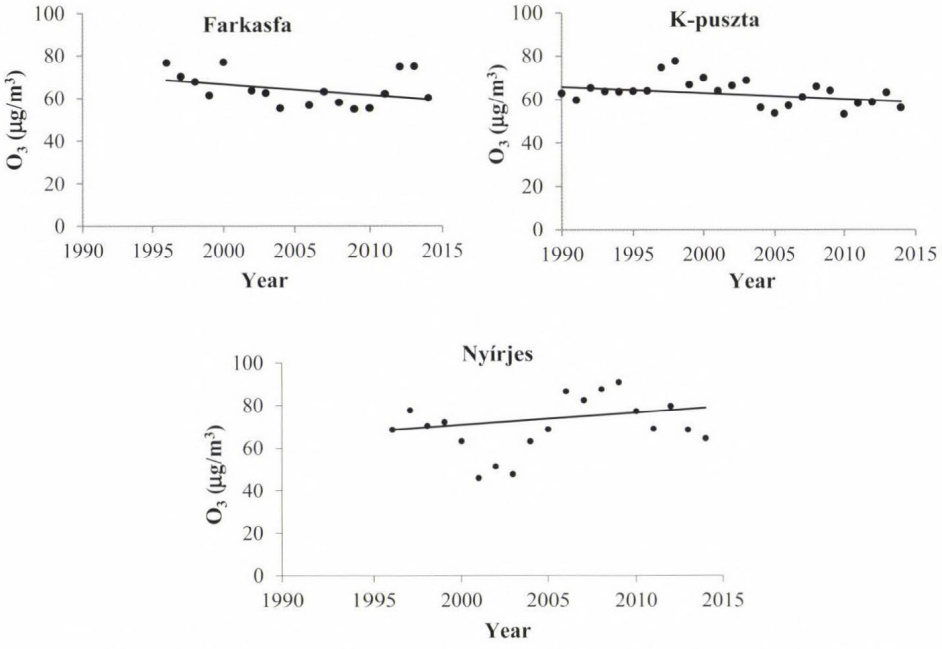

Fig. 2. Ozone trends detected at the Hungarian background air quality monitoring stations (dots = annual mean).

In case of Farkasfa and K-puszta stations, decreasing trends can be observed, while in case of Nyírjes station, the trend is increasing in average but there are intervals when the ozone concentration decreased for a few years (between 1997–2002 and 2009–2014). The trend determined for K-puszta using our 25 years data is –0.276 µg/m^3 per year, but the trend determined by *Wilson et al.* (2012) using

only 10 years (between 1996–2005) shows more intensive decreasing (–1.826 $\mu g/m^3$ per year). Similar results were found by *Sicard et al.,* (2013) over the period 2000–2010, when annual mean concentrations decreased by 0.43% per year at rural sites. Explanation of the maximum values and evolution could be in the local and annual meteorological conditions. At K-puszta, the concentration values usually higher than at Farkasfa that can be explained on one hand by the different meteorological conditions (higher temperature) and higher altitude on the other hand by the ozone plumes coming from Budapest city (*Mészáros et al.,* 2009). The decreasing trends at Farkasfa and K-puszta can be attributed to the reduction in NO_x and VOC emission within Europe. Background concentrations of ozone in Europe are influenced significantly by emissions of precursor gases outside the continent (*Guerreiro et al.,* 2014). Changes of the annual mean of ozone concentrations could have been caused by the precursor gas emission, the effect of the long-range transport of ozone and pre-gases, and the meteorological situation (heat waves, rainfall). *Fig. 3* shows the abatement in NO_x and VOC levels in Hungary that could have caused the reductions in episodic peak ozone levels.

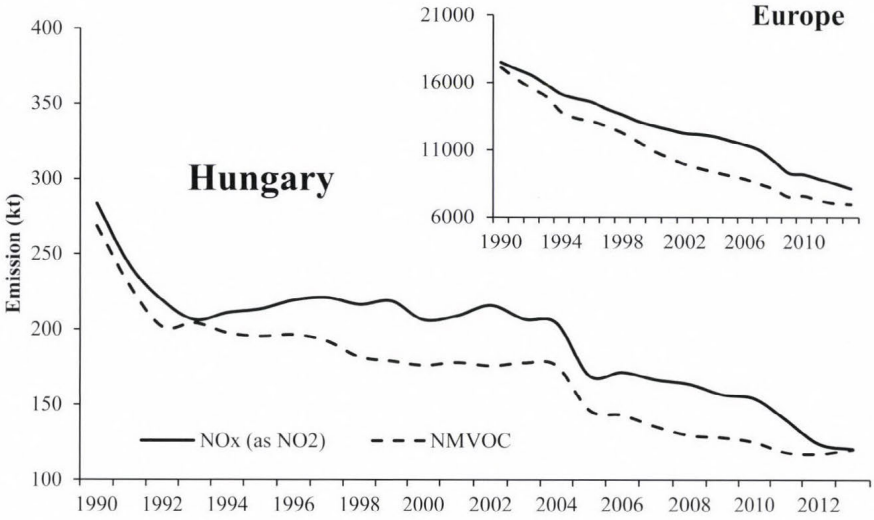

Fig. 3. Anthropogenic NO_x (as NO_2) and NMVOC emissions 1990-2013 for Hungary and Europe (Source: www.ceip.at).

According to *Sicard et al.* (2009), between 1995 and 2003, a rate of –0.48% per year for stations below 1000 m asl and +1.75% per year for stations above 1000 m asl were observed. They mentioned that the possible explanations could be the following:

1.) If ozone is produced in lower field from exhaust and industrial sources, it goes up with the favour of the temperature inversion phenomenon. At high altitude, ozone stagnates to form a reservoir layer.

2.) Altitude sites are not influenced by the ozone destruction by nitrogen oxides. Indeed, the NO concentration, emitted mainly by the road transport, are weak in the higher altitude. In addition, there are biogenic VOC emissions, emitted by the vegetation, which can increase the ozone production.

3.) Approximately 10% of tropospheric ozone is estimated to be of stratospheric origin.

It is also known that background ozone level increases with the height in the lower troposphere. Based on our data (average ozone concentration from 1996 to 2014), a change in the ozone vertical gradient is clearly visible (see *Fig. 4*). The ozone gradient is about +1.4 $\mu g/m^3/m$. This spatial distribution shows an interesting pattern, because the most urban-influenced site (K-puszta) has the lowest concentration, while either the distance or the elevation is not more efficient contribution to reach this high ozone concentration. However, this problem is quite complex, further investigation is needed to explain these findings.

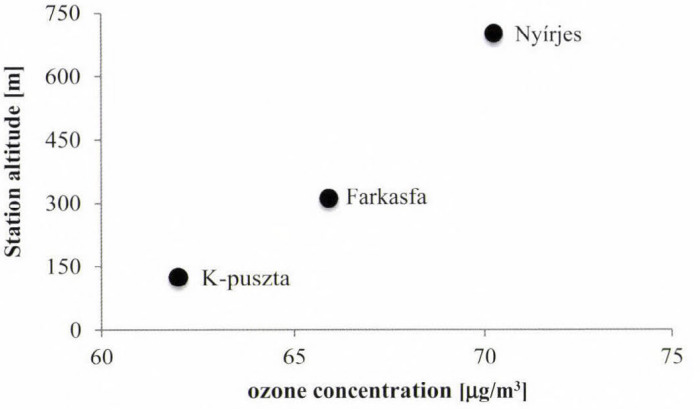

Fig. 4. The total average ozone concentration depending on the station altitude.

2.2. Seasonal trend analysis

The monthly means of ozone concentration were also determined for the three stations. *Fig. 5* presents the results of this investigation. The three diagrams reflect

that the ozone has different yearly variation on the sites. The biggest amplitude can be observed at K-puszta (45.1 μg/m^3), while the lowest at Nyírjes (36.6 μg/m^3). This result is reflects the fact that Nyírjes is a mountain station where the amplitude of the monthly and daily ozone concentrations are much lower than at the plain stations (*Chevalier et al.*, 2007).

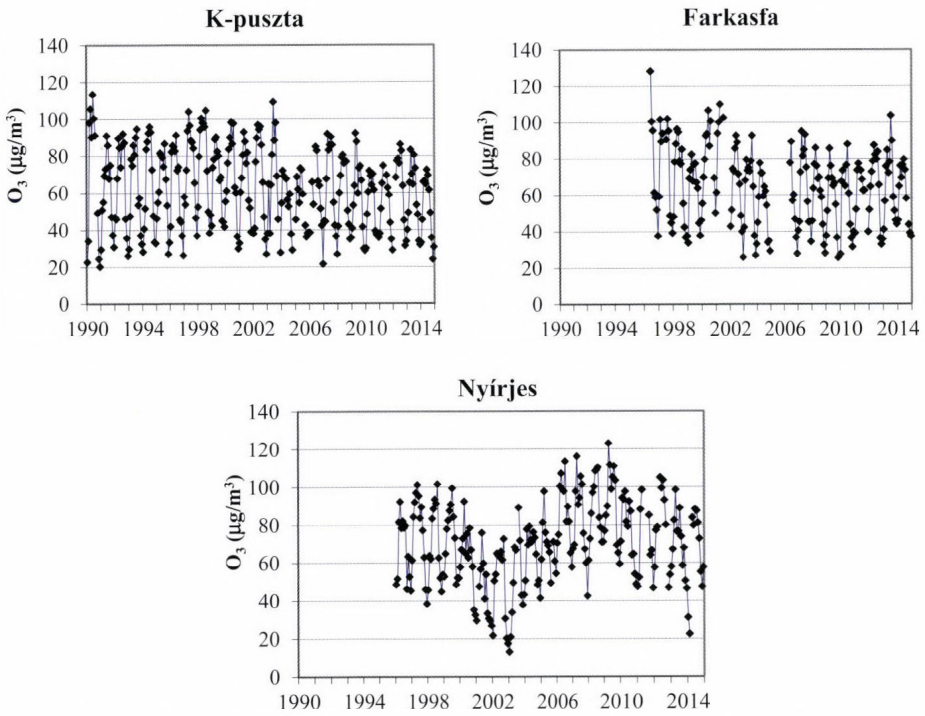

Fig. 5. Temporal variation of observed monthly mean ozone concentrations detected at the Hungarian background air quality monitoring stations (dots = monthly mean).

The trends for the 5th, 50th, and 95th percentiles of ozone concentrations show a decrease for Farkasfa and K-puszta while an increase for Nyírjes (*Fig. 6*). In case of Farkasfa and K-puszta, the 95th percentile decreasing trend is much larger and the 5th percentile decreasing trend is much lower than the median trend. It means that the decreasing trends of the yearly mean values are basically caused by the decreasing maximum concentration values, while the minimum values show a moderate rising.

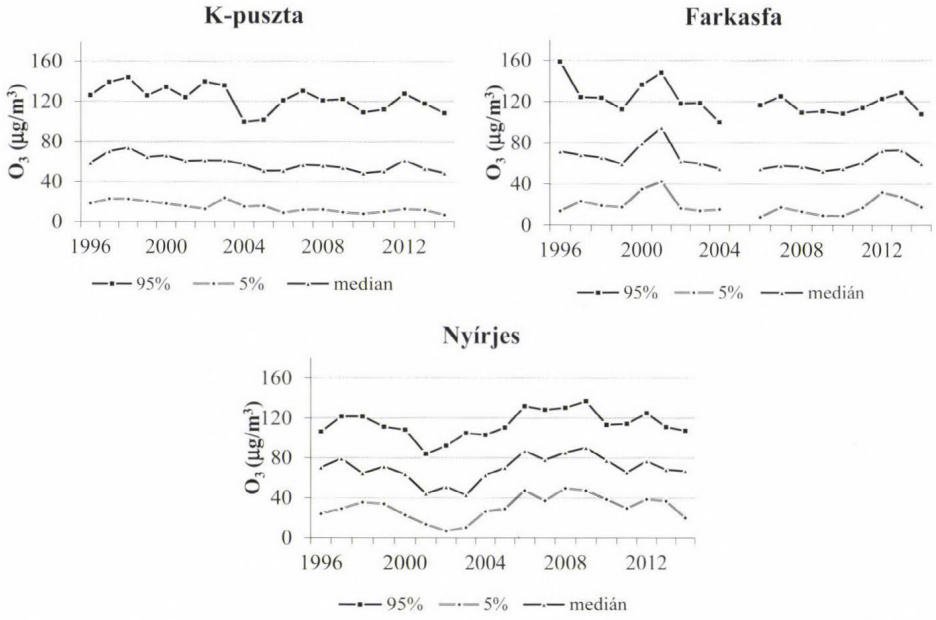

Fig. 6. Temporal variation of the annual 95th, 50th, and 5th percentiles of ozone concentrations detected at the Hungarian background air quality monitoring stations.

In case of Nyírjes, in all three percentiles (95th, 50th, 5th) a rising trend was found (see *Table 1*). The mean ozone concentration is known to strongly increase with altitude in the troposphere mainly in the first 1000 m. The comparison of the results of the three Hungarian stations also shows that the minimum ozone concentration is rising with the altitude. This can be explicable with that the ozone content is eroded near the surface by deposition and titration that dominate in the boundary layer at the yearly time-scale.

Table 1. Mean trends by stations for the 5th, 50th, and 95th percentiles of ozone concentrations

	Trend (µg/m^3/yr)		
Station	**5th percentile**	**median**	**95th percentile**
K-puszta	–0.75	–0.97	–1.24
Farkasfa	–0.20	–0.58	–1.23
Nyírjes	+0.76	0.67	+0.67

Sicard et al. (2013) found that background ozone concentration decreased of –1.1% per year with annual averages and –0.9% per year with median values. They observed that the number of concentration values above 65 $\mu g/m^3$ increased significantly (1% per year), and the 25th percentiles decreased of –0.4% per year over the 2000–2008 period. Based on these and our results the background ozone level seems to increase. However the maximum ozone concentration shows decreasing trend, there are several days when the values reach a threshold. The exceedance days of air quality threshold values for ozone at the Hungarian background air quality monitoring stations decreased in the last 25 years in connection with the emission reduction of precursor gases. The number of days when the O_3 concentration exceeds the previously defined threshold values for ozone was also determined using the Hungarian monitoring data (*Fig. 7*). At our stations, the ground-level ozone has never exceeded the population warning threshold in the examined period, but the ozone concentrations were quite often above the other threshold values. The ozone concentration exceeded the health protection threshold more than 100 times per year only at K-puszta in the time period of 1997–2002. Since K-puszta is a background station, it might be better termed "urban-affected", because of advected urban plumes from Budapest that affect concentration characteristics. Because Nyírjes and Farkasfa are beyond the reach of urban plumes or other anthropogenic effects, they can show small seasonal variations in ozone concentration.

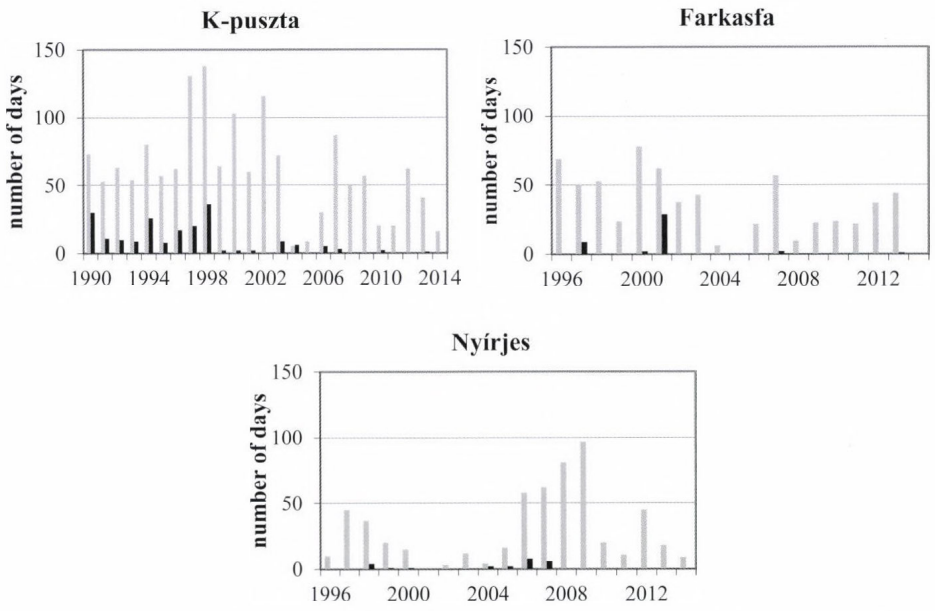

Fig. 7. Exceedance days of air quality threshold values for ozone at the Hungarian background air quality monitoring stations (gray = health protection threshold, black = population information threshold).

The frequency distribution of the hourly ozone concentrations was also calculated. For the comparability of the results, we used only the data from the time period 1996–2014 at all three stations. From many European country's data it can be concluded, that the proportion of ozone concentration range of 40–78 μg/m^3 has increased, while the proportion in the category, 80–118 μg/m^3 has not changed in the summer months. The main differences in terms of frequency distribution can be found in the winter season between the mountain and plain stations. *Fig. 8* shows the results of this examination. The data availability for the stations and for the time period of 1996–2014 was: Farkasfa 80%, K-puszta 90%, Nyírjes 86% (in case of K-puszta, the data availability was 87% for the time period of 1990–2014). The highest ground level ozone concentrations can be expected at Farkasfa in June and July, at K-puszta in June, July, and August, while at Nyírjes only in July.

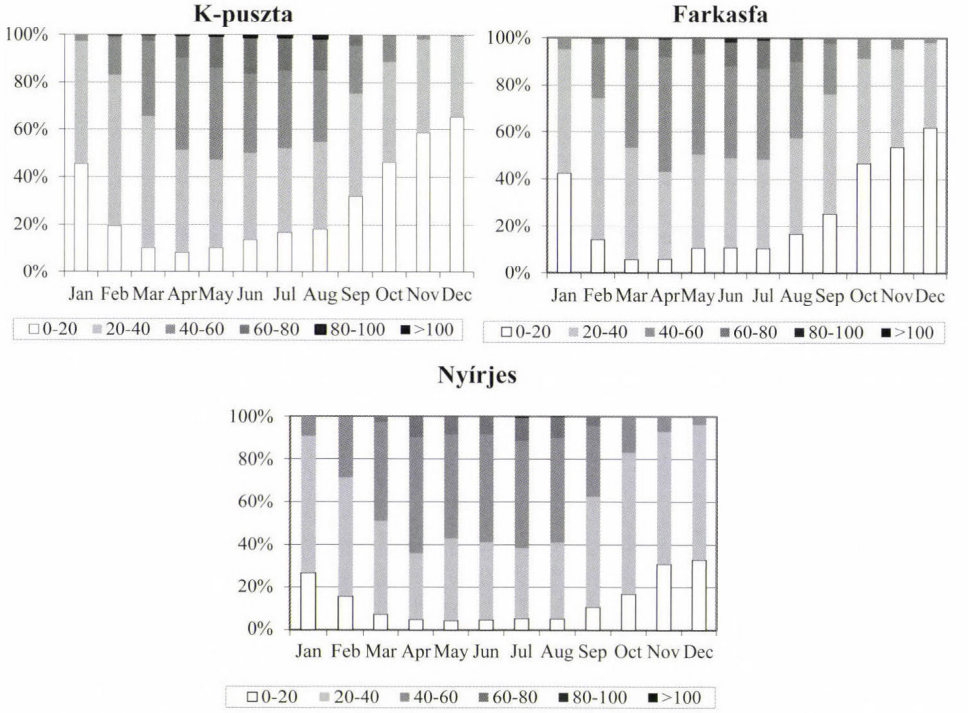

Fig. 8. Frequency distribution of ozone concentrations (hourly values) at the Hungarian background air quality monitoring stations.

2.3. AOT trends

Among the European standards, AOT40 index is generally used for the protection of the vegetation. AOT40 is defined as the sum of differences between the hourly

mean concentration and the 80 μg/m^3 threshold value for each hour when the concentration exceeds 80 μg/m^3. Then these values are summarized each day from May 1 to July 31, for the time period of 8–20 hours. In this study we found significant differences among the stations (see *Fig. 9*).

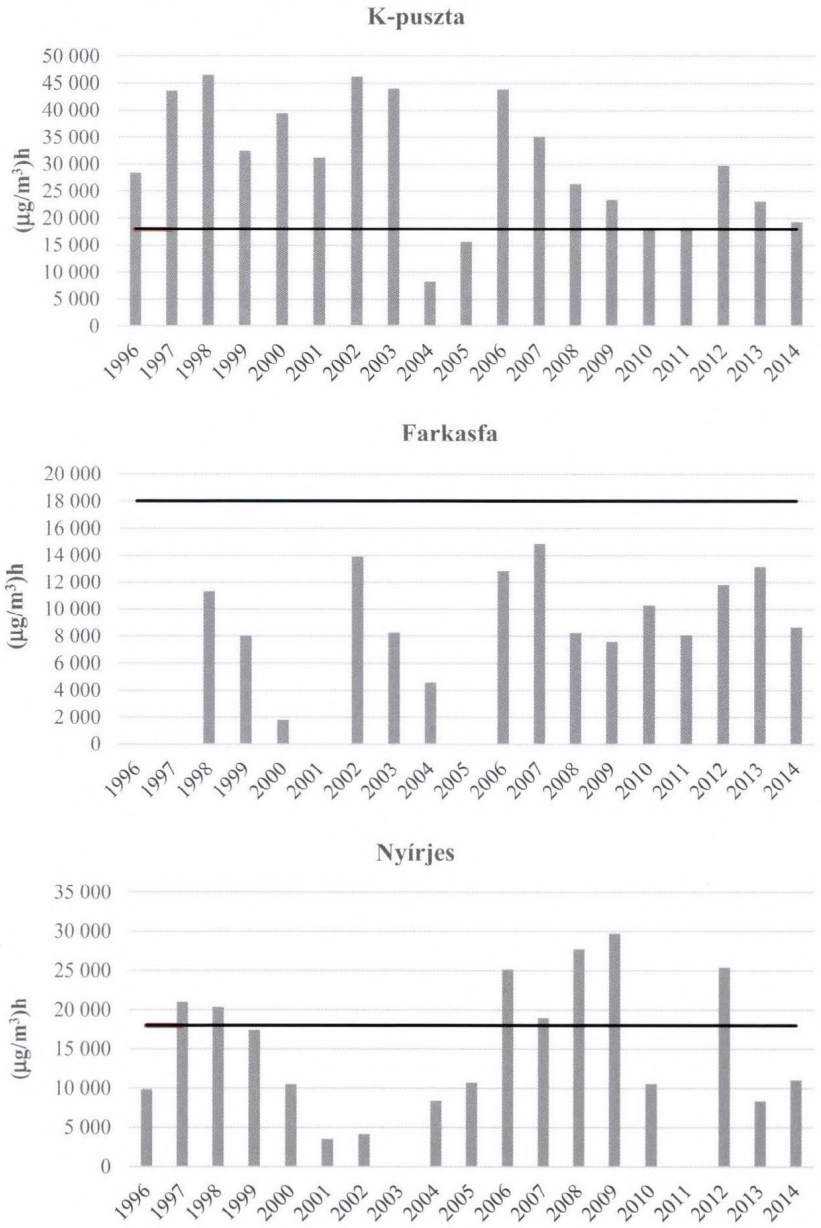

Fig. 9. AOT40 values (μg/m^3)h at the Hungarian background air quality monitoring stations (horizontal black line = threshold value).

Despite the Hungarian declining ozone concentration trends (see *Fig. 2*), AOT40 did not show any trend. In case of K-puszta, the AOT40 exceed the limit value in most cases, while at Farkasfa the calculated AOT40 has never been exceeded the limit value, and at Nyírjes the AOT40 exceeded the limit value only in some cases. Nyírjes and Farkasfa stations are located in areas devoid of local pollution sources, which can be a possible reason for the AOT40 values. In contrast, K-puszta is located in the direction of Budapest's plume, and due to its geographic position, the annual average temperature is higher than in the other stations, which favors for the higher ozone concentration, consequently for higher value of AOT40.

Between 21% and 69% of agricultural crops in the EEA-32 (European Economic Area) were exposed to O_3 levels above the EU target value for protecting vegetation (18 000 ($\mu g/m^3$)h for AOT40) from 2002 to 2010, mostly in southern and central Europe (*EEA*, 2013). Reduction of yield with increasing ozone over a 80 $\mu g/m^3$ threshold, resulting in a 10% reduction in yield for ozone levels commonly found in southern Europe (*Fuhrer et al,* 1997). In Hungary, mainly the beans have shown ozone-injury symptoms.

3. Conclusion

In this paper, recent results on ozone levels and trends at background sites located in Hungary are discussed. Studies have shown that concentrations of ozone in the Hungarian background stations are influenced by emissions of precursor gases outside the continent. The Mann-Kendall test was used to detect the trend from background ozone concentrations. In case of Farkasfa and K-puszta stations, decreased trends (–0.498 $\mu g/m^3$ and –0.277 $\mu g/m^3$) can be observed, while in case of Nyírjes station, the trend is increasing (0.567 $\mu g/m^3$) in average, but there are intervals when the ozone concentration decreased for a few years. In the monthly distribution, the ozone concentrations show different variation. The amplitude decreased due to the increase in altitude, at K-puszta 45.1 $\mu g/m^3$, while at Nyírjes 36.6 $\mu g/m^3$ amplitudes were observed. Since K-puszta is a background station, it might be better termed "urban-affected", because of advected urban plumes from Budapest that affect concentration characteristics. Nyírjes and Farkasfa are beyond the reach of urban plumes or other anthropogenic effect, they can show small seasonal variations in ozone concentration. Based on our data, we found that the ozone gradient is about +1.4 $\mu g/m^3/m$. We observed that in case of Farkasfa and K-puszta, the 95th percentile decreasing trend is much larger and the 5th percentile decreasing trend is much lower than the median trend. It means that the decreasing trends of the yearly mean values are basically caused by the decreasing maximum concentration values. According to AOT40, we found big differences between the stations, however, the data did not show any trend. As Nyírjes and Farkasfa are located in areas devoid of local pollution sources, the

values of AOT40 were low, in contrast to K-puszta, where the AOT40 were higher in every year, consequently.

Acknowledgements: Present article was published in the frame of the project TÁMOP-4.2.2.A-11/1/KONV-2012-0064: „Regional effects of weather extremes resulting from climate change and potential mitigation measures in the coming decades". The project is realized with the support of the European Union, with the co-funding of the European Social Fund.

References

Adams, R.M., Hamilton, S.A., and *McCarl, B.A.,* 1986: The benefits of pollution control: the case of ozone and U.S. Agriculture. *Am. J. Agric. Econ. 68*, 886–893.

Brauer, M., Amann, M., Burnett, R.T., Cohen, A., Dentener, F., Ezzati, M., Henderson, S.B., Krzyzannowski, M., Martin, R.V., Dingenen, R. Donkelaar, A., and *Thurston, G.D.,* 2012: Exposure assessment for estimation of the global burden of disease attributable to outdoor air pollution. *Environ. Sci. Technol. 46*, 652–660.

Chevalier, A., Gheusi, F., Delmas, R., Ordóñez, C., Sarrat, C., Zbinden, R., Thouret, V., Athier, G., and *Cousin, J.-M.,* 2007*:* Influence of altitude on ozone levels and variability in the lower troposphere: a ground-based study for western Europe over the period 2001–2004. *Atmos. Chem. Phys. Discuss 7,* 1327–1356.

Chuang, K.-J., Yan, Y.-H., Chiu, S.-Y., and *Cheng T.J.*, 2011: Long-term air pollution exposure and risk factors for cardiovascular diseases among the elderly in Taiwan. *Occup. Environ. Med., 68*, 64–68.

Dentener, F., Stevenson, D., Cofala, J., Mechler, R., Amann, M., Bergamaschi, P., Raes, F., and *Derwent, R.*, 2005: The impact of air pollutant and methane emission controls on tropospheric ozone and radiative forcing: CTM calculations for the period 1990–2030. *Atmos. Chem. Phys., 5*, 1731–1755.

Delfino, R.J., Murphy-Moulton, A.M., and *Becklake, M.R.,* 1998: Emergency room visits for respiratory illnesses among the elderly in Montreal: association with low level ozone exposure. *Environ. Res. 76*, 67–77.

Derwent, R.G., Jenkin, M.E., Saunders, S.M., Pilling, M.J., Simmonds, P.G., Passant, N.R., Dollardf, G.J., Dumitreanf.P., and *Kent, A.*, 2003: Photochemical ozone formation in north west Europe and its control. *Atmos. Environ 37*, 1983–1991.

EEA, 2013: Exposure of Ecosystems to Acidification, Eutrophication and Ozone (Indicator CSI 005) 2013: http://www.eea.europa.eu/data-and-maps/indicators/exposure-of-ecosystems-to-acidification-2/exposure-of-ecosystems-to-acidification-5.

Fuhrer, J., Skarby, L., and *Ashmore, M.R.,* 1997: Critical levels for ozone effects on vegetation in Europe. *Environ. Pollut. 97*, 91–106.

Gregg, J.W, Jones, C.G., and *Dawson, T.E.,* 2003: Urbanization effects on tree growth in the vicinity of NewYork City, *Nature 424*, 183–187.

Guerreiro, C.B.B., Foltescu, V., and *de Leeuw, F.,* 2014: Air quality status and trends in Europe. *Atmos. Environ. 98,* 376–384.

Guicherit, R. and *Van Dop, H.,* 1977: Photochemical production of ozone in Western Europe (1971–1975) and its relation to meteorology. *Atmos. Environ. 11*, 145–155.

Haszpra, L., Bozó, L., Ferenczi, Z., and *Sándor, V.,* 1997: Formation and transport of tropospheric ozone in Hungary. *Troposph. Ozone Res. 6*, 317–321.

Haszpra, L., Ferenczi, Z., Lagzi, I., and *Turányi, T.,* 2003: Formation of tropospheric ozone in Hungary. Tropospheric Ozone Research, Final Report of Subproject TOR-2, EUROTRAC-2, ISS, Munich, 87–89.

Holland, M., Mills, G., Hayes, F., Buse, A., Emberson, L., Cambridge, H., Cinderby, S., Terry, A., and *Ashmore, M.,* 2002: Economic Assessment of Crop Yield Losses from Ozone Exposure. Report

to U.K. Department of Environment Food and Rural Affairs under Contract 1/3/170. Centre for Ecology and Hydrology, Bangor. Available at: http://www.airquality.co.uk/archive/reports/.

IPCC (Ed.), Climate Change 2001: The Scientific Basis, Cambridge University Press, New York.

Kelly, A., Lumbreras, J., Maas, R., Pignatelli, T., Ferreira, F., and *Engleryd, A.* 2010: Setting national emission ceilings for air pollutants: policy lessons from an ex-post evaluation of the Gothenburg Protocol. *Environ. Sci. Policy 13*, 28–41.

Kim, K.-H., Jahan, S.A. and *Kabir, E.*, 2013: A review on human health perspective of air pollution with respect to allergies and asthma. *Environ. Int. 59*, 41–52.

Marenco, A., Gouget, H., Nédélec, P., and *Pages, J.-P.:* 1994: Evidences of a long term increase in tropospheric ozone in Pic du Midi data series: consequences in the positive radiative forcing. *J. Geophys. Res. 99*, 16617–16632.

Mészáros, R., Szinyei, D., Vincze, C., Lagzi, I., Turanyi, T., Haszpra, L., and *Tomlin, A.S.*, 2009: Effect of the soil wetness state on the stomatal ozone fluxes over Hungary. *Int. J. Environ. Pollut. 36*, 180–194.

Murphy, J.J., Delucchi, M.A., McCubbin, D.R., and *Kim, H.J.*, 1999: The cost of crop damage caused by ozone air pollution from motor vehicles. *J. Environ. Manage. 55*, 273–289.

Paoletti, E. and *Cudlin, P.*, 2012: Ozone, climate change and forests. *Environ. Pollut. 169*, 249.

Sicard, P., Coddeville, P., and *Galloo, J.C.*, 2009: Near-surface ozone levels and trends at rural stations in France over the 1995–2003 period. *Environ. Monit. Assess. 156*, 141–157.

Sicard, P., De Marco, A., Troussier, F., Renou, C., Vas, N., Paoletti, E., 2013: Decrease in surface ozone concentrations at Mediterranean remote sites and increase in the cities. *Atmos. Environ. 79*, 705–715.

Shah, A.S.V., Langrish, J.P., Nair, H., McAllister, D.A., Hunter, A.L., Donaldson, K., Newby, D.E., and *Mills, N.L.*, 2013: Global association of air pollution and heart failure: a systematic review and meta-analysis. *The Lancet 382*, 1039–1048.

Sudo, K. and *Akimoto, H.*, 2007: Global source attribution of tropospheric ozone: Long-range transport from various source regions. *J. Geophys. Res. 112*, D12302.

Wilkinson, S., Mills, G., Illidge, R., and *Davies, W.J.*, 2012: How is ozone pollution reducing our food supply? *J. Experiment. Botany 63*, 527–536.

Wilson, R.C., Fleming, Z.L., Monks, P.S., Clain, G., Henne, S., Konovalov, I.B., Szopa, S., and *Menut, L.*, 2012: Have primary emission reduction measures reduced ozone across Europe? An analysis of European rural background ozone trends 1996–2005, *Atmos. Chem. Phys. 12*, 437–454.

IDŐJÁRÁS

Quarterly Journal of the Hungarian Meteorological Service
Vol. 120, No. 3, July – September, 2016, pp. 283–300

Intra-urban temperature observations in two Central European cities: a summer study

Enikő Lelovics[1], **János Unger**[*1], **Stevan Savić**[2], **Tamás Gál**[1], **Dragan Milošević**[2], **Ágnes Gulyás**[1], **Vladimir Marković**[3], **Daniela Arsenović**[3], and **Csilla V. Gál**[4]

[1] *Department of Climatology and Landscape Ecology, University of Szeged P.O. Box 653, 6701 Szeged, Hungary*

[2] *Climatology and Hydrology Research Centre, Faculty of Science, University of Novi Sad; Trg Dositeja Obradovića 3, 21000 Novi Sad, Serbia*

[3] *Center for Spatial Information of Vojvodina, Faculty of Science, University of Novi Sad, Trg Dositeja Obradovića 3, 21000 Novi Sad, Serbia*

[4] *College of Architecture, Illinois Institute of Technology, Chicago, Illinois 60616-3793, USA*

[*] *Corresponding author E-mail:* unger@geo.u-szeged.hu

(Manuscript received in final form October 8, 2015)

Abstract—This paper presents an urban climatological application of the urban monitoring systems – recently implemented in Szeged, Hungary and Novi Sad, Serbia – using the first set of data collected during the summer of 2014. In order to ensure a representative number and placement of stations, the selection of measurement sites was based on Local Climate Zone (LCZ) maps developed for both cities. Present paper concentrates only on the intra-urban temperature pattern characteristics expressed by the thermal reactions of the different LCZ classes in both cities. The daily temperature indices (e.g., summer days) have the highest values in the densely built up LCZs. The diurnal cycle of surplus temperatures by LCZ classes under anticyclonic weather conditions were found to be similar in the two cities with higher absolute values in the case of Novi Sad. During summer, the diurnal variation of conventional heat island intensity confirms the general knowledge that it remains positive with highest values at night, while negative values occur predominantly during the day.

Key-words: urban climate, Local Climate Zones, monitoring networks, intra-urban and inter-urban temperature comparison, summer, Szeged, Novi Sad

1. Introduction

It is well established that urbanization alters the radiative, thermal, moisture, and aerodynamic properties of the environment, which therefore modifies the water and energy balance of the overlaying atmosphere (*Chandler*, 1965; *Oke*, 1982). The importance of urban climate is highlighted by its effects on urban energy and water management (e.g., *Santamouris et al.*, 2001; *Kolokotroni et al.*, 2006; *Balling* and *Gober*, 2006) as well as on human health (e.g., *Tan et al.*, 2010; *Gabriel* and *Endlicher*, 2011). The urban heat island (UHI) effect – the temperature surplus of built-up areas – is one of the most studied characteristics of the city's modified thermal environment (*Oke*, 1987).

In Central Europe, climate change is expected to increase the frequency, duration, and intensity of heat waves (*IPCC*, 2012; *Pongrácz et al.*, 2013), along with thermal stresses experienced by people (*Tomlinson et al.*, 2011). With reduced nocturnal cooling, the climate of cities is expected to make these already adverse projections worse, as elevated heat loads are linked to higher morbidity and mortality rates (*Petralli et al.*, 2012). Thus, monitoring the spatial and temporal patterns of the elevated urban temperature is an important task that can help both in the mitigation of and in the adaptation to the altered circumstances of the future. Besides monitoring, modeling also plays an important role in this regard. However, modeling requires data obtained from measurements for input and validation.

Air temperature in the city varies according to the properties of the urban environment and the characteristics of the regional climate as modified by hills, water bodies, etc. (*Chandler*, 1965). Urban climatology has traditionally relied on a temperature difference between a pair of stations to describe the climate of cities in reference to its background climate: the 'urban' station is generally located in the inner city (e.g., an old meteorological station of the town), while the 'rural' one, placed outside the city, served as the reference. Through an extensive literature review, *Stewart* (2007) drew attention to the marked difference that exists between station pairs, and which makes inter-urban cross comparisons between different cities almost impossible. For example, in some cases the urban station is located at an airport next to the city, while in other cases it is placed in a paved parking lot or in an urban park. As a consequence, the local climatic differences that exist between measurement sites are the sum of the background climate and urban effects, and the two cannot be separated (*Lowry*, 1977).

In order to investigate the spatial pattern of the air temperature fields in cities, mobile measurements utilizing instrumented vehicles – such as *Bottyán* and *Unger* (2003) – are used. But, they are based on occasional measurements, therefore not suited to monitoring simultaneously both the spatial and temporal development of the urban heat island. However, they are applicable to be the

basis of empirical models that are capable of estimating urban temperature patterns based on surface properties (e.g., *Balázs et al.*, 2009).

One way to automate urban measurements is through remote sensing, as done for example by *Bartholy et al.* (2009). However, this method has its limits as well: first, establishing the linkage between the surface temperatures detected by satellites and the actual temperatures within the urban canopy is not straightforward (*Weng*, 2009); second, data can only be obtained during clear-sky conditions.

Another way of measurement automation is offered by the use of automatic weather stations (AWSs). This is a more suitable approach to study the UHI's spatial and temporal resolution, and it can be refined by increasing the density of the stations as far as it is needed (limited by financial sources). They are also applicable for method development and public information as well. The need of operational urban meteorological networks is underpinned for example by *Grimmond et al.* (2010) and *Muller et al.* (2013a). Existing global AWSs networks are primarily utilized for operative tasks, such as to provide input to numerical weather forecast models or for the notification of the public. These networks are, however, not applicable for urban climate investigations. While urban AWS networks are most suited for such analyses, they are rather rare. Despite the fact that the rules for establishing urban weather stations are less strict (*Oke*, 2006) than those for ordinary meteorological stations (*WMO*, 2008), sensor deployment in urban areas presents other challenges (e.g., safety concerns regarding sensor placement, or the increased network density required for the characterization of small-scale phenomena). There are only a few local scale urban heat island monitoring networks in Europe (*Table 1*), whereas they are more prevalent in other parts of the world such as in Oklahoma, USA (*Basara et al.*, 2011), Tokyo, Japan (*Mikami et al.*, 2003), Taipei, Taiwan (*Chang et al.*, 2010), and Hong Kong, China (*Hung* and *Wo*, 2012).

According to the experiences of former networks, there are three critical issues to solve: (i) placing the instruments – which is necessarily a compromise between WMO standards, safety, and maintenance criteria and representativity; (ii) data storing and transferring; (iii) power supply. As in this case a relatively dense network is needed (several sensors), it is expected that the instruments should be small, low-cost, and have possibility to transfer data via wireless methods (e.g., *Petralli et al.*, 2011; *Chapman et al.*, 2014). In general, existing networks have two shortcomings from the viewpoint of urban climatology: the placement of measurement sites is either not representative of the built characteristics of the city (as e.g., in Berlin, where only LCZ classes with natural land cover and open built-up characteristics are investigated by *Fenner et al.* (2014)), or the description of the sites' environment does not use any standardized method. These issues are originated from different purposes of the networks (e.g., educational, meso-meteorological) and the lack of communication between research groups. Consequently, it is hard to compare their reported results.

Table 1. Local scale urban temperature monitoring systems in Europe with some characteristics

Country, city	Number of sensors	Area (km^2)	Operating	Aim, instruments, experiences
England, Birmingham	111		2013–	– denser network in the downtown area and sparser in the outskirts (*Young et al.*, 2012) – data are transmitted through WiFi – Vaisala WXT-520s, low-cost Aginova sensors (*HiTemp*, 2014; *Chapman et al.*, 2012)
England, London	91	1580	2009–	– educational aim, located at schools – data are transmitted through WiFi (*Davies et al.*, 2011)
Finland, Helsinki	100	150	2005–	– research in mesoscale meteorology –Vaisala WXT-510 – data are transmitted via the mobile phone network (*Dabberdt et al.*, 2005)
Germany, Berlin	10	890	2000–	– different types of sensors and radiation shields – five sites (classified as LCZ A, LCZ A, LCZ B, LCZ 5 and LCZ 6, respectively) – data are transmitted through Ethernet cable (*Muller et al.*, 2013a; *Fenner et al.*, 2014)
Italy, Florence	35		2004–	– located randomly in districts characterized by distinct spatial configurations – HOBO PRO Temp/Rh Data Loggers (, 2013)

Urbanized areas can be classified according to their ability to interact with near-surface atmosphere and establish their typical local-scale thermal environments. Classification can either be used for mapping and spatial analysis, or for the characterization of measurement sites based on their induced local climate. Over the past years, the increased need to use well-established and universally applicable system of categories for the description of measurement sites (e.g., *Muller et al.*, 2013b) stimulated efforts to develop an appropriate site classification system. One such approach is the frequently used Local Climate Zones (LCZ) system (*Stewart* and *Oke*, 2012). It is based on a worldwide survey of urban climate studies (*Stewart*, 2007, 2011) and is influenced by earlier concepts (*Auer*, 1978; *Ellefsen*, 1991; *Oke*, 2006). The LCZ system was developed to standardize measurement site description and, therefore, to facilitate intra-urban and inter-urban cross comparisons. The major advantages of LCZ system is that it is a global classification scheme, it contains limited number of classes, and the classes are

separated by the main thermal characteristic of the urban surface. The LCZ system does not cover entirely the spatial heterogeneity of the thermal pattern because it is affected by far more and complex processes, but it describes the most important features, thus it can be a good basis for local and regional scale climate models in order to estimate the intra-urban temperature patterns.

The objective of this paper is twofold. First, it introduces the urban climate monitoring and visualization systems recently implemented in two Central European cities. Second, the paper presents the analysis on temperature and partly on humidity data in the first complete summer (2014) period: (1) the validation of the measurement equipment used in the networks; (2) intra-urban and inter-urban comparison of the sites' (representing different LCZs) thermal behavior; and (3) the evaluation of the systems' usefulness.

2. Study areas

Szeged (Hungary) and Novi Sad (Serbia) are located in the Pannonian Plain in Central Europe. They have similar geographical and climatic environments. According to the climate classification system developed by Köppen, both cities belong to the Cfb climate category – temperate warm climate with a rather uniform annual distribution of precipitation (*Kottek et al.*, 2006).

Szeged has 160,000 inhabitants and its terrain is almost completely flat with average height around 79 m a.s.l. While the administrative area of Szeged is 281 km^2, the urbanized area is only about 30 km^2. The avenue-boulevard structure of the city was built to follow the axis of the river Tisza. It is characterized by a densely built up city center, with blocks of flats in the northern part of the city, as well as family homes and warehouses at the outskirts.

Novi Sad consists of two parts. The larger part is located between 80 and 86 m a.s.l. on a plain, whereas the smaller, southern part is situated on the northern slopes of the Fruška Gora hills. With an area of 80 km^2, it is the second largest city of Serbia with a population of 340,000. The River Danube flows through the southern and south-eastern edges of the city. It has a densely built-up central area and an industrial zone at the northern part of the city (*Savić et al.*, 2013).

3. Monitoring networks and data

The development of the online urban climate monitoring systems in Szeged, Hungary and Novi Sad, Serbia is funded by the Hungary-Serbia IPA Cross-border Co-operation EU Programme (*URBAN-PATH*, 2015) (*Fig. 1*). The systems record directly measured temperature and relative humidity, along with a calculated human comfort index which is not applied in our study. The systems present the data by maps and graphs, which together with the archived materials are freely available on the project's website (www.urban-path.hu). The

development of the monitoring systems is based on the LCZ mapping method (for the details see *Lelovics et al.*, 2014). According to *Unger et al.* (2014), there are 24 and 27 stations in the seven and eight LCZ classes occurring in and around Szeged and Novi Sad, respectively (*Fig. 1*).

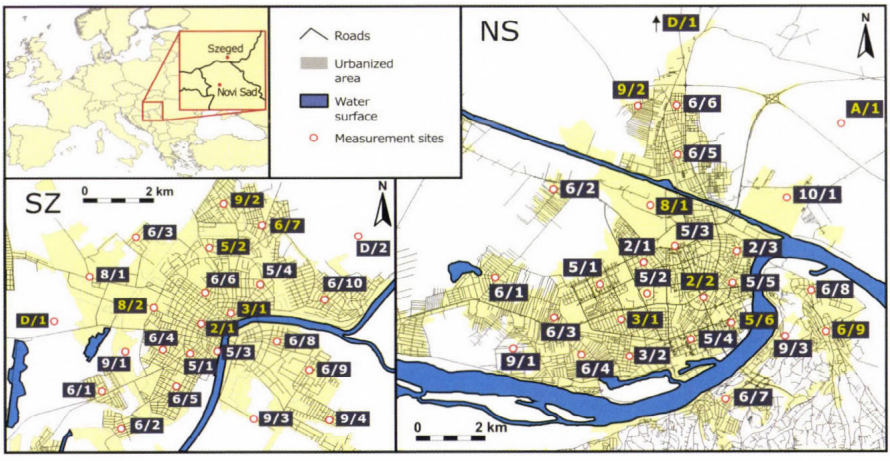

Fig. 1. Maps of the urban monitoring networks in Szeged (SZ), Hungary and Novi Sad (NS), Serbia. In the sites' identification number, the first digit refers to the LCZ class (*Stewart* and *Oke*, 2012) and the second one is an assigned number. Yellow identification numbers are the selected stations for the analysis presented in this paper. The details about the stations and their environs are listed in *Table 2*.

In the case of our networks, the response for the challenges mentioned in Section 1 is (i) to select sites with homogeneous neighborhood and mount them onto lamp posts; (ii) to store data on microSD card and transfer automatically through a 3G network; and (iii) to use batteries charged from the power supply of the city lights. Once the appropriate sites for the stations were selected, the instruments were mounted on lamp posts at 4 m above ground level for security reasons. For further technical details see *Unger et al.* (2015).

In this study, seven and eight measurement sites were selected for the analysis in Szeged and Novi Sad, respectively, representing the LCZ types occurring in the study areas. These sites are in the center of their LCZ areas, and also the surroundings are the most homogenous. The selected sites per LCZ classes and the typical values of surface parameters of their 250 m radius environment are listed in *Table 2*. The aerial photographs in *Fig. 2*. show a set of selected sites as examples with their surroundings.

Table 2. Typical surface properties of the 250 m radius environment around the selected sites. Abbrevations refer to surface properties: ISF – impervious surface factor, BSF – building surface factor, PSF – pervious surface factor, ALB – albedo, SVF – sky view factor, HRE – height of roughness elements. Upper lines refer to Szeged, bottom lines to Novi Sad

LCZ class (after 36)	Number of sites	HRE [m]	SVF	BSF	ISF	PSF	ALB	land use: 1: EEA Urban Atlas (*EEA*, 2010) for Szeged 2: Corine Land Cover (*Bossard et al.*, 2000) for Novi Sad
LCZ2:	1	13.5	0.6099	0.4316	0.4454	0.1229	0.1503	60% urban continuous, 20% industrial, 17% roads, 3%
compact midrise	3	16.2–20.8	0.4715–0.5892	0.2598–0.3752	0.5930–0.6293	0.0186–0.1472	0.1545–0.1677	green[1] 100% urban discontinuous[2]
LCZ3:	1	9.5	0.6746	0.3681	0.4682	0.1637	0.1514	70% urban continuous, 13% roads, 12% industrial, 4% green[1]
compact lowrise	2	12	0.5860–0.6102	0.2168–0.2704	0.6435–0.6621	0.0861–0.1211	0.1676–0.1701	100% urban discontinuous[2]
LCZ5:	4	11.7–20.6	0.6909–0.8015	0.1183–0.3338	0.3718–0.5162	0.2526–0.5099	0.1441–0.1453	7–77% urban continuous, 0–43% urban dense, 0–31% urban
open midrise	6	15.9–25.7	0.6407–0.8840	0.0852–0.3499	0.4553–0.6749	0.0763–0.3314	0.1631–0.1836	medium, 4–41% industrial, 10–11% roads, 0–5% urban green, 0–35% water bodies[1] 60–100% urban discontinuous, 0–40% roads[2]
LCZ6:	10	3.1–5.5	0.8244–0.9562	0.1002–0.2475	0.2829–0.4925	0.2863–0.6101	0.1375–0.1780	0–87% urban continuous, 0–88% urban dense, 0–21% urban medium, 5–14% roads, 0–11% industrial, 0–11%
open lowrise	9	12	0.6268–0.9967	0.1837–0.2136	0.6248–0.8632	0.0819–0.3752	0.1594–0.1827	agricultural, 0–7% urban green[1] 80–100% urban discontinuous, 0–20% urban green, 0–20% roads[2]
LCZ8:	2	4.9	0.9463	0.1545	0.5757	0.2697	0.1347–0.1508	59–81% industrial, 6–9% roads, 0–12% urban continuous, 0–10% water, 0–9% urban dense, 1–7% urban green[1]
large lowrise	1	12	0.8355	0.3050	0.4676	0.2274	0.1701	100% industrial[2]
LCZ9:	4	2.8	0.9965	0.0062–0.2100	0.0209–0.0500	0.7500–0.9729	0.1351–0.1655	0–64% urban medium, 0–67% agricultural, 0–48% urban green, 0–24% urban low density, 0–23% urban dense, 0–18% water bodies, 0–8% urban very low density, 0–9% roads[1]
sparsely built	3	12	0.8233	0.0000–0.0950	0.2551–0.5551	0.3499–0.7922	0.1675–0.1855	20–90% agricultural, 10–80% urban discontinuous[2]
LCZ10:	0	–	–	–	–	–	–	100% industrial[2]
heavy industry	1	12	0.9617	0.0180	0.5683	0.4137	0.1787	
LCZA:	0	–	–	–	–	–	–	100% forest[2]
dense trees	1	0	1.0000	0.0000	0.2078	0.7922	0.1515	
LCZD:	2	0	1.0000	0.0000	0.0000–0.1000	0.8000–1.0000	0.1447–0.1563	83–97% agricultural, 3–14% industrial[1]
low plants	1	0	1.0000	0.0000	0.3119	0.6881	0.1240	100% agricultural[2]

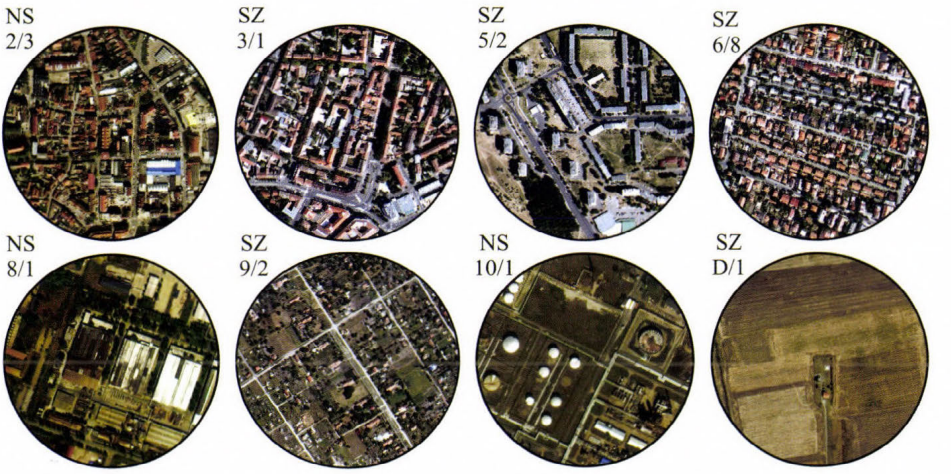

Fig. 2. Aerial photographs illustrating selected measurement sites with their 250 m radius environments (Szeged (SZ), Novi Sad (NS), first number – LCZ class number, second number – station's identity number in the given LCZ class).

In Szeged, data collection began on March 23, 2014, and in Novi Sad on June 10, 2014. In this study, the examined period is from June 1 to August 31, while in Novi Sad the analyzed interval is somewhat shorter – lasting from June 10 to August 9 – due to technical issues. In order to overcome the issues around daylight saving time in summer and to be in line with meteorological standards (*WMO*, 2008), time is given in UTC both in the database and in the analyses below.

In this region, summer is generally the most critical season from the viewpoint of health and human comfort. Although with 321 mm precipitation recorded in Szeged, this summer was unusually wet compared to the seasonal average of 169 mm measured in the period of 1901–2000 (*HMS*, 2008). As a consequence, the number of days with favorable weather conditions – conducive to the development of micro- and local climates – was lower than usual.

4. Results and discussion

As we utilize a number of widely known methods during the data evaluation, these methods are mentioned at the beginning of the relevant subsections.

4.1. Sensor performance verification

The Hungarian Meteorological Service's (HMS) SYNOP station 12982 is located next to the urban network's D/1 station in Szeged (*Fig. 1*). Since the station of the HMS is part of the international surface synoptic network, it meets the requirements of the WMO. HMS utilizes Vaisala HMP-35D and HMP-45D temperature and relative humidity sensors and Vaisala MILOS-500 data loggers and transmitters. It records data with 10 minute resolution. As stations 12982 and D/1 are also mounted on the same platform and their radiation shields are the same, the former can be used as a reference for the validation of the latter. The sensor performance verification compared temperature and relative humidity values from the stations and utilized 25,780 pair of data from April 1 to September 29, 2014 in the process. The scatter plots of these values and their differences are presented in *Fig. 3*. We calculated mean absolute error (MAE), root mean square error (RMSE), standard deviation (STDEV), and mean error (MA).

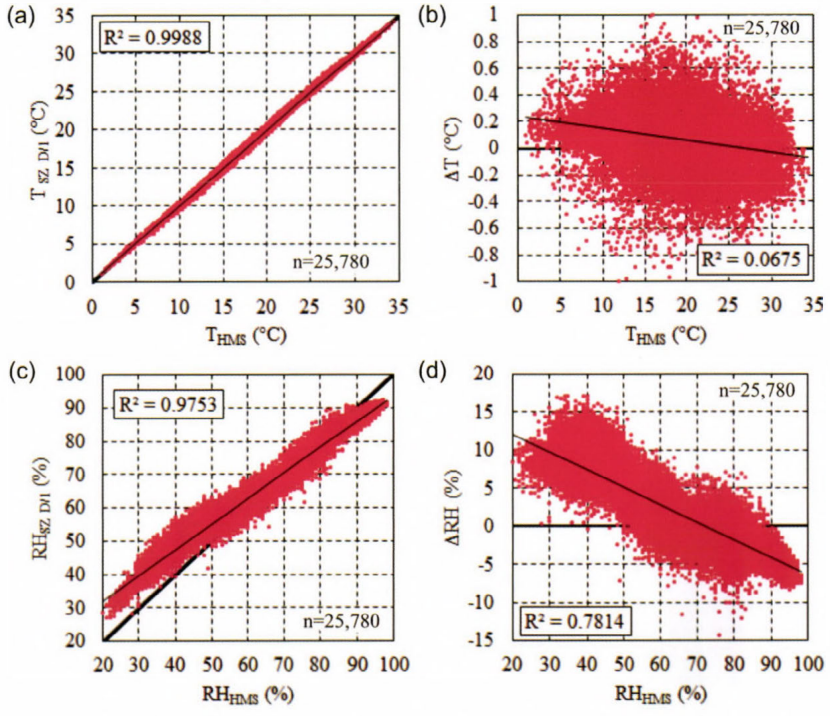

Fig. 3. Scatter plot of temperature (a), relative humidity (c), and their biases (b and d, $\Delta X = X_{SZ\,D/1} - X_{HMS}$) in Szeged.

The performance of the temperature sensor is adequate (*Fig. 3a*). As illustrated in *Fig. 3b*, the errors are small (MAE=0.1745 °C, RMSE=0.2194, while $STDEV_{D/I}$=5.78 °C and $STDEV_{HMS}$=5.83 °C) and almost balanced with a slight overestimation (ME=0.0769 °C). The relative humidity sensor underperforms (ME=0.6044%, MAE=4.2054%, RMSE=5.2277, $STDEV_{D/I}$=15.43%, $STDEV_{HMS}$=19.83%). Although the results shown in *Fig. 3c* do not meet the WMO standards (*WMO*, 2008) – requiring 1% accuracy for high and 5% accuracy for mid-range relative humidity levels –, the sensor was nevertheless deemed adequate for the purpose of the project, as 1–2% difference in RH has little effect on people's thermal comfort sensation in summer (e.g., *Oliveira* and *Andrade*, 2007). In contrast to the temperature sensor where bias is almost independent from its value (*Fig. 3b*), the relative humidity sensor systematically overestimates at lower values and underestimates at higher ones (*Fig. 3d*).

4.2. Intra-urban and inter-urban comparisons

4.2.1. Daily temperature indices

Two temperature indices were determined utilizing daily minimum (T_{min}) and maximum (T_{max}) temperature values: summer days, defined as days with T_{max}>25 °C; and tropical nights, where daily T_{min}>20 °C (*Karl et al.*, 1999). These indices were selected because of their acceptance as reliable indicators of heat stress (e.g., *Gabriel* and *Endlicher*, 2007; *Petralli et al.*, 2011). It was recognized that applying daily minima and maxima causes a kind of time asynchronity, but from the viewpoint of human health and heat stress, these time differences are not significant.

In order to make the daily temperature indices comparable between the two cities, days without data gaps in both locations were selected. The analysis used 48 days that met the criterion. The relative frequencies of these indices for each LCZ class are presented in *Fig. 4*.

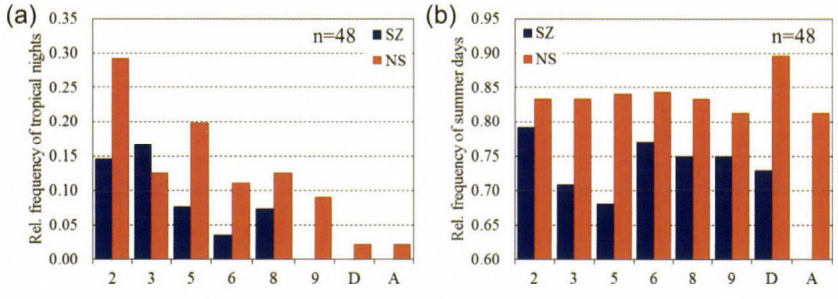

Fig. 4. Relative frequency of tropical nights (a) and summer days (b) by LCZ classes in Szeged and Novi Sad calculated for the selected common set of days.

In the case of tropical nights (Fig. *4a*), the differences between LCZ classes are relatively large, their number varies between 0 (LCZ D and LCZ 9) and 8 days (LCZ 3) in Szeged, while this range is between 1 (LCZ D and LCZ A sites) and 17 (LCZ 2) days in Novi Sad. It is important to note that the highest frequencies of tropical nights occur in the most densely built LCZs (2, 3, and 5). In contrast to tropical nights, the distribution of summer days is relatively even among the different LCZs (*Fig. 4b*). In the case of Novi Sad, LCZ D is an outlier, as it lacks shading from both buildings and taller plants. The cooling effect from shading is the reason behind the lower values recorded at LCZ 3 and 5 in Szeged. In the case of the latter site, the evapotranspiration from the higher amount of vegetation also contributes to this effect.

4.2.2. Diurnal variation of temperature under anticyclonic conditions

For the analysis of the thermal effect of the different LCZs, ideal weather conditions should be examined, because in these conditions the effect of the urban surface for the temperature are undisturbed. In order to eliminate the effects of unfavorable weather conditions and thus to bring forth the characteristic diurnal temperature cycles of various LCZ classes, we applied the average weather factor, Φ_w (*Oke*, 1998) calculated for 3-hour intervals using the data from the HMS SYNOP station 12982. Finally, we selected two time periods with prevailing anticyclonic conditions when Φ_w was greater than 0.7. They run from July 3 to 5, 2014 and from July 19 to 20, 2014 and lasted 72 and 48 hours in length, respectively. *Figs. 5* and *6* present the diurnal variation of absolute and relative temperatures – expressed relative to LCZ D as $T_{LCZ\,X} - T_{LCZ\,D}$.

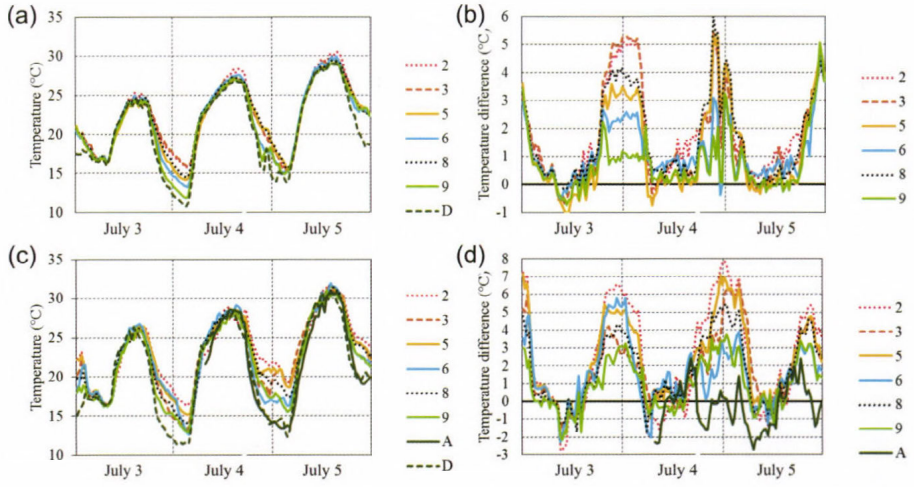

Fig. 5. Absolute and relative (difference from LCZ D) temperature variations at selected sites in Szeged (a, b) and Novi Sad (c, d) (July 3 to 5, 2014).

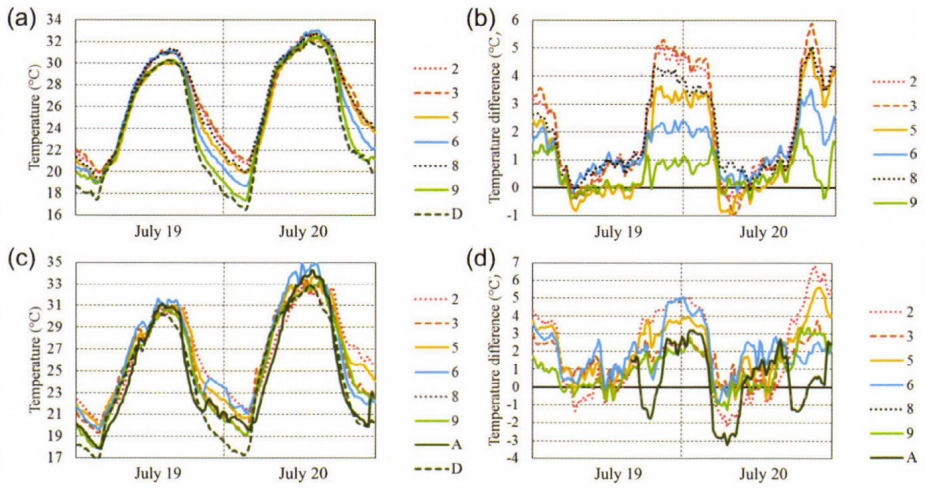

Fig. 6. Absolute and relative (difference from LCZ D) temperature variations at selected sites in Szeged (a, b) and Novi Sad (c, d) (July 19 to 20, 2014).

The measurement sites belonging to various LCZs have distinct daily temperature cycles. The differences between the classes are most pronounced in the case of Szeged, where LCZ 2 and LCZ 3 have an over 5°C temperature surplus at 00:00 UTC, July 4 (*Figs. 5a* and *b*) and at 00:00 UTC, July 20 (*Figs. 6a* and *b*). In the case of LCZ 8, LCZ 5, LCZ 6 and LCZ 9 the largest surplus values are 4 °C, 3.5 °C, 2.5 °C and 1 °C, respectively. In Novi Sad, the temperatures are slightly higher, but the classes differ less. The greatest temperature surpluses occur in LCZ 2 and LCZ 6 (between 5–7 °C), while LCZ 5, LCZ 3. and LCZ 8 remain somewhat cooler. The cycles of LCZ A and LCZ D are similar. The temperature difference between the two types remains within the ±3 °C interval, with the largest values occurring around 00:00 UTC.

Fig. 7 shows the examined sites' characteristic daily temperature cycles, calculated from the selected 'ideal' days as hourly averages relative to the average non-urban reference site (LCZ D). While differences are smaller in Szeged – as it is a smaller city with half the population of Novi Sad –, the diurnal cycle of LCZ's in the two cities indicate similar trends. During daytime, when the insolation is high and convective mixing prevails, temperature differences are below ±1 °C. The only exception is LCZ A in Novi Sad during the morning hours, which is the result of lush vegetation that delays warming through shading and evapotranspiration. During the night, when radiative cooling dominates, the differences are larger and mostly

positive. The differences between the LCZ classes are most pronounced during this period due to the unique radiative and thermal properties of the sites. In the case of Szeged, the diurnal cycles of classes are more discernible.

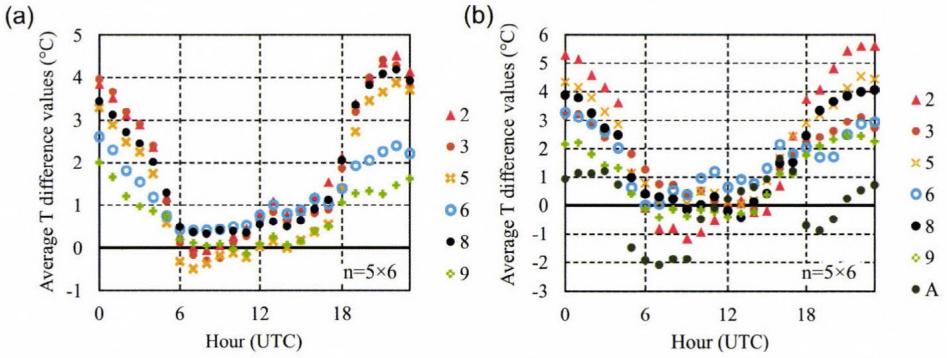

Fig. 7. Average hourly temperature values at selected sites calculated for the five selected days and expressed relative to average LCZ D in Szeged (a) and Novi Sad (b).

4.2.3. Diurnal variation of UHI during summer

This analysis is concerned with the diurnal development of the UHI intensity in the most densely built LCZ areas of Szeged and Novi Sad. Similarly to the conventional heat island studies, the UHI intensity is expressed as the urban conditions relative to non-urban ones. In our case, it was calculated as an average temperature difference between LCZ 2 (urban) and LCZ D (non-urban) sites for half-hour intervals in both cities (*Fig 8*). As noted in Section 3, the investigated period was shorter in Novi Sad due to technical issues.

The shape of isopleths in *Fig. 8* are in line with the general understanding of the thermal behavior of dense urban areas: for the most time, the UHI intensity remains positive with highest values at night, while negative values occur predominantly during the day (urban cool island). The dividing line between these two periods is around 6 UTC and 12 UTC in both cities – see the thick isotherms of 0 °C in *Fig. 8*. The range of UHI intensity is between –1.48 °C and 5.22 °C in Szeged, and between –3.70 °C and 6.85 °C in Novi Sad.

Urban cool island occurs in both cities during the day. It is typically around –1 °C in Szeged and –2 °C in Novi Sad. An exception around 18:00 UTC on July 27 in Szeged (shown in *Fig. 8a*) is caused by the cooling effect of a

convective precipitation – 36.4 mm precipitation was measured at the outskirts and 83.0 mm in the inner city. It resulted in large temperature differences between different parts of the city, and produced an outflow with 8.3 ms^{-1} wind speed at the outskirts and 9.3 ms^{-1} in the center. As a consequence, the cooling was much faster in the central area and produced the mentioned anomaly.

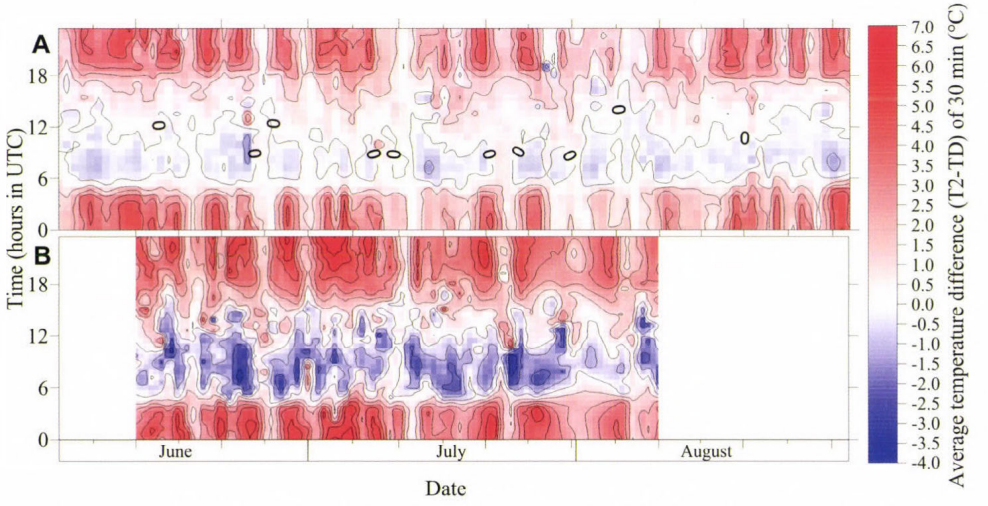

Fig. 8. Average temperature differences [°C] between LCZ 2 and LCZ D (a) in Szeged and (b) Novi Sad (thin isotherms – integer °C, thick isotherms – 0 and 5°C).

5. Conclusions

Monitoring urban temperature patterns is an important task that can assist in formulating adaptation and mitigation strategies to meet the challenges of climate change. The use of automatic weather stations is the most suited method for understanding the spatial and temporal characteristics of the urban climate. Although the global network of AWSs is well developed, their presence in cities is still rather rare. The developed urban climate monitoring systems in Szeged, Hungary and Novi Sad, Serbia visualize the observed temperature and relative humidity data along with calculated human comfort index. The results are freely available online. The selection of measurement sites utilized LCZ maps to ensure a representative number and placement of stations within different LCZs.

This study introduces these monitoring networks through a number of analyses using data from the summer of 2014. The temperature and relative humidity sensors at site D/1 in Szeged were validated against the sensors of the Hungarian Meteorological Service's SYNOP station 12982. In the case of temperature, the sensor performance was found satisfactory with slight underestimation. The relative humidity sensor underperformed, but it was deemed acceptable for the purpose of the project.

The evaluation of the daily temperature indices (summer days and tropical nights) revealed that the highest frequencies of tropical nights occur in the most densely built LCZ classes (2, 3, and 5). Based on these results, the control of building densities or the spatial confinement of dense LCZs could be viable adaptation strategies.

Further, in order to assess the thermal behavior of different LCZs under 'ideal' conditions, two periods with anticyclonic conditions were selected. In the case of Szeged, the distinction between the daily temperature cycles of different LCZ classes was quite pronounced. In contrast, while the nighttime temperature surpluses and the daytime temperature deficits were greater in Novi Sad, the thermal cycle of different LCZs was less distinct. The average daily cycle of each LCZ highlights the differences between day- and nighttime processes.

During summer, the diurnal variation of conventional heat island intensity confirms the general knowledge, that is, it remains positive with highest values at night, while negative values occur predominantly during the day.

Overall, it can be stated that the monitoring networks installed in Szeged and Novi Sad serve their intended purposes – as informing the citizens about the most recent temperature, humidity, and thermal comfort measurements – well. Based on the site visit data of the public display (www.urban-path.hu) of the monitoring system, the daily visitor number is around 200 and the two-thirds of it are new visitors from these two cities. Hopefully, this publicity helps the local authorities to decrease the disadvantageous effects of urban climate. They provide beneficial information about the climate of these cities to the public, moreover, the results (based on a short time period) presented in this paper show that the scientific application of the obtained data is also conductive. The spatial and temporal resolution of the network is adequate, and the accuracy of the sensors is satisfactory. The results indicate that the site selection was appropriate, as the sites belonging to different LCZs exhibit distinct thermal behaviors. The planned operation time of these networks will be over 5 years. Future data series will allow for more detailed and versatile climatological analyses in relation to intra-urban climate variations.

Acknowledgement: The study was supported by the Hungary-Serbia IPA Cross-border Co-operation EU Programme (HUSRB/1203/122/166 – URBAN-PATH), the Hungarian Scientific Research Fund (OTKA K-111768, PD-100352). *Tamás Gál* was supported by the János Bolyai Research Scholarship of the Hungarian Academy of Sciences.

References

Auer, A.H., 1978: Correlation of land use and cover with meteorological anomalies. *J.Appl. Meteorol. 17*, 636–643.

Balázs, B., Unger, J., Gál, T., Sümeghy, Z., Geiger, J. and *Szegedi, S.*, 2009: Simulation of the mean urban heat island using 2D surface parameters: empirical modeling, verification and extension. *Meteorol. Appl. 16*, 275–287.

Balling, R.C. and *Gober, P.*, 2006: Climate variability and residential water use in the City of Phoenix, Arizona. *J. Appl. Meteorol. Climatol. 46*, 1130–1137.

Bartholy, J., Pongrácz, R., Lelovics E., and *Dezső, Z.*, 2009: Comparison of urban heat island effect using ground-based and satellite measurements. *Acta Climatol. Chorol. 42-43*, 7–15.

Basara, J.B., Illston, B.G., Fiebrich, C.A., Browder, P.D., Morgan, C.R., McCombs, A., Bostic, J.P., McPherson, R.A., Schroeder, A.J., and *Crawford, K.C.*, 2011: The Oklahoma City Micronet. *Meteorol. Appl. 18*, 252–261.

Bossard, M., Feranec, J., and *Otahel, J.*, 2000: CORINE land cover technical guide – Addendum 2000. EEA Technical report No 40.

Bottyán, Z., and *Unger, J.*, 2003: A multiple linear statistical model for estimating the mean maximum urban heat island. *Theor. Appl. Climatol. 75*, 233–243.

Chandler, T.J., 1965: *The Climate of London*. London: Hutchinson.

Chapman, L., Muller, C.L., Young, D.T., Cai, X-M., and *Grimmond, C.S.B.*, 2012: An introduction to the Birmingham Urban Climate Laboratory. *8th Int. Conf. on Urban Climate*, Dublin, Ireland, Paper 19.

Chang, B., Wang, H-Y., Peng, T-Y. and *Hsu, Y-S.* 2010: Development and evaluation of a city-wide wireless weather sensor network. *Edu. Technol. Soc. 13*, 270–280.

Chapman, L., Muller, C.L., Young, D.T., Warren, E.L., Grimmond, C.S.B., Cai, X-M., and *Ferranti, E.J.S.*, 2015: The Birmingham Urban Climate Laboratory: An open meteorological testbed and challenges of the smart city. *Bull. Am. Meteorol. Soc. 96*, 1545–1560.

Dabberdt, W., Koistinen, J., Poutiainen, J., Saltikoff, E., and *Turtiainen, H.*, 2005: The Helsinki mesoscale testbed: an invitation to use a new 3-D observation network. *Bull. Am. Meteorol. Soc. 86*, 906–907.

Davies, L., Bell, J.N.B., Bone, J., Head, M., Hill, L., Howard, C., Hobbs, S.J., Jones, D.T., Power, S.A., Rose, N., Ryder, C., Seed, L., Stevens, G., Toumi, R., Voulvoulis, N., and *White, P.C.L.*, 2011: Open air laboratories (OPAL): a community-driven research programme. *Environ. Poll. 159*, 2203–2210.

EEA, 2010: *Urban Atlas*. http://www.eea.europa.eu/data-and-maps/data/urban-atlas, Accessed: 2015-01-28.

Ellefsen, R., 1991: Mapping and measuring buildings in the canopy boundary layer in ten U.S. cities. *Energy and Buildings 15-16*, 1025–1049.

Fenner, D., Meier, F., Scherer, D., and *Polze, A.*, 2014: Spatial and temporal air temperature variability in Berlin, Germany, during the years 2001–2010. *Urban Climate 10*, 308–331.

Gabriel, K.M., and *Endlicher, W.R.*, 2011: Urban and rural mortality rates during heat waves in Berlin and Brandenburg, Germany. *Environ. Poll. 159*, 2044–2050.

Grimmond, C.S.B., Roth, M., Oke, T.R., Au, Y.C., Best, M., Betts, R., Carmichael, G., Cleugh, H., Dabberdt, W., Emmanuel, R., Freitas, E., Fortuniak, K., Hanna, S., Klein, P., Kalkstein, L.S., Liu, C.H., Nickson, A., Pearlmutter, D., Sailor, D., and *Voogt, J.*, 2010: Climate and more sustainable cities: climate information for improved planning and management of cities (producers/capabilities perspective). *Procedia Environ. Sci. 1*, 247–274.

HiTemp, 2014: *High Density Measurements within Urban Environment.* http://www.birmingham.ac.uk/schools/gees/centres/bucl/hitemp/index.aspx Accessed: 2014-08-12.

HMS, 2008: *Climate Data Series of Szeged, 1901-2000. Description of instruments.* http://owww.met.hu/eghajlat/eghajlati_adatsorok/sz/Navig/102_EN.htm, Accessed: 2014-10-01.

Hung, T.K., and *Wo, O.C.*, 2012: Development of a community weather information network (Co-WIN) in Hong Kong. *Weather 67*, 48–50 .

IPCC, 2012: *Managing the Risks of Extreme Events and Disasters to Advance Climate Change Adaptation*, A Special Report of Working Groups I and II of the IPCC. Cambridge, UK and New York, USA: Cambridge University Press.

Karl, T.R., Nicholls, N., and *Ghazi, A.*, 1999: CLIVAR/GCOS/WMO workshop on indices and indicators for climate extremes: Workshop summary. *Climatic Change 42*, 3–7.

Kolokotroni, M., Giannitsaris, I., and *Watkins, R.*, 2006: The effect of the London urban heat island on building summer cooling demand and night ventilation strategies. *Sol. Energy 80*, 383–392.

Kottek, M., Grieser, J., Beck, C., Rudolf, B., and *Rubel, F.*, 2006: World Map of the Köppen-Geiger climate classification updated. Meteorologische Zeitschrift 15, 259-263.

Lelovics, E., Unger, J., Gál, T., Gál, C.V., 2014: Design of an urban monitoring network based on Local Climate Zone mapping and temperature pattern modelling. *Clim. Res. 60*, 51–62.

Lowry, W.P., 1977: Empirical estimation of urban effects on climate: A problem analysis. *J. Appl. Meteorol. 16*, 129–135.

Mikami, T., Ando, H., Morishima, W., Izumi, T., and *Shioda, T.*, 2003: A new urban heat island monitoring system in Tokyo. 5th Int. Conf. on Urban Climate, Lodz, Poland, O.3.5.

Muller, C.L., Chapman, L., Grimmond, C.S.B., Young, D.T., and *Cai, X-M.*, 2013a: Sensors and the city: a review of urban meteorological networks. *Int. J. Climatol. 33*, 1585–1600.

Muller, C.L., Chapman, L., Grimmond, C.S.B., Young, D.T., and *Cai, X-M.*, 2013b: Toward a standardized metadata protocol for urban meteorological networks. *Bull. Am. Meteorol. Soc. 94*, 1161–1185.

Oke, T.R., 1982: The energetic basis of the urban heat island. *Quart. J. Roy. Meteorol. Soc. 108*, 1–24.

Oke, T.R., 1987: *Boundary Layer Climates.* 2nd ed. London–New York: Routledge.

Oke, T.R., 1998: An algorithmic scheme to estimate hourly heat island magnitude. 2nd Urban Environment Symp., Albuquerque, New Mexico, 80–83.

Oke, T.R., 2006: Initial guidance to obtain representative meteorological observations at urban sites. Geneva: WMO/TD No. 1250.

Oliveira, S., and *Andrade, H.*, 2007: An initial assessment of the bioclimatic comfort in an outdoor public space in Lisbon. *Int. J.Biometeorol. 52*, 69–84.

Petralli, M., Massetti, L., and *Orlandini, S.*, 2011: Five years of thermal intra-urban monitoring in Florence (Italy) and application of climatological indices. *Theor. Appl. Climatol. 104*, 349–356.

Petralli, M., Morabito, M., Cecchi, L., Crisci, A., and *Orlandini, S.*, 2012: Urban morbidity in summer: ambulance dispatch data, periodicity and weather. *Central European J. Medicine 7*, 775–782.

Petralli, M., Massetti, L., Brandani, G., and *Orlandini, S.*, 2013: Urban planning indicators: useful tools to measure the effect of urbanization and vegetation on summer air temperatures. *Int. J. Climatol. 34*, 1236–1244.

Pongrácz, R., Bartholy, J., and *Bartha, E.B.*, 2013: Analysis of projected changes in the occurence of heat waves in Hungary. *Adv. in Geosciences 35*, 115–122.

Santamouris, M., Papanikolaou, N., Livada, I., Koronakis, I., Georgakis, C., Argiriou, A., and *Assimakopoulos, D.N.*, 2001: On the impact of urban climate on the energy consumption of buildings. *Sol. Energy 70*, 201–216.

Savić, S., Milošević, D., Lazić, L., Marković, V., Arsenović, D., and *Pavić, D.*, 2013: Classifying urban meteorological stations sites by "Local Climate Zones": Preliminary results for the City of Novi Sad (Serbia). *Geographica Pannonica 17(3)*, 60–68.

Stewart, I.D., 2007: Landscape representation and urban-rural dichotomy in empirical urban heat island literature, 1950-2006. *Acta Climatol. Chorol. 40-41*, 111–121.

Stewart, I.D., 2011: A systematic review and scientific critique of methodology in modern urban heat island literature. *Int. J. Climatol. 31*, 200–217.

*Stewart, I.D.,*and *Oke, T.R.*, 2012: Local Climate Zones for urban temperature studies. *Bull. Am. Meteorol. Soc. 93*, 1879-1900.

Tan, J., Zheng, Y., Tang, X., Guo, C., Li, C., Song, G., Zhen, X., Yuan, D., Kalkstein, A.J., Li, F., and *Chen, H.*, 2010: The urban heat island and its impact on heat waves and human health in Shanghai. *Int. J. Biometeorol. 54*, 75–84.

Tomlinson, C.J., Chapman, L., Thornes, J.E., and *Baker, C.J.*, 2011: Including the urban heat island in spatial heat health risk assessment strategies: a case study for Birmingham, UK. *Int. J. Health Geographics 10*, 1–14.

Unger, J., Savic, S., Gál, T., and *Milosevic, D.*, 2014: Urban climate and monitoring network system in Central European cities. Novi Sad (ISBN: 987-86-7031-341-5), 101 p.

Unger, J., Gál, T., Csépe, Z., Lelovics, E., and *Gulyás, Á.*, 2015: Development, data processing and preliminary results of an urban human comfort monitoring and information system. *Időjárás 119*, 337-354.

URBAN-PATH homepage, 2015: http://www.urban-path.hu, Accessed: 31-01-2015.

Weng, Q., 2009: Thermal infrared remote sensing for urban climate and environmental studies: Methods, applications, and trends. *ISPRS J. Photogramm. Rem. Sens. 64*, 335–344.

WMO, 2008: *Guide to Meteorological Instruments and Methods of Observation.* 8th ed. Geneva, Switzerland: World Meteorological Organization.

Young, D.T., Chapman, L., Muller, C.L., and *Cai, X-M.*, 2014: A low-cost wireless temperature sensor: evaluation for use in environmental monitoring applications. *J. Atmos. Oceanic Tech. 31*, 938–944.

IDŐJÁRÁS

Quarterly Journal of the Hungarian Meteorological Service
Vol. 120, No. 3, July – September, 2016, pp. 301–313

Short-term weather fluctuation and quality assessment of oxbows

János Tamás Kundrát[1*], Edina Simon[1], István Gyulai[2], Gyula Lakatos[1], and Béla Tóthmérész[3]

[1]*University of Debrecen, Department of Ecology, Egyetem tér 1, H-4032 Debrecen, Hungary*

[2]*University of Debrecen, Department of Hydrobiology, Egyetem tér 1, H-4032 Debrecen, Hungary*

[3]*MTA-DE Biodiversity and Ecosystem Services Research Group, Egyetem tér 1, H-4032 Debrecen, Hungary*

**Corresponding author E-mails: kundratt@gmail.com*

(Manuscript received in final form December 7, 2015)

Abstract—Our aim was to study the effects of short-term weather fluctuations on the quality of oxbows, based on the physico-chemical parameters of the water. The present study explored the effect of precipitation, temperature, and the water level of the main river on the quality of oxbows. We assessed the quality of four oxbows in the Upper Tisza region (north Hungary) over a two-year period. Water samples were collected in the summer in 2011 and 2012, and 12 physico-chemical parameters were investigated.

We found positive correlations between the dissolved oxygen, water temperature, concentration of hydro carbonate, nitrate, pH, conductivity and the average temperature. Canonical discriminant analysis showed that the studied oxbows were similar in 2011 and 2012, based on physico-chemical parameters. Significant differences were found between the years, in terms of the water temperature, the content of suspended solids, and the concentrations of carbonate and chloride. Our results show that only short-term weather changes such as less precipitation and higher temperature cause the quality of oxbows to deteriorate.

Our results demonstrated that the water quality of oxbows is influenced by the River Tisza, because the decrease in the water level of the Tisza was also responsible for the differences between the years, based on the physical-chemical parameters of the water.

Key-words: physico-chemical parameters of water, weather change, drought index, degradation, emerse vegetation, submerse vegetation

1. Introduction

Conservation of oxbows is of central importance both in Europe and around the world. Although these oxbows are also endangered aquatic habitats, the management and conservation of freshwater resources mainly focuses on running water and larger water bodies (*Oertli et al.,* 2009). Due to their biodiversity, small oxbows are equally significant from a socio-economic and from a conservation biology point of view (*Oertli et al.,* 2009). Many oxbows were found in the Upper Tisza region, which is characterized by abandoned river channels, meanders, and periodical and permanent water marshy areas. Most of the oxbows were created during the regulation of the River Tisza (*Varga et al.,* 2013). There are about 70 oxbows along the Upper Tisza river. They are connected to the river during the floodplain events, when large quantities of suspended particles are transported into the floodplain (*Nguyen et al.,* 2009).

Weather fluctuation has effects on aquatic ecosystems: (i) the temperature increase causes an increase in water temperature which may result in an increase in conductivity that may in turn reduce the level of oxygen and severely stress aquatic fauna (*Bond et al.,* 2008); (ii) the seasonal changes in precipitation alter the hydrological relations existing in aquatic systems (*Georgi* and *Pal*, 2004). Regional patterns in precipitation and temperature predict changes which have the potential to alter natural flow regimes (*Palmer et al.,* 2009). However, the cumulative changes in temperature and precipitation may have both direct and indirect effects on oxbows, because these water bodies have substantial exchanges with atmospheric water in the form of precipitation and evapotranspiration (*Michener et al.,* 1997; *Winter,* 2000). The hydrologic conditions directly affect the chemical and physical processes, and the dynamic of nutrients and suspended solids (*Fink* and *Mitsch,* 2007).

Aquatic macrophytes influence the physical and chemical environment of lakes and oxbows (*Lukács et al.,* 2009, 2011). Macrophytes play a key role in biochemical cycles, organic carbon production, and phosphorus mobilization. They also have a direct influence on hydrology and sediment dynamics (*Bornette* and *Puijalon,* 2011). Numerous studies have demonstrated that they can dramatically alter the material and energy flows between lakes and oxbows (*Frodge et al.,* 1990). Earlier studies have also demonstrated that macrophytes have an influence on the physico-chemical parameters of water on a macro-scale; consequently, the vegetation and the physico-chemical parameters of water are closely related (*Barendregt* and *Bio,* 2003; *Heegaard et al.,* 2001).

The aim of our study was to assess the impact of short-term weather fluctuations, such as reduced precipitation and higher temperature. We also investigated the effect of the water level of the main river and vegetation types on the quality of oxbows, based on the physico-chemical parameters of the water. The physico-chemical parameters of the surface water of oxbows were

studied during two years, 2011 and 2012. To compare the studied years a drought index was used, based on the mean temperature and rainfall of the years in question. At the same time, the effect of the water level of the Tisza on the quality of oxbows was also studied. The poor state of oxbows was evident in the field; thus, our hypothesis was that the weather parameters and water level of the Tisza may cause the deterioration of the physico-chemical parameters of the water, which leads to the degradation of the water quality. Thus, the aim of our study was to demonstrate that the precipitation, temperature, and water level of the River Tisza influenced the quality of these oxbows, and that the meteorological parameters and water level affected the oxbow fill up rate, even over a short time period. Our second hypothesis was that the macrophytes also had an effect on the physico-chemical parameters of the water, which may cause a change in the quality of oxbows. The present study explored the factors affecting the quality of oxbows, the precipitation and temperature, the water level, and/or the structure of vegetation.

2. Data and methods

2.1. Study sites

We studied the oxbows in the Upper Tisza region. The area studied covers 95 ha; it is an undisturbed area in the UpperTisza region, in the north part of Hungary. There are many oxbows in this region, and the following four oxbows were studied: the Kis-Zátony oxbow, the Nagy-Zátony oxbow, the Nagy-Pap oxbow, and the Sulymos oxbow (*Fig. 1*). In our study, two vegetation types (submersed and emersed) and open water were studied. The submersed vegetation type was characterized by *Ceratophyllum demersum Nymphaea alba* and *Schoenoplectus lacustris.* The emersed vegetation type was characterized by the following species: *Typha angustifolia, Typha latifolia,* and *Phragmites australis* (*Cook*, 1996). In the open water, there were no macrophytes. In the Kis-Zátony oxbow there were seven sampling points (two open water, four emersed, and one submersed vegetation). In the Nagy-Zátony oxbow, there were three sampling points (one open water, one submersed, and one emersed). In the Nagy-Pap oxbow, there were three sampling points (two emersed and one open water). In the Sulymos oxbow, there were six sampling points (one open water, one submersed, and four emersed vegetation type).

2.2. Water chemistry

We collected surface water samples in 1-liter plastic bottles; the bottles were rinsed out with deionized water three times. Until laboratory processing, samples were stored at 4 °C. We measured the physical and chemical parameters of the water. The following parameters were measured in the field: conductivity,

temperature, content of dissolved oxygen (DO) with portable field instruments (WTW cond. 340i), and pH (WTW pH 315i).

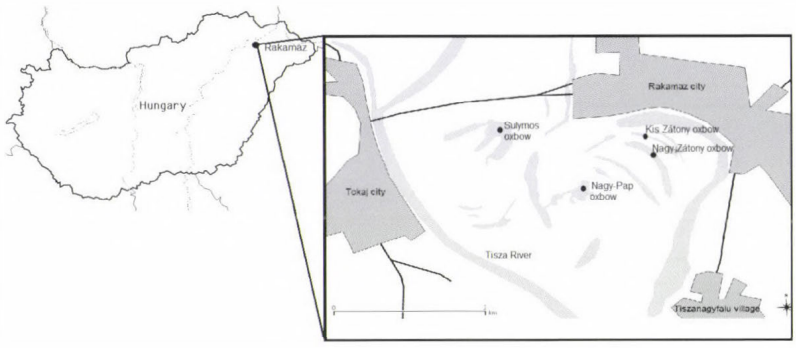

Fig. 1. Locations of oxbows.

We measured suspended solids from the original samples. For nitrite, nitrate, ortho-phosphate, carbonate, hydro-carbonate, carbon-dioxide and chloride concentration we used filtered samples. Water chemistry analysis was performed by the *USEPA* (1983) and *APHA* (2000) methods. For the assessment of quality, the *MSZ 12749* (1993) standard classification was used.

The local meteorological conditions of the study sites were based on the data from the websitwe of the MetNet Association (www.metnet.hu). The following parameters were used: rainfall, number of rainy days, and average temperature (*Table 1*). For our study, the results of four summer months were used. The water level of the Tisza was based on the data of the National Water Warning Service (www.hydroinfo.hu) (*Fig. 2*).

Table 1. Summary of meteorological data from May, June, July, and August (mean ± SE). The average temperature is the mean of the day, and the mean of rainfall is the average of the month

Year	Temperature (°C)	Rainfall (mm)	Number of raining days
2011	20 ± 2	68 ± 26	15 ± 7
2012	22 ± 3	47 ± 3	11 ± 4

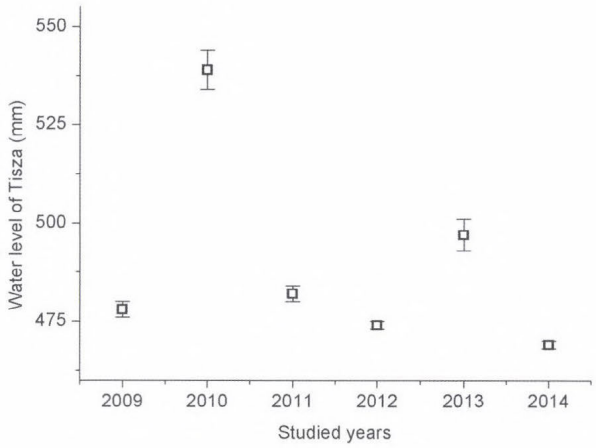

Fig. 2. The water level of the River Tisza (mean ± SE) over the past six years.

2.3. Drought index

To compare the years, a drought index (PaDI) was used. This index is a ratio of the mean temperature during the period from April to August and the rainfall from October to August (*Tsakiris* and *Vangelis,* 2004; *Tate* and *Gustard,* 2000). The following drought categories were used: PaDI < 4 represents a drought free year, 4 < PaDI < 6 a slight drought year, 6 < PaDI < 8 a moderate drought year, 8 < PaDI < 10 a medium moderate drought year, 10 < PaDI < 15 a severe drought year, 15 < PaDI < 30 a very severe drought year, and PaDI > 30 an extreme drought year.

2.4. Statistical analysis

SPSS/PC+ and Canoco for Windows statistical software packages were used during the calculations. Using redundancy analysis (RDA) we studied the correlation between the physico-chemical parameters of water and precipitation, and the temperature in the studied oxbows. canonical discriminant analysis (CDA) was used to study the physico-chemical parameters of oxbows. The physico-chemical parameters of the oxbows were compared by ANOVA, where the years and vegetation types were fixed factors. In the case of any significant differences, the Tukey's multiple comparison test was used to explore these significant differences.

3. Results

The correlation between the first component (RDA1) of redundancy analysis and the water physico-chemical parameters and weather parameters was 0.955, while for the second component (RDA2), the correlation was 0.562. The cumulative percentage variances were 31.3 (RDA1) and 7.5 (RDA2). In the case of water physico-chemical parameters and weather parameters, the relation was 79.5% (RDA1) and 19.1% (RDA2). For carbon dioxide, suspended solids, and carbonate, a positive correlation was found between concentration and rainfall and the number of rainy days (*Fig. 3*). A positive correlation was found between dissolved oxygen, water temperature, and the concentration of hydro carbonate, nitrate, pH, conductivity, and the average temperature (*Fig. 3*).

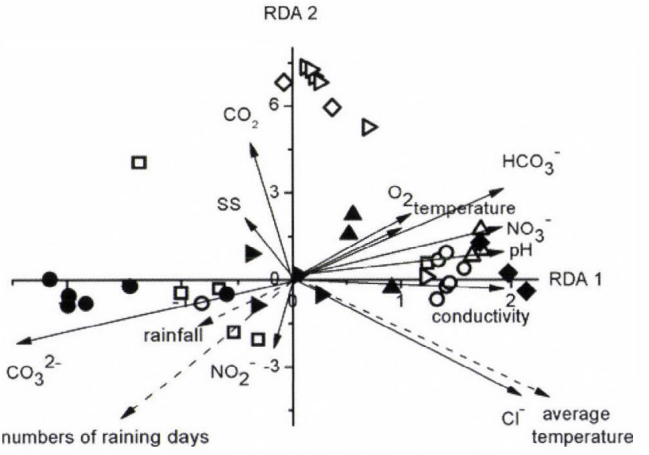

Fig. 3. Redundancy analysis biplot to show the interaction between the physico-chemical parameters of water and the meteorological conditions. Notations: solid arrow – physico-chemical parameters of water, dash arrow – precipitation and temperature.

Based on the physical and chemical parameters of water, the separation of the studied oxbows was similar in 2011 and 2012, based on the canonical discriminant analysis (*Fig. 4A-B*). There were differences between 2011 and 2012 only in the Nagy-Zátony oxbow. The canonical variance percentage was 99.6 in the first and 0.3 in the second axis, based on the 2011 data. The canonical variance percentage was 83.9 in the first and 10.0 in the second axis, based on the 2012 data.

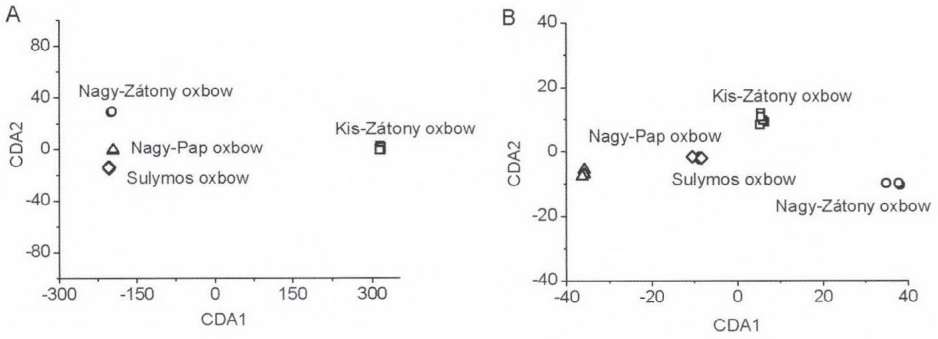

Fig. 4. Canonical discriminant biplot based on the physical and chemical parameters in the studied oxbows in 2011 (A) and 2012 (B).

Based on the vegetation types, the separation was also similar in both years (2011 and 2012). A slight change was found in the case of submersed vegetation types in 2011 and 2012 (*Fig. 5A-B*). The variance percentage was 93.3 in the first and 6.7 in the second axis in 2011. However, in 2012, the variance percentage was 70.8 in the first and 29.2 in the second axis.

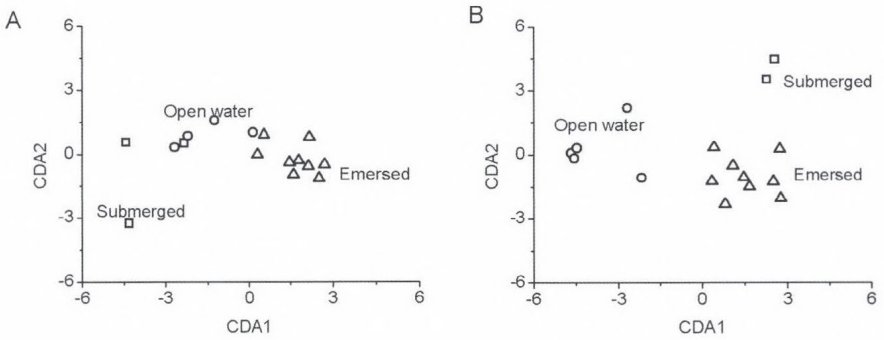

Fig. 5. Canonical discriminant biplot based on the physical and chemical parameters in the vegetation types in 2011 (A) and 2012 (B).

The result for the drought index was similar in the studied years. In 2011 the drought index value was 4.2, while in 2012 the value was 5.9. The index values suggest that each year was a slight drought year. In spite of this, when

comparing the water physico-chemical parameters, a difference was found between the years, but differences were not found among vegetation types using two-way ANOVA. There was a significant difference between the years in the water temperature, the suspended solid content, and the concentration of carbonate and chloride (*Table 2*). A significantly higher temperature, suspended solid content, and carbonate and chloride concentration were found in 2012 than in 2011. Significantly higher water temperatures were found in 2011 than in 2012 in the Kis-Zátony oxbow (t_5=–5.413, p=0.003), the Nagy-Pap oxbow (t_3=–52.200, p<0.001), and the Sulymos oxbow (t_8=–26.960, p<0.001). However, the water temperature did not differ between the two years (t_8=–26.960, p<0.001) in the Nagy-Zátony oxbow. The concentration of carbonate was significantly higher in 2012 than in 2011 in the Kis-Zátony oxbow (t_5=–5.541, p=0.003) and the Sulymos oxbow (t_8=–26.960, p<0.001). The concentration of hydro-carbonate was significantly higher in 2011 than in 2012 in the Kis-Zátony oxbows (t_5=7.194, p=0.001). In the Nagy-Zátony oxbow, the concentration of hydro-carbonate was significantly higher in 2012 than in 2011 (t_2=–111.449, p<0.001). Significantly higher concentrations of chloride-ion were observed in 2012 than in 2011 in the Nagy-Pap (t_3=–24.498, p<0.001) and Sulymos oxbows (t_8=–32.680, p<0.001). In the Nagy-Zátony oxbow, the concentration of chloride-ion did not differ between the years (t_2=–2.452, p=0.134) (*Table 3*). There was no significant difference among habitat types in their physical-chemical parameters.

Table 2. Results of ANOVA based on the physical and chemical parameters of years and vegetation types.

	year		vegetation type	
	F	***p***	**F**	***p***
temperature (°C)	10.294	0.003	0.232	0.795
pH	2.914	0.099	1.581	0.224
conductivity(μS/cm)	0.239	0.629	0.281	0.757
dissolved oxygen (mg/l)	0.855	0.363	0.526	0.597
suspended solid (mg/l)	11.286	0.002	0.426	0.657
carbonate (mg/l)	11.097	0.002	0.019	0.981
hydro carbonate (mg/l)	2.970	0.096	0.596	0.558
carbon dioxide (mg/l)	0.701	0.409	0.537	0.590
chloride (mg/l)	5.627	0.025	0.202	0.819
orthophosphate (mg/l)	0.109	0.744	0.421	0.661
nitrite (N mg/l)	2.296	0.141	0.630	0.540
nitrate (N mg/l)	1.712	0.201	0.396	0.677

Table 3. Physical and chemical parameters in the surface water of the studied oxbows (mean ± SD). Notations: n.m. means not measured, n.d. means not detected.

	Kis- Zátony oxbow		Nagy- Zátony oxbow		Nagy-Pap oxbow		Sulymos oxbow	
	2011	2012	2011	2012	2011	2012	2011	2012
temperature (°C)	25.1 ± 0.3	27.5 ± 0.2	22.6 ± 0.2	20.7 ± 0.1	18.8 ± 0.04	29.7 ± 0.2	18.4 ± 0.2	29.4 ± 0.3
pH	7.2 ± 0.01	7.4 ± 0.1	7.1 ± 0.2	7.1 ± 0.2	7.0 ± 0.1	9.0 ± 0.2	7.0 ± 0.1	7.9 ± 0.2
conductivity (µS/cm)	615 ± 8	699 ± 25	825 ± 7	875 ± 27	694 ± 4	558 ± 7	805 ± 57	621 ± 9
dissolved oxygen (mg/l)	8.2 ± 0.1	4.2 ± 0.4	n.d.	n.d.	2.4 ± 1.6	6.3 ± 0.7	8.2 ± 0.4	5.0 ± 0.5
suspended solid (mg/l)	7.4 ± 1.1	18.9 ± 2.3	10.1 ± 2.8	14.9 ± 4.5	15.4 ± 5.5	54.4 ± 12.9	16.8 ± 5.1	40.7 ± 12.9
carbonate (mg/l)	6.3 ± 3.0	27.1 ± 3.9	n.d.	4.5 ± 0.1	n.d.	n.d.	n.d.	3.8 ± 0.4
hydro carbonate (mg/l)	81 ± 1	5.0 ± 1.7	n.d.	102 ± 3	n.d.	n.d.	n.d.	79.4 ± 0.9
carbon dioxide (mg/l)	28.1 ± 2.4	35.8 ± 4.2	22.5 ± 1.6	42.9 ± 7.4	22.7 ± 2.3	n.d.	13.1 ± 3.1	5.7 ± 1.1
chlorine (mg/l)	25.5 ± 2.2	15.7 ± 1.4	13.6 ± 1.9	18.5 ± 1.0	n.d.	24.3 ± 2.5	n.d.	24.8 ± 2.5
orthophosphate (mg/l)	0.2 ± 0.01	0.1 ± 0.04	0.1 ± 0.01	0.1 ± 0.01	0.1 ± 0.01	0.2 ± 0.04	0.1 ± 0.03	0.2 ± 0.01
nitrite (N mg/l)	0.05 ± 0.03	0.02 ± 0.01	0.01 ± 0.001	0.01 ± 0.01	0.01 ± 0.01	0.03 ± 0.02	0.2 ± 0.1	0.002 ± 0.001
nitrate (N mg/l)	0.2 ± 0.03	0.02 ± 0.01	0.1 ± 0.01	0.05±0.00	0.05±0.01	0.11±0.07	0.02±0.01	0.1 ± 0.01

4. Discussion

The chemical composition of lakes and oxbows is determined by natural and anthropogenic factors; these include geological, climatic, and biological factors (*Moiseenko et al.,* 2013). Many papers have reported the effects of climatic and weather factors on oxbows (*Cullum et al.,* 2006; *Hunyady,* 2010, *Zhao et al.,* 2013). Earlier studies demonstrated that dry seasons and dry years cause worse water quality, similarly to our findings (*Pesce* and *Wunderlin,* 2000, *Vega et al.,* 1998).

The quality of the Kis-Zátony oxbow and the Nagy-Pap oxbow were good, while the Nagy-Zátony oxbow and the Sulymos oxbow were contaminated in 2011, based on the conductivity findings (*MSZ*,1193). A similar conductivity was found in the second year – 2012 – in each oxbow, except for the Sulymos oxbow, where the quality was good in 2012. *Michalska-Hejduk et al.* (2009) found similar conductivity values and the use of their classification shows that the oxbows we studied are ion-rich.

Of the chemical parameters, dissolved oxygen is an important component of the surface water (*Michalska-Hejduk et al.,* 2009). In our study, based on the concentration of dissolved oxygen, the quality of the Kis-Zátony and Sulymos oxbows was excellent in 2011. The quality of the Nagy-Pap oxbow was contaminated in 2011, but in 2012 it was good. Concentrations of dissolved oxygen in the Kis-Zátony and Sulymos oxbows were contaminated in 2012. Anthropogenic activities were not detected in the area of this oxbow; thus, the lower oxygen concentration is probably the result of a decreasing water level. The water level decrease may result in higher organic matter, which has a direct effect on the dissolved oxygen concentration in the water ecosystem (*Michalska-Hejduk et al.,* 2009).

Kröger et al. (2013) found a positive correlation between the concentration of suspended solids and wind speeds. They demonstrated that turbidity has an indirect effect on suspended solid concentrations (*Kröger et al.,* 2013). Similarly to their findings, our results also indicated that weather parameters have an effect on the concentration of suspended solids. We found higher results in 2012 than in 2011 in every oxbow.

The concentrations of anions, including carbonate, hydro carbonate, chloride, nitrite, and nitrate are dependent on atmospheric deposition and conditions, as it is shown in the redundancy analysis. Based on the nitrite concentrations, the quality of the Nagy-Zátony, Nagy-Pap, and Sulymos oxbows was good, while the quality of the Kis-Zátony oxbow was tolerable in 2011. Nevertheless, in 2012, the water quality of the Kis-Zátony oxbow improved to the same level as that of the other oxbows. This could be explained by higher microbial activity, which may have caused the higher temperature and lower water level in this year (*Davidson et al.,* 1998). Similarly to the earlier finding, the conductivity is related to alkalinity which may regulate the aquatic

production (*Zablotowicz et al.,* 2010). The concentration of orthophosphate was similar among the oxbows and also between years. Water quality was contaminated in the Kis-Zátony oxbow, based on orthophosphate concentrations in 2011. The other oxbows were tolerable in 2011. In the next year, the quality of water was contaminated in the Nagy-Pap and Sulymos oxbows, while in the Nagy-Zátony and Kis-Zátony oxbows it was tolerable. In spite of earlier findings (*Moiseenko et al.,* 2013), we did not find an increase in the orthophosphate concentration, despite the increase in the daily temperature.

Unlike earlier studies (*Lukács et al.,* 2009, 2011) we did not find any differences between the vegetation types based on the physico-chemical parameters of water. *Lukács et al.* (2009) demonstrated that nitrogen and carbonate were the most important variables for vegetation development. *Lukács et al.* (2011) also observed that among water chemical parameters, calcium, chemical oxygen demand, nitrite, magnesium, and chloride-ion were important in differentiating the vegetation. Our study showed that the physico-chemical parameters of water did not differ among vegetation types, which was probably caused by the low level of the water.

In spite of the poor state of the oxbows which was visible in the field, differences were not found between the weather parameters in the years under investigation. Based on the drought index, each year experienced a slight drought, although with some parameters, such as water temperature, suspended solids content, and the concentration of carbonate and chloride, significant differences between the years were found. Using the water level data for the River Tisza, the results show that in the past years the water level of the river has changed remarkably.

5. Conclusions

We demonstrated that precipitation and temperature influenced the open-water surface area, the water level, and the physico-chemical parameters of oxbows. These oxbows were connected to the main river only during floods; thus, the water level of the main river also had a remarkable effect on the quality of oxbows. The physico-chemical parameters indicated that the anthropogenic activities did not cause the degradation in the state of the oxbows. Our findings suggest that the degradation of the water quality of the oxbows is only slightly influenced by precipitation and temperature. The degradation depends on the water level of the main river, and the frequency and duration of the flooding.

Acknowledgements: This research was supported by the TÁMOP 4.2.1./B-09/1/KONV-2010-0007, and TÁMOP- 274 4.2.2/B-10/1-2010-0024 projects, the European Union and the State of Hungary, co-financed by the European Social Fund. E. Simon was supported by the TÁMOP-4.2.2.A-11/1/KONV. The study was supported by the SROP-4.2.2.B-15/1/KONV20150001 project.

References

APHA, 2000: American Public Health Association, Washington (DC).

Barendregt, A., and *Bio, A.F.M.*, 2003: Relevant variables to predict macrophyte communities in running waters. *Ecol. Modell. 160,* 205–217.

Bond, N.R., Lake, P.S., and *Arthington, A.H.*, 2008: The impacts of drought on freshwater ecosystems: an Australian perspective. *Hydrobiologia 600*, 3–16.

Bornette, G., and *Puijalon, S.*, 2011: Response of aquatic plants to abiotic factors: a review. *Aquat. Sci. 73*, 1-14.

Cook, C.D.K., 1996: Aquatic Plant. Academic Publishing, Amsterdan/New York.

Cullum, R.F., Knight, S.S., Cooper, C.M., and *Smith, S.*, 2006: Combined effects of best management practices on water quality in oxbow lakes from agricultural watersheds. *Soil. Till. Res. 90,* 212–221.

Davidson, E.A., Belk, E., and *Boone, R.D.*, 1998: Soil water content and temperature as independent or confounded factors controlling soil respiration in a temperate mixed hardwood forest. *Glob. Change. Biol. 4,* 217–227.

Fink, D.F., and *Mitsch, W.J.*, 2007: Hydrology and nutrient biogeochemistry in a created river diversion oxbow wetland. *Ecol. Eng. 30*, 93–102.

Frodge, J.D., Thomas, G.L., and *Pauley, G.B.*, 1990: Effects of canopy formation by floating and submergent aquatic macrophytes on the water quality of two shallow Pacific Northwest lakes. *Aquat. Bot. 38*, 231–248.

Georgi, F.X., and *Pal, J.*, 2004: Mean, interannual variability and trends in a regional climate change experiment over Europe. II: climate change scenarios (2071–2100). *Clim. Dynam. 23*, 839–858.

Heegaard, E., Birks, H.H., Gibson, C.E., Smith, S.J., and *Wolfe-Murphy, S.*, 2001: Species–environmental relationships of aquatic macrophytes in Northern Ireland. *Aquat. Bot. 70,* 175–223.

Hunyady, A., 2010: Projected climate change effects on water level of an oxbow. *Phys. Chem. Earth. 35*, 70–75.

Kröger, R., Dibble, E.D., Brandt, J.R., Fleming, J., Huenemann, T.W., Stubbs, R.B., Prevost, J.D., Tietjen, T.E., Littlejohn, K.A., and *Pierce, S.C.*, 2013: Spatial and temporal changes in total suspended sediment concentrations in an Oxbow Lake from implementing agricultural landscape management practices. *River Res. Appl. 29*, 56–64.

Lukács, B.A., Dévai, G., and *Tóthmérész, B.*, 2011: Small scale macrophyte-environment relationship in an oxbow-lake of the Upper-Tisza valley (Hungary). *Community Ecol. 12*, 259–263.

Lukács, B.A., Dévai, Gy., and *Tóthmérész, B.*, 2009: Aquatic macrophytes as bioindicators of water chemistry in nutrient rich backwaters along the Upper-Tisza river (in Hungary). *Phytocoenologia 39*, 287–293.

Michalska-Hejduk, D., Kopeć, D., Drobniewska, A., and *Sumorok, B.*, 2009: Comparison of physical and chemical properties of water and floristic diversity of oxbow lakes under different levels of human pressure: A case study of the lower San River (Poland). *Int. J. Ecohydrol. Hydrobiol. 9*, 183–191.

Michener, W.K., Blood, E.R., Bildstein, K.L., Brinson, M.M., and *Gardner, L.R.*, 1997: Climate change, hurricanes and tropical storms, and rising sea level in coastal wetlands. *Ecol. Appl. 7*, 770–801.

Moiseenko, T.I., Skjelkvale, B.L., Gashkina, N.A., Shalabodov, A.D., and *Khoroshavin, V.Y.*, 2013: Water chemistry in small lakes along a transect from boreal to arid ecoregions in European Russia: Effects of air pollution and climate change. *Appl. Geochem. 28*, 69–79.

MSZ, 1993: MSZ 12749. Hungarian Standard Association.

Nguyen, H.L., Braun, M., Szalóki, I., Baeyens, W., Van Grieken, R., and *Leemarkers, M.* 2009 Tracing the metal pollution history of the Tisza River through the analysis of a sediment depth profile. *Water Air Soil Pollut. 200*, 119–132.

Oertli, B., Céréghino, R., Hull, A., and *Miracle, R.*, 2009 Pond conservation: from science to practice. *Hydrobiologia 634*, 1–9.

Palmer, M.A., Lettenmaier, D.D., Poff, N.L., Postel, S.L., Richter, B., and *Warner, R.*, 2009: Climate Change and River Ecosystems: Protection and Adaptation Options. *Environ. Manage. 44*, 1053–1068.

Pesce, S.F., and *Wunderlin, D.A.*, 2000: Use of water quality indices to verify the impact of Córdoba City (Argentina) on Suquía River. *Water Res. 34*, 2915–2926.

Tate, E.L., and *Gustard, A.*, 2000: Drought definition: A hydrological perspective. In (eds.: *Voght, J.V.*, *Somma, F.*) Drought and drought mitigation in Europe. Kluwer Academic Publishers, Dordrecht.

Tsakiris, G., and *Vangelis, H.*, 2004: Towards drought watch system based on spatial SPI. *Water Resour. Manag. 18*, 1–12.

USEPA, 1983: United States Environmental Protection Agency, Washington (DC).

Varga, K., Dévai, G., and *Tóthmérész, B.*, 2013: Land use history of a floodplain area during the last 200 years in the Upper-Tisza region (Hungary). *Reg. Environ. Change. 13*, 1109–1118.

Vega, M., Pardo, R., Barrado, E., and *Deban, L.*, 1998: Assessment of seasonal and polluting effects on the quality of river water by exploratory data analysis. *Water Res. 32*, 3581–3592.

Winter, T.C., 2000: The vulnerability of wetlands to climate change: a hydrologic landscape perspective. *J. Am. Water Resour. As. 36*, 305–311.

Zablotowicz, R.M., Zimba, P.V., Locke, M.A., Knight, S.S., Lizotte, R.E., and *Gordo, R.E.*, 2010: Effects of land management practices on water quality in Mississippi Delta oxbow lakes: Biochemical and microbiological aspects. *Agr. Ecosyst. Environ. 139*, 214–223.

Zhao, Y., Xia, X., and *Yang, Z.*, 2013: Growth and nutrient accumulation of *Phragmites australis* in relation to water level variation and nutrient loadings in a shallow lake. *J. Environ. Sci. 25*, 16–25.

IDŐJÁRÁS

Quarterly Journal of the Hungarian Meteorological Service
Vol. 120, No. 3, July – September, 2016, pp. 315–329

Comparison of simulated and objectively analyzed distribution patterns of snow water equivalent over the Carpathian Region

Hristo Chervenkov* and **Kiril Slavov**

National Institute of Meteorology and Hydrology – Bulgarian Academy of Sciences
66, Tsarigradsko Shose blvd, Sofia 1784, Bulgaria
E-mails:hristo.tchervenkov@meteo.bg, kiril.slavov@meteo.bg

**Corresponding author*

(Manuscript received in final form February 8, 2016)

Abstract—Snow is a very important component of the climate system which controls surface energy and water balances. Its high albedo, low thermal conductivity, and properties of surface water storage impact regional to global climate. The various properties characterizing snow are highly variable and thus have to be determined as dynamically active components of climate. However, on large spatial scales, the properties of snow are not easily quantified either from numerical modeling or observations. Thus, it is vital to estimate the model performance in comparison with consistent datasets of assimilated data. Snow water equivalent data simulated with four different model configurations of the RegCM climate model over Central Europe for a time window of 10 consecutive winters are compared with the objective analysis data from the high-resolution CARPATCLIM database on monthly and seasonal basis. The CARPATCLIM snow water equivalent data are also modeled, but based on the gridded daily observation of the temperature, precipitation, and relative humidity. The results reveal good commensurability over the bigger, mostly flat part of the domain, however, they show significant discrepancies, mainly overestimation, over the Carpathian Region.

Key-words: *snow water equivalent, numerical simulation, RegCM*

1. Introduction

Snow is a very important component of the climate system which controls surface energy and water balances, and it is the largest transient feature of the land surface according *Yang et al.* (2001). It has an effect on atmospheric circulation through changes to the surface albedo, thermal conductivity, heat capacity, and aerodynamic roughness, as it has been documented in numerous

observational and modeling studies (e.g., *Barnet et al.* 1989, *Gong et al.* 2003). The snow properties of the surface water storage control the availability of water in many ecosystems and to a sixth of the world's population (*Clifford,* 2010). Therefore, it is vital that snow is properly represented in geophysical models if we want to understand and make predictions of weather, climate, carbon cycle, flooding, and drought.

The various properties characterizing snow are highly variable and thus have to be determined as dynamically active components of climate. These include the snow depth (h_s) snow water equivalent (*SWE*), density, and snow cover area (*SCA*). To understand global snow water trends in the necessary depth, the most fundamental metric to assess is *SWE*, with h_s as a close second. However, on large spatial scales, the properties of snow are not easily quantified either from modeling or observations. For example, station based snow measurements often lack spatial representativeness, especially in regions, where the topography, vegetation, and overlaying atmosphere produce considerable heterogeneity of the snow-pack distribution (*Liston,* 2004). Thus, despite the weaknesses of the land surface models, the quantitative assessment of the snow properties by the means of the numerical simulation is a pragmatic approach for obtaining of the spatial and temporal continuous distribution of the snow pack. The utilization of regional climate models (RCMs) in the Bulgarian National Institute of Meteorology and Hydrology is within the framework of the common effort for composition of detailed picture of the snow cover and its dynamics over Southeast Europa with focal point to the central part of the Balkan peninsula. So, the latest version of the well-known RegCM regional climate model is applied for quantitative estimation of many surface variables, including *SWE*, for 14 consecutive winters between 2000 and 2013, and the subset 2000–2009 is used in the present study. As in many validation studies, however here even in greater extent, part of the difficulties in exploring the simulation ability issue of the model is rooted in the lack of validation data for small-scale features and reliable measurements. It is clear that datasets as the mentioned model simulation with such time gaps are highly insufficient for any model validation study. Nevertheless, hence such procedure is often treated in similar numerical experiments as a necessary (first) step in verification/model performance evaluation, such comparisons are preformed and the results are described (*Chervenkov et al.,* 2015). Main conclusion from this work is that the comparisons of the measurements with the model output from all runs yield generally similar results. Further, the overall (i.e., over the whole time span) biases are acceptable, but, however, with large discrepancies in the day-by-day comparisons, which is typical for climate modeling studies.

Satellite earth snow observation products have the needed spatial and temporal consistency, which allows comparisons with model output over continuous area and time frames. So, utilizing satellite data is a significant step ahead in the quantitative snow cover assessment. Satellite retrieval estimates,

however, require inversion algorithms to relate raw signals recorded at the satellite to physical properties of the land surface, and these inverted estimates can contain errors and biases (*Hancock et al.,* 2013). Although among the other products, *SWE* has been proven to be more problematic (*Hancock et al.,* 2013), especially for wet snow and during melt, which is a typical case in southeast Europe, the common treatment of satellite data and model results has been already performed. The gridded digital maps of the Globsnow SWE product (http://www.globsnow.info/swe/GlobSnow_SWE_product_readme_v1.0a.pdf) are compared with the simulation output for the whole 14-year period on monthly basis (*Chervenkov et al.,* 2016). Certain drawbacks of the Globsnow product can point the absence of data for mountainous regions, which, at least from hydrological point of view, are important.

Another informational sources, suitable for assessment studies are the products of objective analysis of measurements. Depending on the leading physical and mathematical concept, involved data streams and, correspondingly, the incorporated processing methods the can vary greatly. The primary importance feature of these products is the data quality and, second, at least from the end-user point of view, the form of the final product, which is a timely continuous digital map of gridded datasets. The relatively long (in climatological sense, i.e., in order of decades) temporary extend, acceptable horizontal resolution, presence of subsets for various variables, and, not at least, the free-of-charge availability of most of these products make it a preferable tool in many applications, as the presented verification study here. Being typical member of this group, the CARPATCLIM dataset is a motivated choice for testing the model performance, and thus this paper, which, in some extend, is the continuation of *Chervenkov et al.* (2015), is dedicated to the comparison of the simulated values of *SWE* with the analyzed ones.

The paper is organized as follows: Short description of the CARPATCLIM database, the used version of the RCM RegCM, and the methodological approach are placed in the first chapter. The performed calculations and the obtained results are described and visualized in the second chapter. Summarizing remarks and the main conclusions are listed in the last chapter.

2. Concept and methodology

The CARPATCLIM database is the result of the common effort of 10 national institutions from 9 Central European countries as well as the Joint Research Centre and the Institute for Environment and Sustainability to overcome the differences caused by the national specification in the meteorological data sampling and management. According to the product description, the main aim of the project is to improve the basis of climate data in the Carpathian Region for applied regional climatological studies such as a Climate Atlas and/or

drought monitoring, to investigate the fine temporal and spatial structure of the climate in the Carpathian Mountains and the Carpathian Basin with unified methods. Manifestation of the success of the project is the freely available, high resolution gridded database for the Larger Carpathian Region (LCR) (see *JRC report* 2010 and the references therein). For ensuring the usage of the largest possible station density, the processing were implemented by the countries themselves using the same methods and software. The commonly used methods were the MASH (Multiple Analysis of Series for Homogenization; *Szentimrey,* 2011) procedure for homogenization, quality control, and completion of the observed daily data series; and the MISH (Meteorological Interpolation based on Surface Homogenized Data Basis; *Szentimrey* and *Bihari,* 2007) for gridding of homogenized daily data series. The harmonization of the datasets was carried out by the exchange of the near border station data of the neighboring countries before and after homogenization.

The evaluation of measured snow cover records at the level of CARPATCLIM area has led to the conclusion that there is a lack of reliable and continuous measured data at the level of the meteorological stations of the region, and it is insufficient for estimating connected variables such as *SWE* and snow depth. This is a chronic problem in many regions of the world, in particular in the Balkan peninsula adjacent to the larger Carpathian Region, as shown in *Chervenkov et al.* (2015). In order to address this gap, a snow cover model employed operationally at the Austrian Central Institute for Meteorology and Geodynamics (ZAMG) was applied to generate a 0.1° latitude/longitude grid of daily mean snow cover and corresponding estimated water equivalent and snow depth simulations. The applied model is based on pre-finished CARPATCLIM grids of mean air temperature, precipitation sum, and relative air humidity. They are processed by the snow cover model regarding three main parts: accumulation of snow cover, ablation of snow cover, and transformation of *SWE* to snow depth. The reader can find more detailed description at http://www.carpatclim-eu.org/docs/computation/SNOW.pdf. The database contains the gridded distributions of 16 variables with horizontal resolution 0.1°×0.1° for domain with longitudinal extent 17 to 27 degrees north and latitudinal extent 44 to 50 degrees east for the period 1961–2010 on diurnal and monthly basis.

RCMs have been developed and extensively applied in the recent decade for dynamically downscaling of the coarse resolution information from different sources, such as global circulation models (GCMs) and reanalysis, for different purposes including past climate simulations and future climate projections. This widely used and productive approach is applied here. The main simulation tool is the freely available latest version of the regional climate model of the International Center of Theoretical Physics in Italy (ICTP). RegCM4 is a 3-dimensional, sigma-coordinate, primitive equation RCM with dynamical core based (version 2 and later) on the hydrostatic

version of the NCAR-PSU Mesoscale Model 5 (MM5) (*Grell et al.,* 1994). The radiative transfer package is taken from the Community Climate Model version 3 (CCM3) (*Kiehl et al.,* 1996). The large-scale cloud and precipitation computations are performed by the Subgrid Explicit Moisture Scheme (SUBEX, *Pal et al.,* 2000), and the land surface physics are performed according to the Biosphere-Atmosphere Transfer Scheme (BATS, *Dickinson et al.,* 1993). The adopted convective scheme for the RCM simulations in the present study is the Grell scheme (*Grell,* 1993)) with the Arakawa and Schubert (*Arakawa* and *Schubert,* 1974) closure assumption. Main manifestation of the flexibility of the modern RCMs, including RegCM4, is the possibility for selection among different initial and boundary conditions datasets (ICBC), parameterization schemes/modules within the model, various constants and closure assumptions, etc., combining them in practically countless model setups. Obviously, the simulation output from such model setups will differ from one another, and, more or less, from the "reality". Thus, multiple runs with different model setups/configurations (further: modcons) have to be performed accenting the inspection of the modules that have major role is the proper description of the considered variables. There is overall agreement in the scientific community that the ICBC plays the most important role in the model performance (see *Xue et al.,* 2014 for details). Although there are numerous tests with different reanalysis data, which are considered as better ICBC compared to those produced by GCMs, there is no single reanalysis data set yielding the best results in every region and/or every season. We have performed simulations with the two most popular and widely used reanalysis datasets: the ERA-Interim of the European Centre for Medium-Range Weather Forecasts (ECMWF) (*Dee et al.,* 2011) with horizontal resolution 1.5°×1.5° for RegCM simulations, noted further as EIN15 and the reanalysis 2 of the USA National Centers for Environmental Predictions and the National Center for Atmospheric Research (NCEP/NCAR) (*Kanamitsu et al.,* 2002) with horizontal resolution 2.5°×2.5°, noted further as NNRP2. It is physically reasonable also to expect, that the module, which describes the surface processes and the interactions with the under- and overlaying soil and atmospheric layers, namely the land surface model, plays relevant role especially in the numerical treatment of the snow cover. A major addition to RegCM4 is the option to use the Community Land Model (CLM), version 3.5. Compared to BATS, CLM is a more advanced package (and, as a result, it is computationally heavier), which is described in detail in *Oleson et al.,* (2004, 2008). It uses a series of biogeophysically based parameterizations to describe the land-atmosphere exchanges of energy, momentum, water, and carbon. So, combining the two ICBC datasets with the two land surface models, four modcons are designed: ERAIN/BATS, ERAIN/CLM, NNRP2/BATS, and NNRP2/CLM, noted further as EB, EC, NB, NC.

The model domain is centered over Bulgaria and consists of 72×77 20 km×20 km gridcells and covers the CARPATCLIM one without the most northern latitudinal band in width 1.4° only. The simulation period is from November 1 till March 31 for 14 consecutive years between 2000 and 2014. The row model output is the gridded distribution of the *SWE* on a 6-hourly basis (i.e., at 00, 06, 12, and 18 UTC).

Traditional method to judge the model performance is to assess the degree of agreement between the model output and the analyzed data using well elaborated statistical methods, among them the most frequently applied is the calculation of statistical scores, which is widely used in validation studies.

3. Performed calculations and obtained results

Due to the practical absence of horizontal mixture processes, specific feature of the snow cover is the relatively high heterogeneity (in comparison to the atmospheric lower-level parameters). Thus, even on small distances in order of couple of kilometers, considerable differences in the snow properties can be observed, and the inspection of the CARPATCLIM *SWE* dataset confirms this peculiarity: the differences in some months and regions even for neighboring gridcells can be more than an order of magnitude. Hence, is reasonable to expect that the adequate resolution of the analysis and the model data, and the comparability of both of them is vital. As long as the resolution of the CARPATCLIM (roughly 10 km) is properly selected, the RegCM resolution of 20 km for the current implementation seems insufficient. Additionally, intending initially to obtain the mainly overall picture for a significantly larger domain, the subgridding option was not switched on in the model simulations, which is not applicable for the CLM option. Since interpolation procedures can not reveal smaller scale features than those presented in the original data, and generally all of these leads to smoothing of the field, is methodologically correct to interpolate the finer CARPATCLIM grid to the RegCM one and not vice versa. This is done in the most natural way, by simple spatial averaging of every neighboring 2×2 gridcells with definite values.

Although in some years and gridcells there is already snow cover before the 1st of November, the start of the model simulations at this date ensures generally the practical absence of significant snow pack over the bigger part of the domain. Starting relevantly later would cause systematic underestimations. Ten winters of the period 2000–2009 were taken in consideration in this study.

Usually January is treated as the representative month for the corresponding winter. The inspection of the CARPATCLIM atlas (available at http://www.carpatclim-eu.org/pages/atlas/), however, reveals that the snow cover over the bigger part of the domain for most of the considered years is thicker in February, and thus the average *SWE* for this month is the first

considered climate characteristics. The second one is the monthly weighted average *SWE* for the winter, namely December, January, and February. Each month is weighted with the number of days per month.

Hence main aim of this work is to present the comparison between the simulated and analyzed *SWE*, rather than the actual *SWE* climatology, only an indicative sight is given here *Figs. 1* and *2*. It is worth to emphasize, however, its spatial and temporal variation – generally speaking, the *SWE* in the plains is roughly 10–50 mm, when over the Carpathian ridge it is up to 150–200 mm.

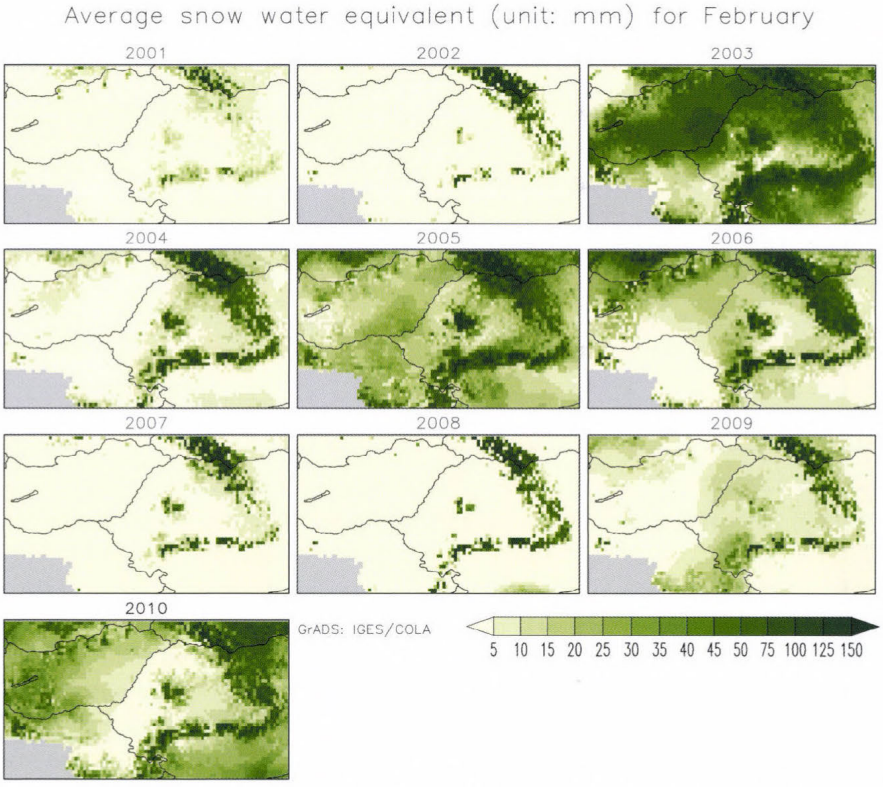

Fig. 1. Monthly average CARPATCLIM *SWE* (unit: mm) distribution for February in the original grid.

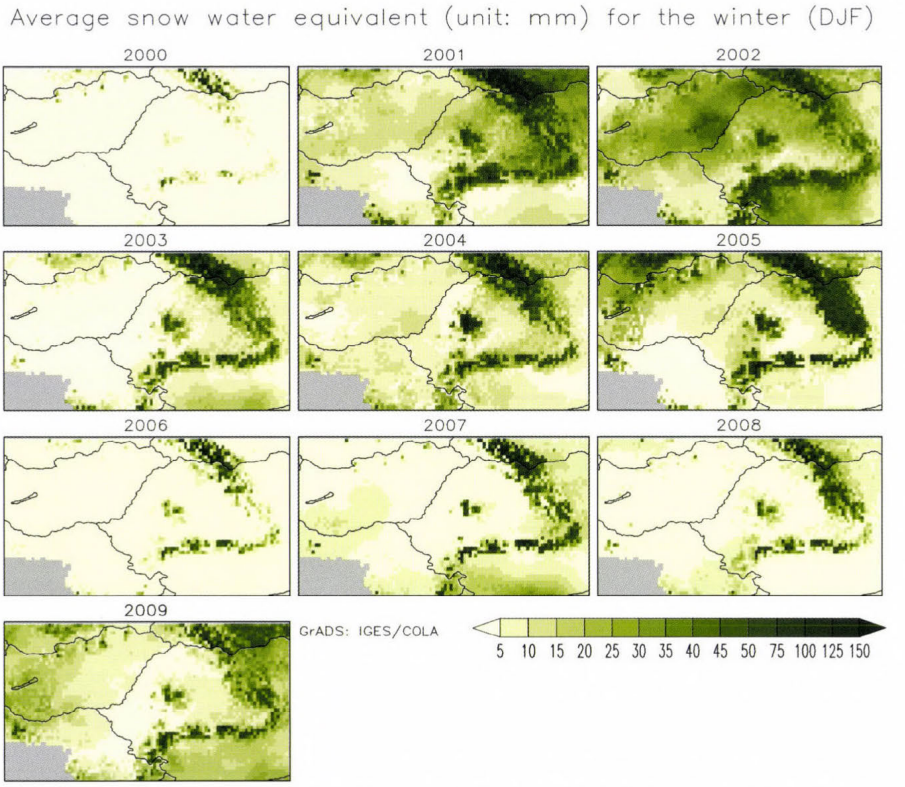

Fig. 2. Winter average (i.e., monthly weighted for December, January, and February) CARPATCLIM *SWE* (unit: mm) distribution in the original grid.

Keeping in mind the above described reasons about the resolution choice and intending to facilitate the comparisons, the modeled data are interpolated to the new, coarser CARPATCLIM 0.2°×0.2° grid. The files with the row RegCM output are handled with the powerful and easy-to-use operator suite climate data operator (*CDO,* 2015). The postprocessing of the model and analysis data is performed with purposely developed own programs, all tasks are automated via Linux bash scripts, and the visualization is done with GrADS scripts.

Most traditional approach for estimation of the departure of the model results from the analysis is applied: the absolute difference between the CARPATCLIM *SWE* and the modeled one (i.e., BIAS) for every winter month and for the monthly weighted winter average are calculated, but, due to the above commented relative importance, only those for February (in *Figs. 3–6*) and for the seasonal mean (in *Figs. 7–10*) are presented.

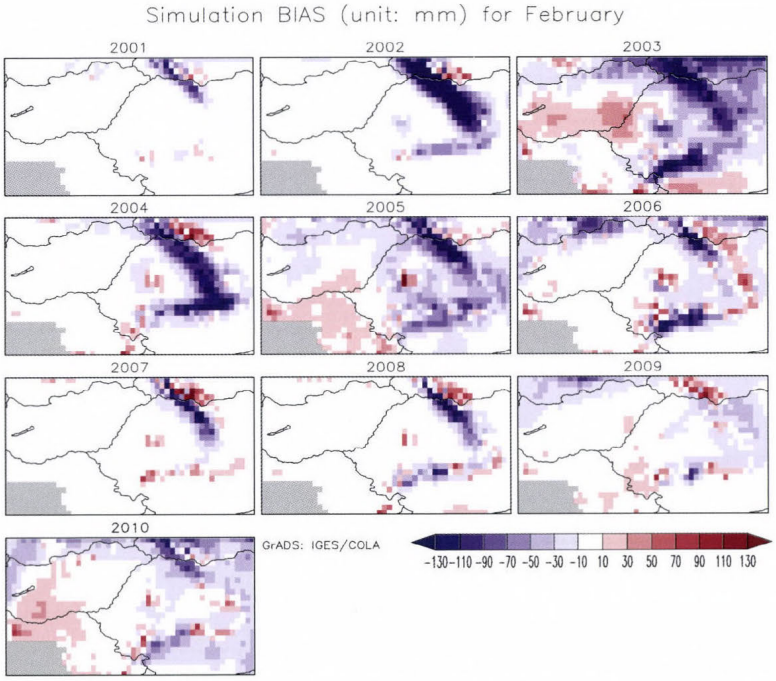

Fig. 3. BIAS (unit: mm) for the modcon 'EB' for February average in the reduced CARPATCLIM grid.

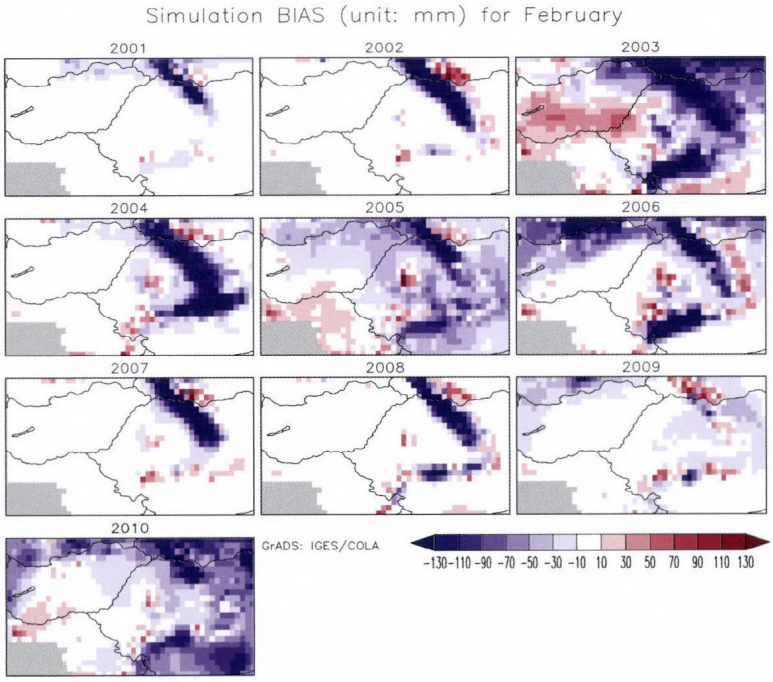

Fig. 4. Same as in *Fig. 3*, but for the modcon 'EC'.

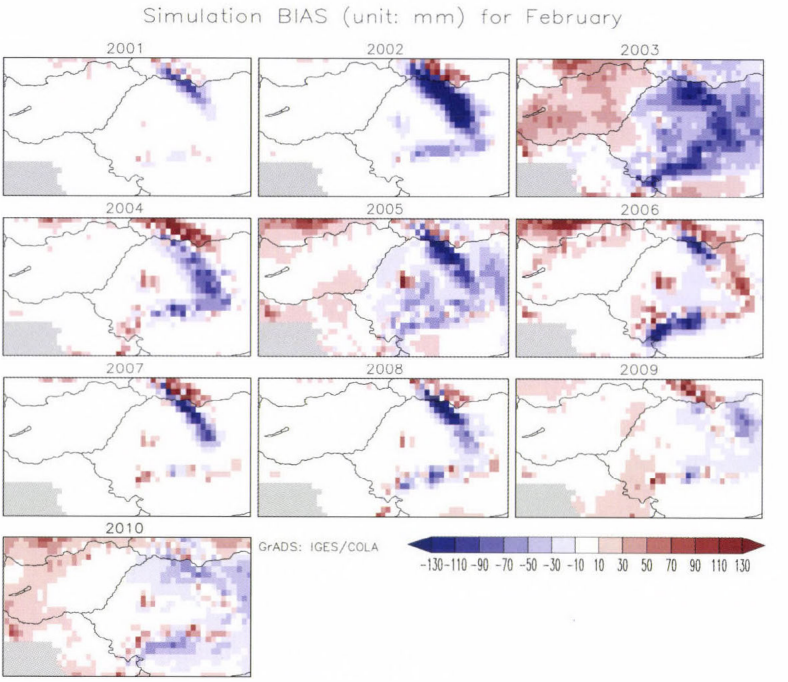

Fig. 5. Same as in *Fig. 3*, but for the modcon 'NB'.

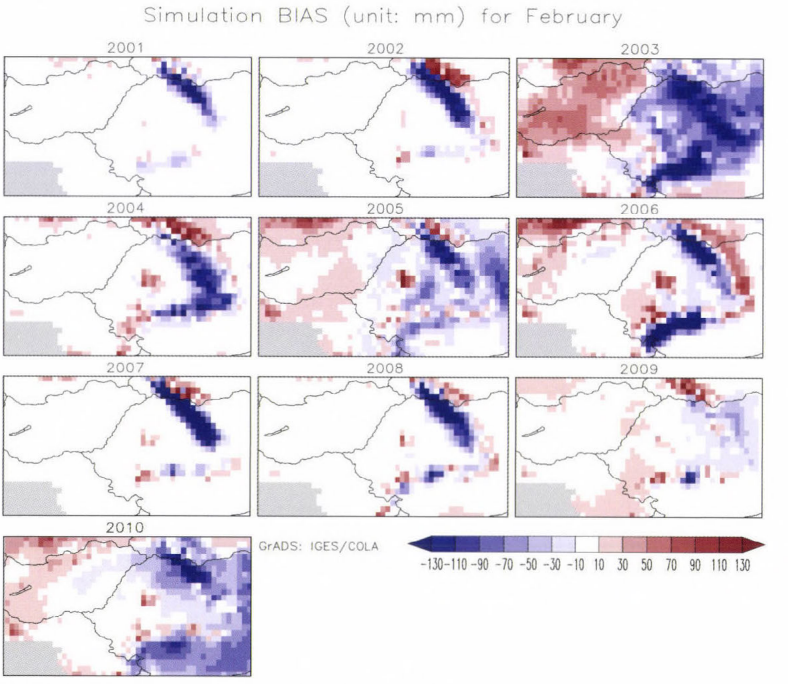

Fig. 6. Same as in *Fig. 3*, but for the modcon 'NC'.

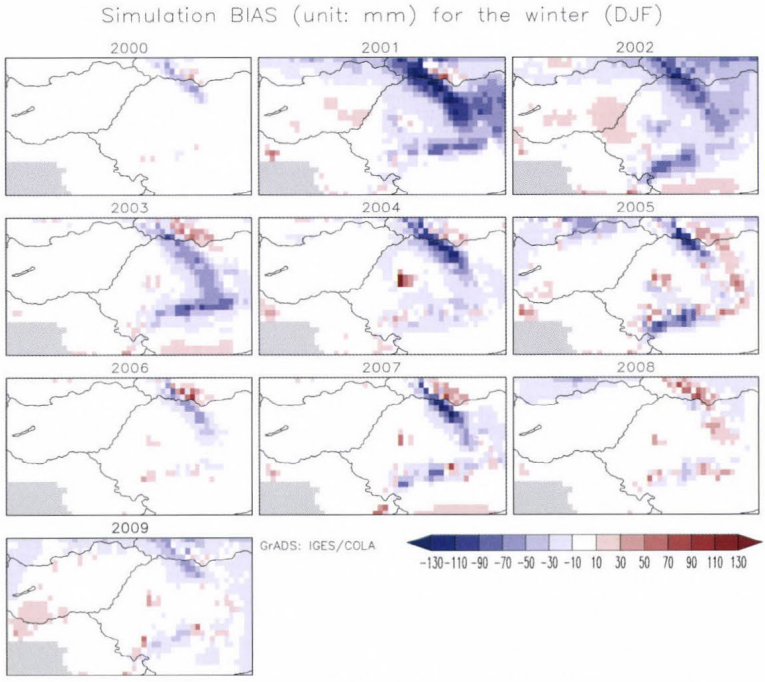

Fig. 7. BIAS (unit: mm) for the modcon 'EB' for the winter average in the reduced CARPATCLIM grid.

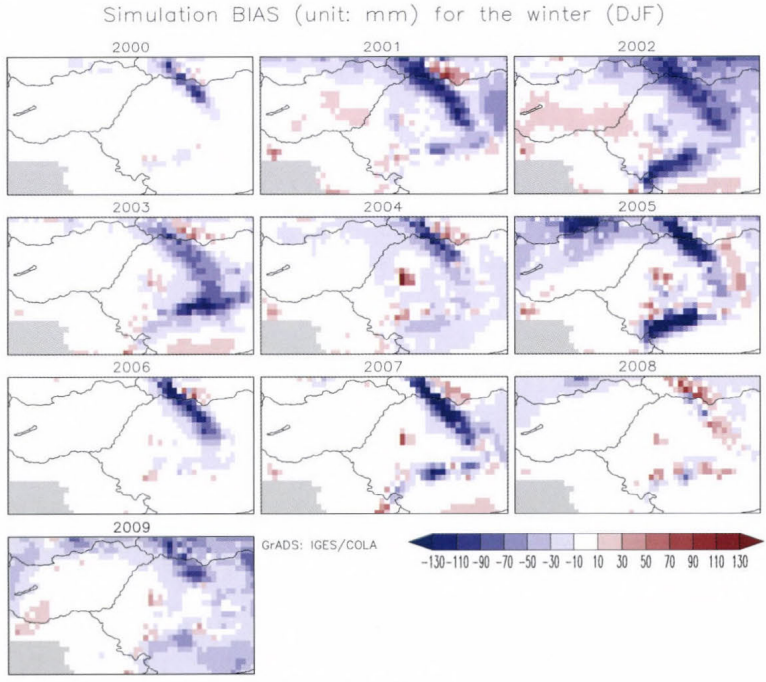

Fig. 8. Same as in *Fig. 7*, but for the modcon 'EC'.

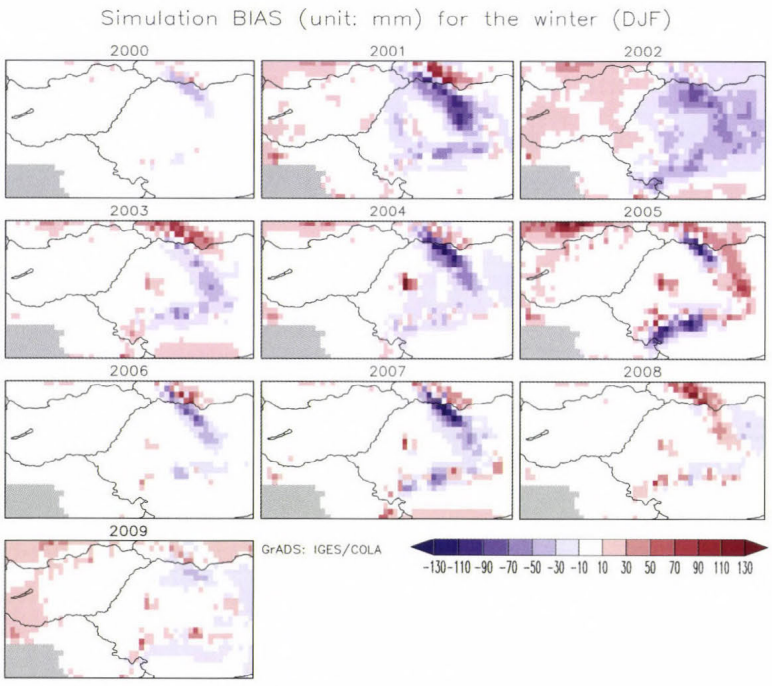

Fig. 9. Same as in *Fig. 7*, but for the modcon 'NB'.

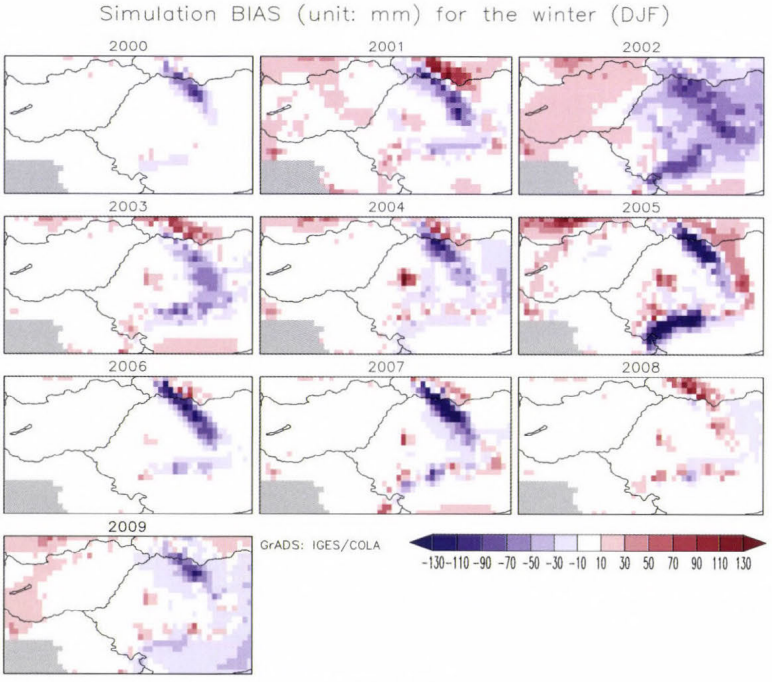

Fig. 10. Same as in *Fig. 7*, but for the modcon 'NC'.

The BIAS is formulated as:

$$BIAS = \frac{1}{N} \cdot \sum_{i=1}^{N} (O_i - M_i), \tag{1}$$

where O_i are the observed, in this case the CARPATCLIM values, M_i are the modeled ones and N is the number of pairs (comparisons).

Hence the spatial variability of the BIAS is significant, it is important to provide also the root mean square error (RMSE) averaged over the domain index, presented in *Table 1*. Using the notation of Eq. (1), the RMSE is equal to:

$$RMSE = \sqrt{\frac{1}{N} \sum_{i=1}^{N} (O_i - M_i)^2} . \tag{2}$$

This index can serve for the first (and rough) judgment of the spatially integrated criterion of the model performance. It is not latitudinal weighted, but, due to the relatively small extent of the domain along the meridian, this effect can be neglected.

Table 1. Values of the root mean square error (unit: mm)

Modcon	**EB**				**EC**				**NB**				**NC**			
Winter	**D**	**J**	**F**	**DJF**	**D**	**J**	**F**	**DJF**	**D**	**J**	**F**	**DJF**	**D**	**J**	**F**	**DJF**
2000	2.1	6.3	13.1	6.6	3.3	12.9	25.1	13.1	2.0	5.7	12.2	6.0	2.2	9.5	21.0	10.2
2001	30.0	46.1	45.9	35.9	28.3	41.3	44.1	31.9	15.0	28.8	35.3	22.8	16.2	31.8	31.8	22.4
2002	9.2	31.8	50.4	28.8	12.2	42.1	69.8	38.9	6.5	27.2	44.3	24.3	9.1	34.1	60.2	32.1
2003	5.9	23.7	36.7	20.6	6.3	31.4	52.7	28.0	5.3	18.0	27.2	15.7	5.5	20.4	33.4	18.2
2004	11.0	22.0	35.8	20.9	11.0	22.2	44.6	22.6	10.8	21.7	32.9	20.0	11.0	20.4	37.5	20.2
2005	11.9	26.3	32.9	22.1	20.3	50.7	63.6	42.9	15.0	31.3	33.9	25.8	20.0	43.7	48.8	36.4
2006	3.2	9.0	22.3	10.2	4.8	17.0	45.2	20.4	3.5	11.8	23.0	11.1	5.0	18.2	38.7	18.6
2007	14.5	21.9	22.9	19.1	21.1	31.1	38.1	29.1	13.1	22.0	23.6	18.7	16.3	26.1	33.1	24.1
2008	8.7	13.7	18.6	12.0	9.6	15.5	22.1	13.9	10.6	15.3	19.1	13.4	10.5	15.8	19.8	13.4
2009	6.5	14.9	27.6	14.3	7.7	25.2	58.3	27.8	4.8	14.4	23.4	12.0	5.1	17.5	42.4	18.5
average	**10.3**	**21.6**	**30.6**	**19.1**	**12.5**	**28.9**	**46.4**	**26.9**	**8.7**	**19.6**	**27.5**	**17.0**	**10.1**	**23.8**	**36.7**	**21.4**

4. Summary and conclusions

The interpretation of the results can be specified in many directions, but the most important and obvious conclusions are listed as follows:

- Over the bigger, mostly flat part of the domain, the modeled values of the *SWE* are relatively close to the analysis. The BIAS here shows high spatial

and temporal (i.e., from month-to-month and from season-to-season) variability, but generally the BIAS remains in the interval of (–10)–10 mm.

- The most significant discrepancies, mainly in direction overestimation (negative BIAS), are detected clearly over the Carpathian ridge, especially over the northern half.
- For all modcons the absolute value of the BIAS for February is greater than for the winter average, suggesting overall proportionality of the BIAS and the *SWE* values.
- The presented figures and *Table 1* do not outline any model configuration which output is clearly better/worse than the others.

Despite the high variability of the BIAS, even in adjacent gridcells, the detected negative BIAS for all modcons over the Carpathian ridge, especially over its northern part, seems systematic, and this is the main issue of this work. The comparison of the model results with the Globsnow product (*Chervenkov et al.,* 2016) shows significant dispersion of the BIAS, but also with prevailing negative values. Being the "final outcome" of complex atmospheric processes and interactions with the land surface, the snow cover can be influenced in many pathways along the simulation chain. Thus, for example, the relatively poor model performance in 2003 and 2010 can be rooted in the inadequate description of the large scale precipitation over the domain. Finally, the fact that the CARPATCLIM snow products are not pure observations suggests its possible deviation from the "truth state".

The model RegCM is constantly developed and, respectively, its simulation capabilities are steadily increasing. Further numerical experiments have to be performed, in particular including other parameterization schemes. The study confirms, however, that horizontal resolutions over 10 km are highly insufficient for regional snow cover modeling, especially over topographic heterogeneous terrain as the larger Carpathian Region. This fact have to be regarded by selecting the simulation tool and the model configuration. This is very important due to the fact that the mountainous snow covers are, generally speaking, those with the longest duration and thickness, with its all hydrological, ecological, and socio-economical consequences.

Acknowledgments: Deep gratitude to the organizations and institutes (ICTP, CARPATCLIM, ECMWF, NCEP-NCAR, Unidata, MPI-M, and all others), which provides free of charge software and data. Without their innovative data services and tools, this study would be not possible.

References

Arakawa, A. and *Schubert, W.H.*, 1974: Interaction of a cumulus cloud ensemble with the large-scale environment, Part I. *J. Atmos. Sci. 31*, 674–701.

Barnett, T.P., Dumenil, L., Schlese, U., Roechner, E. and *Latif., M.,* 1989: The effect of Eurasian snow cover on regional and global climate variations, *J. Atmos. Sci. 46,* 661–685.

CDO, 2015: Climate Data Operators. Available at: http://www.mpimet.mpg.de/cdo

Chervenkov, H., Todorov, T., and *Slavov, K.,* 2015: Snow Cover Assessment with Regional Climate Model - Problems and Results., Lecture Notes in Computer Science vol. 9374, (Eds. *Lirkov et al.*) Large-Scale Scientific Computing: 10th International Conference, LSSC 2015, Sozopol, Bulgaria, June 8-12, 2015. Springer, 327–334.

Chervenkov, H. and *Slavov, K.*, 2016 Simulated versus Satellite Retrieval Distribution Patterns of the Snow Water Equivalent over Southeast Europe, *Int J Environ. Agricult. Res. 2*, 115–122.

Clifford, D., 2010: Global estimates of snow water equivalent from passive microwave instruments: history, challenges and future developments. *Int. J. Remote Sens. 31*, 3707–3726.

Dee, D.P., Uppala, S.M., Simmons, A.J., Berrisford, P., Poli, P., and *Kobayashi, S.,* 2011: The ERA-Interim reanalysis: Configuration and performance of the data assimilation system. *Q. J. Roy Meteorol. Soc. 137*, 553–597.

Dickinson, R., Henderson-Sellers, A., and *Kennedy, P.J.,* 1993: Biosphere-Atmosphere Transfer Scheme, BATS: version1E as coupled to the NCAR community climate model. NCAR Tech Note, NCAR/TN-387+STR. National Center for Atmospheric Research, Boulder, CO

Gong, G., Entekhabi, D., and *Cohen, J.,* 2003: Modeled Northern Hemisphere winter climate response to realistic Siberian snow anomalies, *J. Clim. 16*, 3917–3931.

Grell, G.A., 1993: Prognostic evaluation of assumptions used by cumulus parametrizations. *Mon. Weather Rev. 121*, 764–787.

Grell, G.A., Dudhia, J, and *Stauer, D.R.,* 1994: A description of the fifth-generation Penn State/NCAR mesoscale model (mm5)., Tech Rep NCAR/TN-398+ STR, National Center for Atmospheric Research, Boulder, CO

Hancock, St., Baxter, R., Evans, J., and *Huntley B.*, 2013: Evaluating global snow water equivalent products for testing land surface models, *Remote Sens. Environ. 128*, 107–117.

JRC, 2010: Climate of the Carpathian Region. Technical Specifications (Contract Notice OJEU 2010 /S 110-166082 dated 9 June 2010)

Kanamitsu, M., Ebisuzaki, W., Woollen, J., Yang, S.K., Hnilo, J.J., Fiorino, M., and *Potter, G.L.,* 2002: NCEP-DOE AMIP- II reanalysis (R-2). *B. Am. Meteorol. Soc. 83*, 1631–1643.

Kiehl, J.T., Hack, J.J., Bonan, G.B., Boville, B.A., Breigleb, B.P., Williamson, D., Rasch, P., 1996: Description of the NCAR community climate model (ccm3). Tech Rep, NCAR/TN-420+ STR. National Center for Atmospheric Research, Boulder, CO.

Liston, G.E., 2004: Representing subgrid snow cover heterogeneities in regional and global models. *J. Clim., 17,* 1381–1397.

Oleson, K.W., Dai, Y., Bonan, G., and *Bosilovich, M.,* 2004: Technical description of the Community Land Model. National Center for Atmospheric Research Tech Note NCAR/TN-461+ STR, NCAR, Boulder CO.

Oleson, K.W., Niu, G.Y., Yang, Z.L., and *Lawrence, D.M.*, 2008: Improvements to the Community Land Model and their impact on the hydrologic cycle. *J. Geophys. Res. 113*, G0102.

Pal, J.S., Small, E.E., and *Eltahir, E.A.B.*, 2000: Simulation of regional-scale water and energy budgets: representation of subgrid cloud and precipitation processes within RegCM. *J Geophys Res, 105,* 29579–29594.

Szentimrey, T., 2011: Manual of homogenization software MASHv3.03, Hungarian Meteorological Service.

Szentimrey, T. and *Bihari, Z.*, 2007: Mathematical background of the spatial interpolation methods and the software MISH (Meteorological Interpolation based on Surface Homogenized Data Basis). Proceedings from the Conference on Spatial Interpolation in Climatology and Meteorology, Budapest, Hungary, 2004, COST Action 719, COST Office, 17 –27.

Yang, F., Kumar, A., Wang, W., Juang, H.-M. H., and *Kanamitsu, M.,* 2001: Snow-albedo feedback and seasonal climate variability over North America. *J. Climate 14,* 4245–4248.

Xue, Y., Janjic, Z., Dudhia, J., Vasic, R., and *De Sales, F.,* 2014: A review on regional dynamical downscaling in intraseasonal to seasonal simulation/prediction and major factors that affect downscaling ability, *Atmos. Res. 147–148*, 68–85.

IDŐJÁRÁS

Quarterly Journal of the Hungarian Meteorological Service
Vol. 120, No. 3, July – September, 2016, pp. 331–351

Climate-based seasonality model of temperate malaria based on the epidemiological data of 1927–1934, Hungary

Attila Trájer[1,2]* and **Tamás Hammer**[1]

[1]*University of Pannonia, Department of Limnology, Egyetem út 10, H-8200, Veszprém, Hungary*

[2]*MTA-PE Limnoecology Research Group, Egyetem út 10, H-8200, Veszprém, Hungary*

**Corresponding author* E-*mail: atrajer@gmail.com*

(Manuscript received in final form October 4, 2015)

Abstract—The potential resurgence of malaria in the temperate areas of Europe due to climate change is an actual topic of epidemiology. Although several ecological forecasting models were built for the prediction of the potential re-emergence of malaria in the recently non-endemic areas of the world, the simulations are mainly based on the recent climatic thresholds of the tropical and subtropical vectors and *Plasmodium* parasites, mainly of *Plasmodium falciparum*. We aimed to reanalyze the primarily *Plasmodium vivax* caused autochthon malaria disease data of the past model period of 1927-1934 in Hungary to gain reliable knowledge about the climatic thresholds and the determinants of the malaria season for a temperate climate in a Central European country. Multivariable and simple linear correlation and regression was performed to analyze the malaria data of 96 months dividing the season a first and a second half parts of the year. Two models were built on the gained correlations using unstandardized and standardized correlation weights. It was found, that both in the first and second halves of the year, the ambient mean temperature was the most important predictor of the relative malaria incidence, while precipitation influenced the first half of the season. Summer sum of precipitation above 200 mm was found as one of the most important determinant of the absolute annual case number of benign tertian malaria. The unstandardized weights-based modeled malaria seasons returned well the observed autochthon malaria seasons.

Key-words: *Plasmodium vivax*, malaria, temperate climate, seasonality, archive data

1. Introduction

Malaria is one of the most important vector-borne diseases in the world affecting at least 3.2 billion people (*World Malaria Report*, 2005) and causing about 700.000 to 2.7 million people deaths per a year (*Patz* and *Olson*, 2006). The disease is caused by different *Plasmodium* species and transmitted by several *Anopheles* mosquitos. About 40% of the mankind live in malaria endemic areas (*Mendis et al.*, 2001). Once in the wide areas of Europe malaria was endemic, however, due to the active eradication programs of the 20th century, malaria became a non-endemic or rare disease in the old continent. Malaria was highly endemic also in Hungary, in the hearth of Central Europe, even to the mid-20th century, when the results of a combination of several actions, malaria became eradicated in the country. For example, in the 1920's, malaria caused six to eight thousand newly acquired cases per year in the continuous regions of the north-east and south-west parts of Hungary (*Lőrincz*, 1981–82). In the territory of the Kingdom of Hungary, the Ministry of the Interior adopted decree against malaria in 1901, but the malaria data was regularly collected from 1927 (*Szénási et al.*, 2003). The year of 1930 was a milestone in the history of the malaria in Hungary indicating the start of the active intervention, although the more intensive epidemiological interventions due to the start of the establishment of the observation stations in the endemic areas started only in 1937 (*Szénási et al.*, 2003). The intent public health efforts, the elimination of the wetland areas and the introduction of DDT led to the eradication of the malaria to 1956 in Hungary, although officially the WHO delivered Hungary to a malaria-free country in 1963.

In contrast to the recent epidemiological situation, the climate models predict the resurgence and worldwide increasing risk of malaria transmission due to the anthropogenic climate change (*Martens et al.*, 1999). It was found that small increases in temperature at low temperatures can increase the risk of malaria transmission substantially (*Lindsay* and *Birley*, 1996), although the potential effect of the changing climatic patterns are strongly influenced by socioeconomic developments and malaria control programs (*Martens et al.*, 1995). For example, in the East African highlands, the warming trend from 1950 to 2002 caused the parallel increases in malaria incidence, too. The rapid response of malaria to the changing temperatures patterns is understandable according to the fact that *Anopheles* mosquitos are highly sensible for the meteorological conditions, particularly to the air temperature. Temperature determines the time of the ontogeny and the questing activity of female mosquitos (*MacDonald*, 1957; *Jetten* and *Takken*, 1994). In addition, the highly complex ontogeny of *Plasmodium* parasites is also the function of the ambient temperature. For example, it is known that the lower temperature threshold of the ontogeny of *Plasmodium vivax* and *Plasmodium falciparum* are 14.5–16 and 18 °C, respectively (*MacDonald*, 1957). Even *Hackett* and *Missiroli* (1935)

showed that the pattern of malaria season is in correlation with the latitude of a malaria endemic area, since the latitude essentially determines the annual temperature conditions with other factors, e.g., as the distance from the oceans and the altitude conditions. Before the 20th century, the 15 °C July isotherm appointed the northeast occurrence of the endemic malaria cases (*Menne* and *Ebi*, 2006). Precipitation is also an important factor of the malaria cases determining, with the temperature conditions, the dominance of the *Anopheles* species in Europe (*Kuhn et al.*, 2002). In the Atlantic and continental climate zones of Europe, as the Central European region, *Anopheles atroparvus* van Thiel, in Eastern Europe *Anopheles messeae* Falleroni, and in the Balkan Peninsula *Anopheles superpictus* Grassi are the main potential vectors of the human pathogen *Plasmodium* species. Recently, seven *Anopheles* species are known from Hungary, although the presence of *Anopheles sacharovi* Favre is also possible in the southern border areas (*Tóth* and *Kenyeres*, 2012). The malaria pathogen transmission potential of the different *Anopheles* species are different, the members of the so-called Maculipennis complex (named after the *Anopheles maculipennis* Meigen malaria mosquito) are known to be the most important vector species. In Hungary, *Anopheles atroparvus, Anopheles maculipennis,* and *Anopheles messeae* are the plausible potential vectors of the *Plasmodium* parasites according to the historical data (*Szénási et al.*, 2003). It is also known that before the eradication of the malaria in Hungary, *Plasmodium vivax* caused the 90% and *Plasmodium falciparum* the 10% of the malaria cases.

The resurgence of malaria in Europe is more than a fiction: *Plasmodium*-infected people introduced tropical malaria during the 1997 heat-wave in Germany (*Krüger et al.*, 2001) and Italy (*Baldari et al.,* 1998), when local female *Anopheles* mosquitos bite infected passengers returning from endemic areas. The reverse case is also known, when introduced, infected malaria vectors caused malaria infection in the airport staff or the people living in the neighborhood of the airport (*Giacomini et al.*, 1997). However, the well-developed simulations provide information of the vector potential of the *Anopheles* species in the near future; there are no well-based evidences about the potential seasonality of malaria in the continental areas as the Carpathian Basin. In turn, seasonality and the determinants of the annual run of the disease season can be more important factors of the possibility of reemergence of malaria than the simple presence of the malaria vectors. Since either the tropical vectors or the parasites are not or only partly equivalent to their continental counterparts, the model results require further validation. According to the above described causes, only the historical data of an area in a temperate region can provide a reliable basis and model for the potential near future seasonality of malaria in the temperate regions, even the climate is changing. In contrast to the northern regions of Europe, where malaria spontaneously disappeared in the early 20th century (*Bruce-Chwatt* and *de*

Zulueta, 1980), in Hungary the malaria eradication was the consequence of the joint effort of public health services. Although, autochthon malaria cases were observed in Hungary from the medieval ages to the 1950's, the analyzable period is limited to the start of the regular data collecting activity and the start of the more active public health interventions in the second part of the 1930's.

Our aim was to analyze the autochthon malaria case data of Hungary after the start of the data collection, but before the pre-intervention era in the period of 1927 to 1934. While the threshold of the tropical vectors and parasites is well-known, the threshold of the extinct European strains is still debate (*Menne* and *Ebi*, 2006). We also aimed to gain information about the former seasonality patterns, the effect of the temperature and precipitation on the autochthon malaria cases and to build a phonological malaria seasonality model based on the results. In addition, the re-modeling of the adult female malaria mosquito season was performed for the studied period.

2. Methodology

2.1. Statistics and software

The multivariable and the simple linear correlation and regression were performed by the simple and multiple regression tool of VassarStats on-line statistical program (*Lowry*, 2004). Microsof Office 2010 Excel was used in the visualization of the graphs. ArcGis 10.0 software was used in the performance of the spatial data.

2.2. Climate data

Since the climatic and topographical conditions are very homogenous in the country, Hungary was considered in climatic sense as a homogenous unit. The daily mean temperature data were derived from the European Climate Assessment Dataset (*Haylock et al.,* 2008).

2.2.1. Temperature and precipitation data for the period 1927–1934

We gained the monthly mean temperature and the monthly sum of precipitation data from the dataset of CRU TS3.22 (land) model for 1901–2013. Average values were calculated from the 0.5° grid within the domain including almost the entire Hungary. The latitudinal range was 45.50°N–48.50°N, while the longitudinal was 16.00°E–23.00°E. The monthly mean temperature and the monthly sum of precipitation values were derived from the period of January 1927–December 1934.

2.2.2. Temperature and precipitation data for the period 1970-1999

We gained the mean daily temperature data from the dataset of E-OBS model (1950-now). Average values were calculated from the 0.5° grid within the domain including almost the entire Hungary (*Fig. 1*). The latitudinal range was 45.50°N-48.50°N, while the longitudinal was 16.00°E–23.00°E. The monthly mean temperature values were derived from the period of January 1970–December 1999. The daily data was converted into monthly mean temperature values.

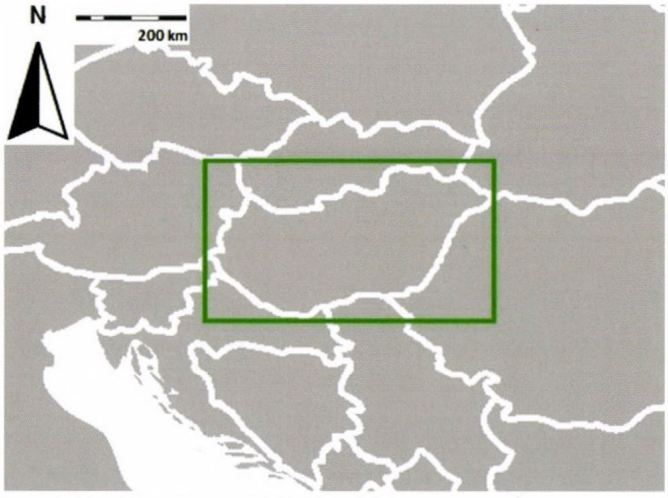

Fig. 1. The domain of Hungary in Central Europe.

2.3. Malaria data

2.3.1. Monthly autochthon malaria data of 1927-1934 in Hungary

The monthly malaria case number of 1927–1934 was based on the article of Zoltán Alföldy (*Alföldy,* 1935). The results of this study are shown in *Fig. 2 left.* Due to the lack of the written data, after the digitalization of the figure, the monthly case numbers were read directly from the figure using a precise covering grid. Although, malaria became a mandatory reportable disease in 1930 in Hungary, the regular collection of the disease started in the autumn of 1926. Since the data of 1926 is incomplete, in the latter analysis we neglected this data. Despite the fact that the studied eight years may seems at first inspect to be a short period, the absolute malaria case number showed a notable fluctuation. While the lowest malaria case number was observed in 1930 with less than 150 cases per year, the highest malaria case number exceeded the 1900 case per year value in 1934. Summer cases formed the most notable part of the annual malaria incidence with a synclinal pattern during the studied period (*Fig. 2 right*).

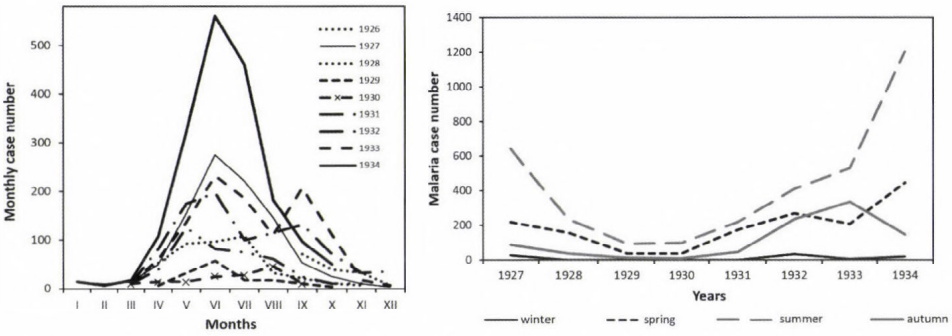

Fig. 2. Left: the autochthon monthly malaria cases in Hungary, in the autumn of 1926 and 1927–1934, *right*: changes of the number of the seasonal autochthon malaria cases in 1927–1934, Hungary.

2.3.2. Spatial data of the malaria cases of 1936 and its georeferencing

To show the former spatial occurrence of malaria in Hungary, the year of 1936 was selected as a characteristic example of the 1930's. In this year the malaria morbidity was 20.8 per 100.000. The spatial distribution data of the malaria cases of 1936 was based on the publication of *Szénási et al.* (2003) (*Fig. 3, Malaria morbidity in Hungary in 1936*). The original spatial data was displayed in the former "járás" (*processus*, the lowest-level administrative unit) system, which corresponds roughly to the present day NUTS4 district areas. We used the site appointing function of Google Earth imagery to mark the central points of the former NUTS4 areas. Each marked points were named after its case number interval. Six intervals of annual case number were used according to the original: the 1 to 5, 6 to 14, 15 to 29, 30 to 59, 60 to 149, and 150 to 284. We converted the designated spatial data into keyhole markup language (*kml*) file format (altitude or gamma intensity data). After opening the *kml* data, we converted them into shape file format in the ArcGIS 10.1 software. To create color images, we linked the points with the mean of the annual case number intervals. The different values were assigned to the referred points and were sorted into attribute table. We interpolated the values of the spatial data by the IDW interpolation function of the spatial analyst tool in the ArcGIS. The aquatic habitats illustrating cut off the second military surveying of the Habsburg Empire were derived from the Mapire homepage (*Mapire,* 2015), which is a digitized and georeferenced raster mosaic of the original individual sheets (*Molnár* and *Timár,* 2009).

2.4. *Mosquito data*

The relative abundance, *RA* (in %), value of the female imago individuals of *Anopheles messeae*, a member of the *Anopheles maculipennis* complex was gained from the three decades (1970's, 1980's, and 1990's) covering countrywide mosquito collecting data of *Tóth* (2004). We assorted the number of collected female mosquitos according to the months of the year and used the summarized monthly female mosquitos in the model. The number of the collected number of the mosquitos was termed as a relative abundance (*RA*). Since the monthly value of *RA* depends on the number of monthly trapping occasions, we used the quotient of *RA* and the number of the trapping occasions (termed as the normalized relative abundance value, *NRA*):

$$NRA = \frac{RA_i}{N_t}, \tag{1}$$

where *NRA* is the normalized relative abundance, RA_i is the the normalized relative abundance of the *i*th month of the year, and $N_t$is the the number of trapping occasions in the ith month of the year.

Since this number is based on the summarized amount of collected mosquitos, this data was utilized to build only a relative model predicting the seasonal run of the malaria mosquito season.

2.5. *Modeling approaches*

To analyze the phenology of the malaria season, two different approaches were used: a climate-based model and a vector (*Anopheles messeae*)-based model. In the first approach, we also used the temperature and precipitation data to predict, at first, the annual relative incidence (*RI*, in %) and after the percentage of the malaria case number according to the whole period's case number (*R*). Since, in contrast to the past malaria data, we used the 30 years summarized monthly number of the mosquitos, in the vector-based model only the temperature and the annual normalized relative abundance of the potential vectors (*NRA*, in %) were used. Both *NRA* and *RI* values mean the percentage of the monthly cases or number according to the annuals'. The *R* value was calculated according to the incidence values of the period of 1927–1934.

2.5.1. *The first approach*

The model was built to analyze the determinant climatic factors of the former run of the annual malaria case curve in Hungary and to reconstruct the curve in the studied period. At first, we calculated the relative case number values form the monthly cases, as in the period of 1927 to 1934. The case number of malaria showed the above described high variance, and the relative case number (relative

malaria incidence, RI_m) values were used instead of absolute incidence or case number values as the basis of the model. The model was constructed to calculate the RI_m values of a certain month based on the monthly mean temperature (T_m) and the monthly sum of precipitation (P_m). Since RI_m may be related to the abundance of the actual questing, hungry active female *Anopheles* population, we hypothesized that malaria can positively correlate with the outdoor temperature and the precipitation. Our approach was that the annual *RI* is the amount of the monthly values of the temperature and precipitation dependent abundance related relative monthly malaria case numbers in the first (RI_{m1}; from the 1st to the 6th months) and second part of the year (RI_{m2}; from the 7th to the 12th months). Although the correlation between the relative monthly malaria incidence and the sum of the monthly precipitation values was negligible in case of the second part of the season, keeping the consistency of the model, precipitation was involved. *RI* is the product of the following equation:

$$RI = \sum_{i=1}^{6} RI_{m1} + \sum_{i=7}^{12} RI_{m2}, \tag{2}$$

where *RI* is the relative annual malaria incidence ,RI_{m1} is the relative malaria incidence (%) of the months of first half part of the year, and RI_{m2} is the relative malaria incidence (%) of the months of second half part of the year.

The monthly relative malaria incidence was described as a multivariable linear regression function of the T_m and P_m according to the gained coefficients of the multiple linear regression analyses in Eq.(3):

$$RI_m = a + \beta_1 T_m + \beta_2 P_m, \tag{3}$$

where RI_m is the relative monthly malaria incidence, a is a constant, $_{1,2}$ are correlation weights, T_m is the mean monthly temperature, and P_m is the sum of the monthly precipitation (mm).

Since the multiple linear regression analyses gave unstandardized and standardized coefficients, two groups of the models were built according to the used coefficients. $Model_a$ was built on the unstandardized, $Model_b$ on the standardized coefficients.

At the second step, we aimed to converse the output (the *RI*) of the relative annual model into the relative (*R*) values of the whole period. The conversation of the case numbers into incidence values was not considered to be necessary due to the relatively short period. Since the summer cases formed the more than 50% of the cases, the correlation between the summer precipitation and the summer malaria case number was analyzed. It was hypothesized that the ratio of the modeled summer case number according to the mean can be used as the multiplier of the annual case number:

$$R = RI_m \frac{N_{modeled\ summer\ malaria}}{N_{mean\ summer\ malaria}}. \quad (4)$$

2.5.2. The second approach

We used a simple linear model to gain correlation between the *NRA* values of the two *Anopheles* species and the mean monthly temperature of the period 1970–1999. Since the domain of the two sources of the temperature data was the same, we calculated the *NRA* values of the malaria mosquitos for the months of the period of 1927–1934. Finally, we compared the *RI* and *NRA* values for the studied period.

3. Results

3.1. The spatial occurrence of malaria in the 1930's

The historical malaria case data of 1936 shows that the former autochthon malaria cases in Hungary had three main focuses, the Upper Tisza region the northeast (*Fig. 3.*1), the river Drava in the southwest (*Fig. 3.*2a), and the south area of Zala hills, adjacent to the Drava valley (*Fig. 3.*2b). The endemic malaria focus in the Upper Tisza valley was partly related to the great Ecsed marsh. The central and northern parts of Hungary were malaria-free areas in 1936. The elevation of the Upper Tisza region focus is 101–118 m above sea level, in case of the southwestern former malaria focuses the topography is very heterogenic, the mean elevation is about 85–170 m, respectively (*Fig. 3,* upper map).The lower maps of *Fig. 3* show the most influenced autochthon malaria regions in 1936 according to the second military survey of the Habsburg Empire. Although the survey itself was carried out in the period from 1853 to 1873, the coverage with wetlands, oxbows, and marches did not differ notably from the conditions of the 1920's and 1930's. In the southern part of the Upper Tisza valley, the marshes formed the dominant potential aquatic habitats of *Anopheles* species, while in the northern part of the Upper Tisza and the Drava valley, these habitats were the oxbows and flood puddles.

3.2. The phenology of the autochthon malaria seasons from 1927 to 1934 in Hungary

The incidence of the autochthon malaria cases was the following: 1.17 (1927), 0.53 (1928), 0.25 (1929), 0.16 (1930), 0.53 (1931), 1.11 (1932), 1.33 (1933), and 2.29 (1934) per 10,000 inhabitants calculating with the population of Hungary according to the census of 1930 (8685109 inhabitants), respectively. The mean of the incidence values was 0.92, the variance was 0.4675, and the standard deviation was 0.7053 per 10,000 inhabitants. In the studied period, the malaria season in 6 cases had unimodal patterns (in 1927, 1928, 1929, 1930, 1931, and 1934), in 2 cases the

season had bimodal feature (in 1932 and 1933). The maximum monthly case numbers were observed in May in 1 case (1931), in June in 5 cases (1927, 1928, 1929, 1930, and 1934), in August in 2 cases (1932 and 1933). In case of 1932, and 1933, a second seasonal peak was observed in September (*Fig. 4*).

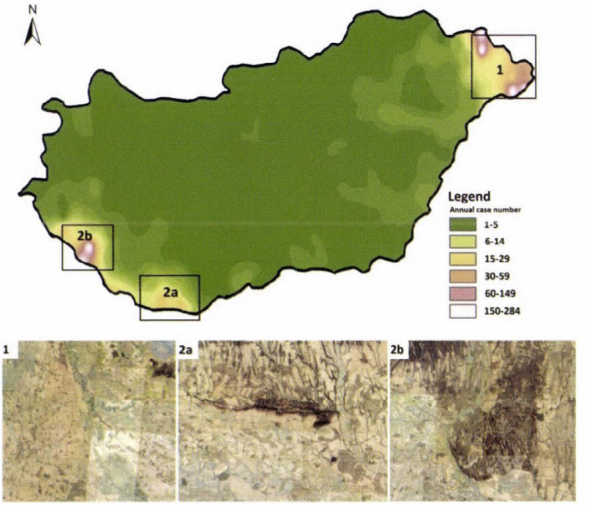

Fig. 3. Spatial distribution of the malaria cases in 1936. 1: Szatmár-Bereg plain, 2a: Drava Plain, and 2b: south Zala hills (upper map) are the most influenced autochthon malaria regions in the 1930's in the maps of the second military survey of the Habsburg Empire. Blue colors refer to the wetlands and rivers of the areas. **1**: the upper Tisza, **2a**: the Drava, and **2b**: the south area of Zala hills, adjacent to the Drava valley (lower maps).

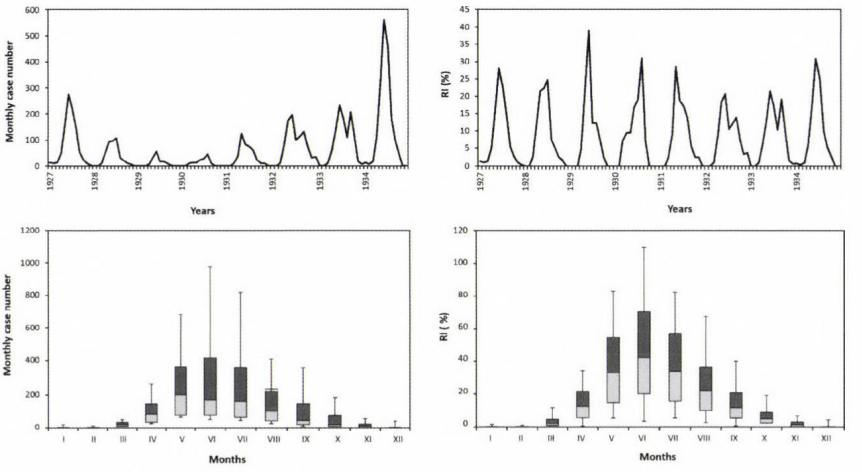

Fig. 4. Upper left: absolute monthly autochton malaria case numbers. *Left*: box and whiskers plots of the monthly case numbers of the years. *Upper right*: relative malaria incidence values. *Lower right*: box and whiskers plots of the annual proportion of the monthly case numbers of the years of 1927–1934 in Hungary.

The season started in March in general, although in 1929 and 1930, the malaria season started in April and May. The summer proportion of the cases according to the annual total case number were the following in the studied years: 1927: 65.69%, 1928: 54.54%, 1929: 63.41%, 1930: 66.66%, 1931: 49.59%, 1932: 43.23%, 1933: 49.00%, 1934: 66.21%. In general, the 57.29% of the annual cases occurred during the summer months in 1927–1934. The seasonal run of the malaria seasons show that the season started when the portion of the monthly malaria case number reached about the 5% of the annual cases. According to this criterion, the malaria season started in April except the year 1930, when the season started in March. The monthly mean temperatures, of the starting months were the following: 9.6 (1927), 10.3 (1928), 6.1 (1929), 6.2 (1930), 7.5 (1931), 9.5 (1932), 7.2 (1933) and 13.0 °C (1934). In general the start of the season occurred at 8.7 °C monthly mean temperature (SD: 2.37 °C). Using the same criterion for the end, the season ended in September in 1927–31 and 1934 and in October in 1932-33. The monthly mean temperatures of the last months were the following: 16.6 (1927), 15.9 (1928), 15.6 (1929), 16.8 (1930), 12.0 (1931), 11.9 (1932), 10.4 (1933), and 16.7 °C (1934). In general the end of the season occurred in 14.5 °C monthly mean temperature (SD: 2.6 °C). The absolute minimum temperature threshold of malaria in the begining and the end and of the season was about 5 °C mean monthly temperature (*Fig. 5 left)*. The peak season month occurred at the following mean temperature and monthly sum of precipitation conditions: 19.0 °C –76.7 mm (1927), 22.3 °C –21.3 mm (1928), 17.2 °C –79.0 mm (1929), 18.8 °C –92.7 mm (1930), 17.5 °C –42.1 mm (1931), 17.0 °C –52.5 mm (1932), 15.6 °C –102.4 mm (1933), and 17.7 °C –116.6 mm (1934) with a mean of 18.1°C (SD: 2 °C) and 72.9 mm (SD: 32.2 mm; *Fig. 5 right*).

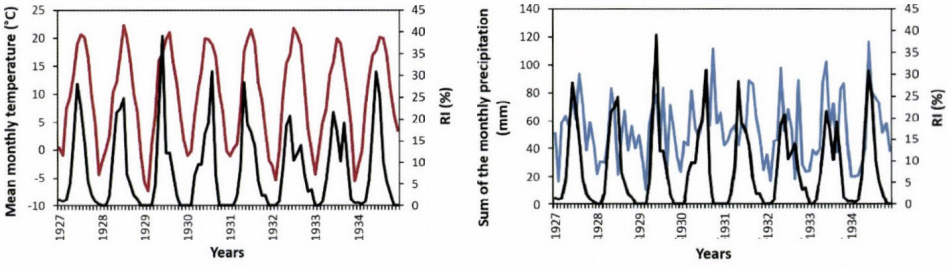

Fig. 5. Left: monthly relative malaria case number and run of the monthly mean temperature values. *Right*: the monthly relative malaria case number and run of the monthly sum of precipitation values.

3.3. *Modeling approach 1*

3.3.1. *The first part of the year*

Strong correlation was found between the *RI* and the mean monthly temperature values ($r^2 = 0.75$). We also found notable correlation ($r^2 = 0.5$) between the *RI* and the sum of the monthly precipitation in the first part of the year. The multiple r^2 of the regression was 0.78; the adjusted r^2 was 0.77 with a standard error of 4.7901. The value of the intercept is –2.5895. The correlation matrix and the gained regression coefficients can be seen in *Tables 1* and *2*.

Table 1. Correlation matrix of the results of the multiple regression in case of the months of the first half of the year; RI_{m1}: relative incidence of the months of first half in the year, T_m: mean monthly temperature, P_m: sum of the monthly precipitation

	T_m	P_m	RI_{m1}
T_m	1	0.656	0.866
P_m	0.656	1	0.71
RI_{m1}	0.866	0.71	1

Table 2. The gained regression coefficients; T_m: mean monthly temperature, P_m: sum of the monthly precipitation, *b*: unstandardized regression weights, *B*: standardized regression weights

	b	*B*	$B \times r_{TmPm}$
T_m	0.8904	0.7025	0.6081
P_m	0.1067	0.2487	0.1765

For the relative malaria incidence of the first six months of the year, RI_{m1}, the following equations can be written:

$$RI_{\mathrm{m1}} = -2.5895 + 0.8904T_m + 0.1067P_m, if\ T_{monthly}^{1927-1934} > 5\ °\mathrm{C} \quad (5.a)$$

$$RI_{\mathrm{m1}} = -2.5895 + 0.7025T_m + 0.2487P_m, if\ T_{monthly}^{1927-1934} > 5\ °\mathrm{C} \quad (5.b)$$

Eq. (5.a) is based on the unstandardized, while Eq. (5.b) is based on the standardized weights, where T_m is the mean monthly temperature and P_m is the sum of the monthly precipitation.

3.3.2. *The second part of the year*

Notable correlation was found between the *RI* and the mean monthly temperature values ($r^2 = 0.57$; *Fig.6 upper part*). In contrast, the correlation between the *RI* and the sum of the monthly precipitation was negligible in the second part of the season ($r^2 = 0.03$, *Fig. 6 lower part*). The multiple r^2 of the regression was 0.58; the adjusted r^2 was 0.56 with a standard error of 5.1746. The value of the intercept is 0.2607. The correlation matrix and the gained regression coefficients can be seen in *Tables 3* and *4*.

Table 3. Correlation matrix of the results of the multiple regression in case of the months of the second half of the year; RI_{m2}: relative incidence of the months of first half in the year, T_m: mean monthly temperature, P_m: sum of the monthly precipitation.

	T_m	P_m	RI_{m2}
T_m	1	0.313	0.758
P_m	0.313	1	0.168
RI_{m2}	0.758	0.168	1

Table 4. The gained regression coefficients; T_m: mean monthly temperature, P_m: sum of the monthly precipitation, *b*: unstandardized regression weights, *B*: standardized regression weights

	b	*B*	$B \times r_{TmPm}$
T_m	0.7727	0.7818	0.5924
P_m	–0.028	–0.0771	–0.0129

For the relative malaria incidence of the first six months of the year, RI_{m1}, the following equations can be written:

$$RI_{\mathrm{m1}} = 0.2607 + 0.7727T_m - 0.0280P_m, if\ T_{monthly}^{1927-1934} > 5\ °\mathrm{C} \quad (6.a)$$

$$RI_{\mathrm{m1}} = 0.2607 + 0.7818T_m - 0.0771P_m, if\ T_{monthly}^{1927-1934} > 5\ °\mathrm{C} \quad (6.b)$$

Eq. (6a) is based on the unstandardized, while Eq. (6b) is based on the standardized weights, where T_m is the mean monthly temperature and P_m is the sum of the monthly precipitation.

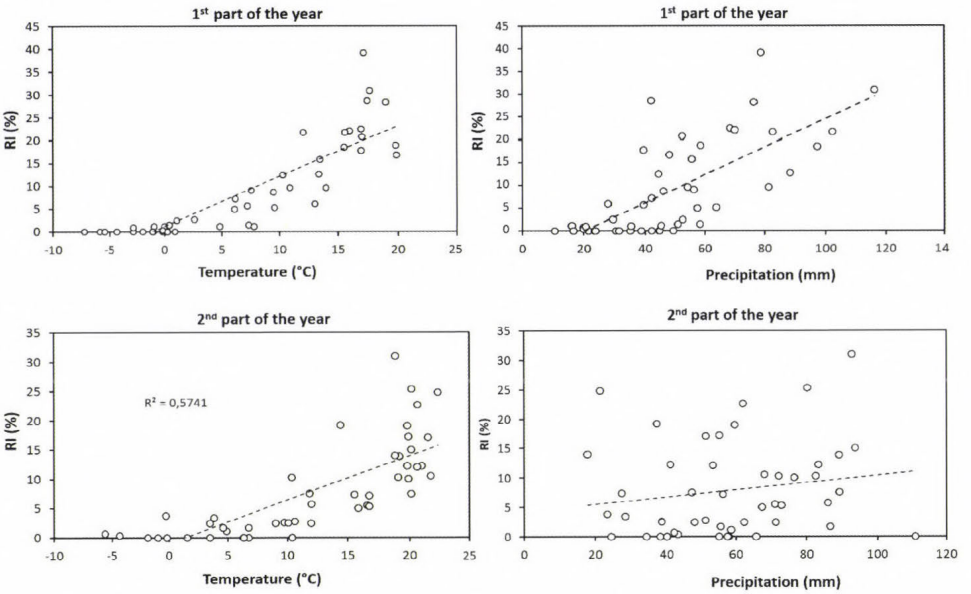

Fig. 6. Upper left: correlation between the monthly relative malaria case number and the run of the monthly mean temperature values in the first part of the year. *Upper right*: correlation between the monthly relative malaria case number and the run of the monthly sum of precipitation values. *Lower left*: correlation between the monthly relative malaria case number and the run of the monthly mean temperature values in the second part of the year. *Lower right*: correlation between the monthly relative malaria case number and the run of the monthly sum of precipitation values.

3.4. Modeled relative seasons

3.4.1. Correlation between the summer precipitation and the number of the summer malaria morbidity

Significant correlation was found between the sum of the summer precipitation and the summer malaria case number:

$$N_{malaria} = 23.437e^{0.0125 \times P_{\Sigma ms}}, \quad (7)$$

where r^2=0.58 and p=0.3557. Results of the Eq. (7) are drawn in *Fig. 7.*

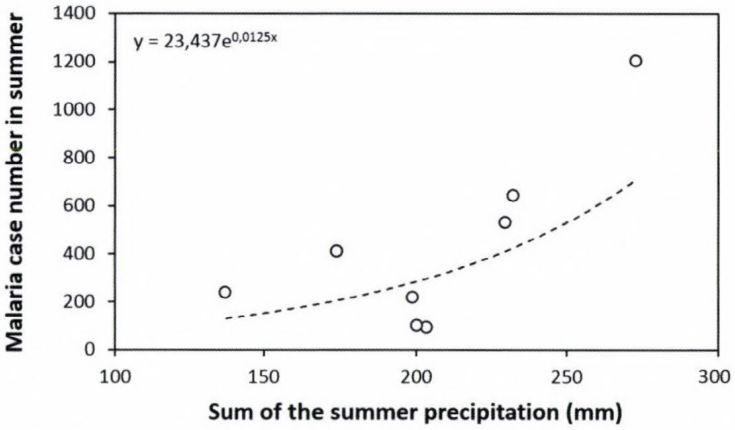

Fig.7. Correlation between the sum of the summer precipitation and the malaria case number in summer

Using unstandardized weights, the sum of the absolute errors is 3.7109, in case of standardized weights it is 4.3859 (*Fig.8 top*). The 12.5% of the malaria case numbers of the period of 1926–1934 occurred in a given year. The ratio of the real case number and the mean of the period were the following: 1927: 1.24, 1928: 0.38, 1929: 0.86, 1930: 0.83, 1931: 0.82, 1932: 0.60, 1933: 1.20, 1934: 2.06. The correlation of the relative malaria cases and the results of the model using unstandardized weights according to the linear and polynomial approximations are $r^2 = 0.6487$and $r^2 = 0.7247$, while in case of standardized weights these values are $r^2 = 0.311$ and $r^2 = 0.341$, respectively. The sum of the absolute errors in case of unstandardized weights was 70.78, in case of standardized weights 82.55, respectively. Although the model somewhat overestimate the relative case number of 1929 and 1930, it predicts the higher season peak values well in case of 1927, 1933, and 1934 (*Fig. 8* bottom).

3.5. The second modeling approach

3.5.1. The temperature dependent seasonality of Anopheles messeae in Hungary

The main part of the mosquito seasons of *Anopheles messeae* started in April and ended in October, however, a few numbers of individuals were collected also in March and November. The main parts (91%) of the female Anopheles maculipennis complex individuals were collected in months with more than 12 °C average temperature (*Fig. 9*).

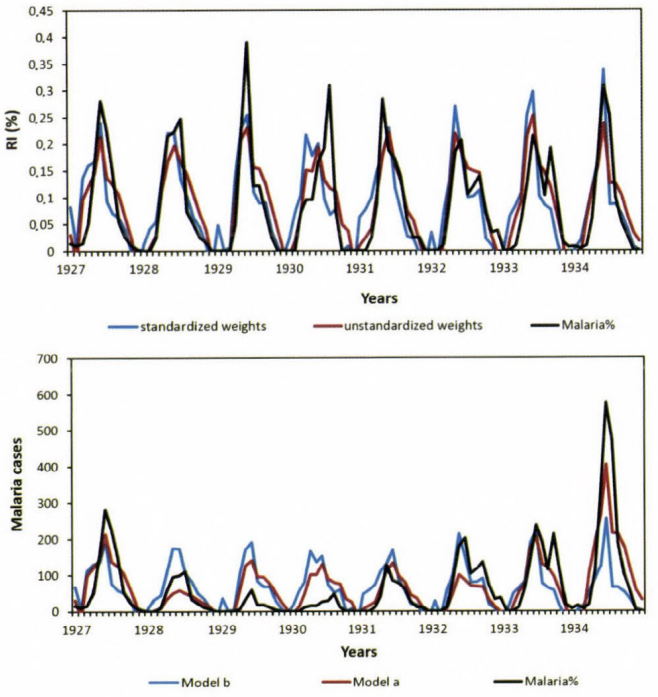

Fig. 8. Top: The observed and modeled relative autochthon malaria seasons according to the unstandardized and standardized weights. *Bottom*: the observed and modeled absolute autochthon malaria seasons according to the unstandardized and standardized weights.

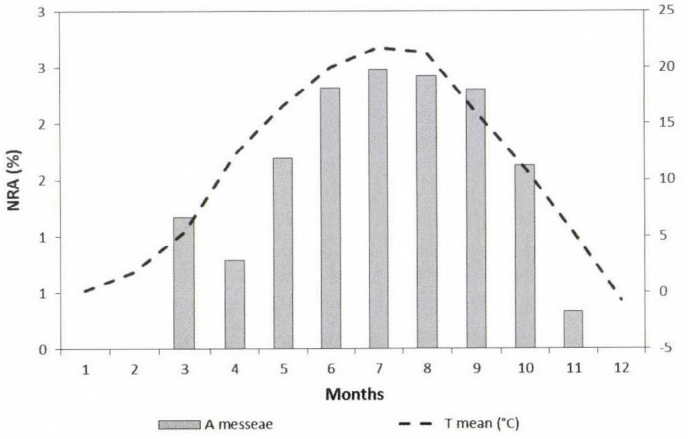

Fig. 9. Seasonality of *Anopheles messeae* and the monthly mean air temperature in the period of 1970–1999.

In case of the normalized relative annual numbers of *Anopheles messeae*, strong significant correlation were found with the monthly mean temperature ($r^2 = 0.89$, $p < 0.0001$). According to the correlation between the monthly mean temperature and the summarized relative (%) number of the collected female individuals of *Anopheles messeae* the following equation was gained:

$$NRA = 0.1147T_m + 0.0117, \tag{8}$$

where *NRA* is the normalized relative abundance (%) and T_m is the monthly mean temperature (°C).

3.5.2. The reconstructed Anopheles messeae seasonality in 1927–1934

Eq. (7) was replayed for the monthly temperature values of 1927–1934 and it was depicted with the relative (%) number of the observed autochthon malaria cases (*Fig. 10*).

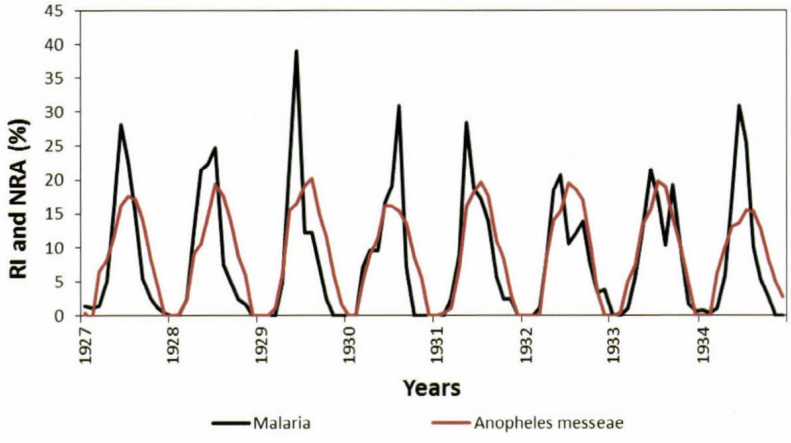

Fig. 10. The observed normalized relative malaria incidences and the modeled relative mean abundance values of *Anopheles messeae.*

4. Discussion

The reanalysis of the historical malaria data in the central part of Europecountry provides a unique feasibility to gain confident data about the former seasonality

of the autochthon malaria in a temperate region of Europe. Historical maps show that the autochthon malaria cases occurred primarily in wetland areas or river basins and not at lakes as lake Balaton. The spatial occurrence of the cases was linked to two major aquatic habitats: marshes and the floodplain of the river valleys. It can be stated that the cases are accumulated in the water collecting area of medium-sized rivers as river Tisza, Drava, or river Körös. The salt lakes of the Danube-Tisza interfluve, the rivers and creeks of the Transdanubian mountain range were not affected by malaria in the studied period. It is plausible that areas with the extent presence of barely or not regulated river sections had the greatest risk for malaria endemicity. Although, the most notable focus in 1926–1934 were linked into south-western and north-eastern parts of Hungary, a major malaria endemic focus is plausible according to the historical records and the FY A Duffy blood group allele in the great plain of Hungary and the south parts of the Carpathian Basin. The recent presence of the local low FY A allele frequency in south Hungary, north Serbia, Vojvodina, and south western Romania (see *Howes et al.,* 2011) may refer to the former presence of a long-persistent malaria endemic area in the south-eastern part of the Carpathian Basin, since malaria resistance is linked to the Duffy-negative phenotype against *Plasmodium vivax* infection. In contrast, the recent distribution of sickle haemoglobin (HbS) allele frequency shows that *Plasmodium falciparum* caused malaria was endemic only in the South Balkan in the historical times (see *Piel et al.,* 2010) and it lacked from the Carpathian Basin which is consistent with the known sensibility of the parasite for cold conditions.

In the historical times, up to the middle of the 20th century, *Plasmodium vivax* was the predominant cause of malaria in the temperate parts of Europe, and *Plasmodium falciparum* persisted only in the Mediterranean coastal regions of the old continent (*de Zulueta*, 1994). The possibility of the overwintering of *Anopheles* mosquitos is not theoretical, since the lethal temperature for some members of the genus is below –15 °C (*Wallace* and *Grimstad*, 2002). It is plausible that relatively cold-resistant *Plasmodium vivax* was the main infectious agent of malaria in Hungary (*Szénási et al.*, 2003), which *Plasmodium* species outside of Africa recently accounts for more than 50% of all human malaria cases (*Mendis et al.*, 2001). *Plasmodium vivax* infection is a re-emerging malaria disease in the eastern part of the Mediterranean basin (*Andriopoulos et al.*, 2013). The occurrence of malaria is strictly limited by precipitation and temperature thresholds. For example, the temperature threshold of the digestion of blood meal in case of *Anopheles maculipennis* is 9.9°C, while the threshold temperature of the extrinsic incubation cycle of *Plasmodium vivax* is 14.5-15°C (*Martens et al.,* 1995).

The absolute minimum limits of the start and the end of the malaria season were about at the 5 °C mean monthly temperature values which are lower than the recent known, at least 14.5 °C ontogeny threshold of the *Plasmodium* species (*MacDonald,* 1957). It is in accordance with the gained, also about 5 °C

minimum activity threshold of adult female *Anopheles messeae* individuals. These observations raise the possibility that the former malaria strains were much cold tolerant in the temperate regions of Europe – similarly to the vectors - than in case of the recent genetic lines of the tropical/subtropical regions.

In contrast to the recent tropical and subtropical examples, malaria in the temperate, continental climate of Hungary had mainly unimodal seasonality with a 3 to 4 months winter diapause. It is also notable that the also mosquito-transmitted, in Hungary recently endemic West Nile fever has a late summer - early autumn peak season with a very low and negligible case number in June (*Trájer et al.*, 2014). The clear difference of the seasonality of the two mosquito-borne diseases could be explained by the different reservoirs, which are birds in case of West Nile fever and humans in case of malaria. While active mosquitos can transmit malaria directly from human to human, West Nile fever epidemics can only break out after that the amount of the circulating virus reaches a given threshold prevalence level in the mosquito population. It should be added, that West Nile virus can overwinter in their mosquito vectors (*Nasci et al.*, 2001). It is somewhat surprising that while the mosquito population could increase during the summer season, the malaria incidence reached its annual peak already in early summer in most of the years. It is possible that infected mosquitos could overwinter in an increased number within the population, since *Plasmodium* infected mosquitos have increased longevity (*Vézilier et al.*, 2012).The observed June maximum in the majority of the years and the early and fast increase of the former malaria season support the hypothesis, that the infected overwintering female imago malaria mosquitos played a notable role in the transmission in the studied former autochthon malaria cases. Another possible interpretation of the former early outbreak and peak of malaria is the role of humans as reservoirs living in wetland areas, since the incubation period varies between 7 and 15 days in general, and the long incubation period can take several months (sometimes years) in case of *Plasmodium vivax* caused malaria without any effective treatment (*ECDC Epidemiological update,* 2013).

The found, 3 to 4 months winter diapause period of the potential vector mosquitos in the cold half of the year led the public health services to the successful intervention. *Szénási et al.* (2003) described that the infected people were re-treated in the spring of the next year, which practice was one of the most important cause of the eradication of malaria in Hungary.

Bismil'din et al. (2000) and *Kuhn et al.* (2003) concluded that there are strong link between the re-emergence of malaria and non-climatic factors. Climate change alone can be insufficient to trigger the reappearance of the autochthon malaria in an area. We found that precipitation is an important determinant factor of the relative incidence in the first half part of the year, and it influences significantly the summer incidence. This finding is in accordance with that rainfall has significant effect on the number of Anopheline vectors as e.g. *Anopheles gambiae* (*Koenraadt et al.*, 2004). We found that in the second

half of the year, precipitation had no notable effect on the malaria incidence. Temperature played important role in the determination of the notable points (the start and the end) of the season although the absolute case number or the possible bimodality of the season was rather determined by the summer precipitation patterns. The effect of the summer precipitation sum above about 200 mm increased rapidly the summer, and consequently, the annual incidence of malaria. The gained similarity of the observed relative malaria and the modeled relative vector seasons confirms the former observations and hypotheses that the native members of Maculipennis complex, e.g., *Anopheles messeae* were the vectors of the malaria in Hungary. It can be concluded that our seasonality model can be well-adapted for the recent *Plasmodium vivax* malaria endemic areas of the world.

Acknowledgement: This study was supported by TÁMOP-4.2.2B-15/1/KONV-2015-0004.

References

Alföldy, Z., 1935: A malária járványgörbéjének évszakos változásáról 1934. *Népegészségügy 16*, 68–75. (In Hungarian)

Andriopoulos P., Economopoulou A., Spanakos, G., and *Assimakopoulos, G.,* 2013: A local outbreak of autochthonous Plasmodium vivax malaria in Laconia, Greece –a re-emerging infection in the southern borders of Europe? *Int. J. Infect. Dis. 17,* e125–e128.

Baldari, M., Tamburro, A., Sabatinelli, G., Romi, R., Severini, C., Cuccagna, G., Fiorilli, G., Allegri, M.P., Buriani, C. and *Toti, M.,* 1998: Malaria in Maremma, Italy. *The Lancet. 351,* 1246–1247.

Bismil'din, F.B., Shapieva, Z., and *Anpilova, E.N.,* 2000: Current malaria situation in the Republic of Kazakhstan. *Med Parazitol (Mosk). 2001*, 24–33.

Bruce-Chwatt, L.J. and *De Zulueta, J.,* 1980: The rise and fall of malaria in Europe: a historico-epidemiological study. Oxford: Oxford University Press, Walton Street.

De Zulueta, J., 1994: Malaria and ecosystems: from prehistory to posteradication. *Parassitologia. 36*, 7–15.

ECDC Epidemiological update: Local cases of malaria in Greece, September- October 2013 25 Nov. Website http://ecdc.europa.eu/en/press/news/_layouts/forms/News_DispForm.aspx?List=8db7286c-fe2d-476c-9133-18ff4cb1b568&ID=912.

Giacomini, T., Axler, O., Mouchet, J., Lebrin P., Carlioz R., Paugam, B., Brassier D., Donetti L., Giacomini, F., and *Vachon, F.* 1997: Pitfalls in the diagnosis of airport malaria. Seven cases observed in the Paris area in 1994. *Scand. J. Infect. Dis. 29*, 433–435.

Hackett, L.W. and *Missiroli, A.,* 1935: The varieties of Anopheles maculipennis and their relation to the distribution of malaria in Europe. *Riv. Malariol. 14*, 1.

Haylock, M.R., Hofstra, N., Klein, Tank, A.M.G., Klok, E.J., Jones, P.D. and *New, M.,* 2008: A European daily high-resolution gridded dataset of surface temperature and precipitation. *J. Geophys. Res (Atmospheres). 113(D20)*,119.

Howes, R.E., Patil, A.P., Piel, F.B., Nyangiri, O.A., Kabaria, C.W., Gething, P.W., Zimmermann, P.A., Barnadas, C., Beall, C.M., Gebremedhin, A., Ménard, D., Williams, T.N., Weatherall, D.J., and *Hay, S.I.,* 2011: The global distribution of the Duffy blood group. *Nat. Commun. 2*, 266.

Jetten, T.H. and *Takken, W., 1994:* Anophelism without malaria in Europe. A review of the ecology and distribution of the genus Anopheles in Europe. Landbouwuniversiteit Wageningen (Wageningen Agricultural University), Wageningen.

Koenraadt, C.J.M., Githeko, A.K., and Takken, W., 2004: The effects of rainfall and evapotranspiration on the temporal dynamics of Anopheles gambiae ss and Anopheles arabiensis in a Kenyan village. *Acta Trop. 90,* 141–153.

Krüger, A., Rech, A., Su, X.Z., and *Tannich, E.,* 2001: Two cases of autochthonous Plasmodium falciparum malaria in Germany with evidence for local transmission by indigenous Anopheles plumbeus. *Trop. Med. Int. Health. 6,* 983–985.

Kuhn, K.G., Campbell-Lendrum, D.H., Armstrong, B., and *Davies, C.R.,* 2003: Malaria in Britain: past, present, and future. *Proc. Natl. Acad. Sci. 100,* 9997–10001.

Kuhn, K.G., Campbell-Lendrum, D.H., and *Davies, C.R.,* 2002: A continental risk map for malaria mosquito (Diptera: Culicidae) vectors in Europe. *J. Med. Entomol. 39,* 621–630.

Lindsay, S.W., and *Birley, M.H.,* 1996: Climate change and malaria transmission. *Ann. Trop. Med. Parasit. 90,* 573–588.

Lowry, R., 2004*:* VassarStats*:* Website for statistical computation. Vassar College. Accessed: 30 04 2015. Website http://vassarstats.net/

Lőrincz, F., 1981–82: Malária Magyarországon régen és ma. Visszaemlékezés. *Parasit Hung. 14,* 13–16. (In Hungsarian)

MacDonald, G., 1957: The epidemiology and control of malaria. London: Oxford Univ. Pr., Oxford.

Mapire, 2015: The Historical maps of the Habsburg Empire. Website http://mapire.eu/hu/

Martens, P., Kovats, R.S., Nijhof, S., De Vries, P., Livermore, M.T.J., Bradley, D.J., Cox, J., and *McMichael, A.J.,* 1999: Climate Change and Future Populations At Risk Of Malaria. *Global Environ. Chang. 9(Suppl 1),*89–107.

Martens, W.J., Niessen, L.W., Rotmans, J., Jetten, T.H., and *McMichael, A.J.,* 1995: Potential impact of global climate change on malaria risk. *Environ. Health Persp. 103:* 458.

Mendis, K., Sina, B.J., Marchesini, P., and *Carter, R.,* 2001: The neglected burden of Plasmodium vivax malaria. *Am. J. Trop. Med. Hyg. 64(Suppl 1),* 97–106.

Menne, B. and *Ebi, K.L. (Eds.),* 2006: Climate change and adaptation strategies for human health. Steinkopff Verlag/Springer, Darmstad.

Molnár, G. and *Timár, G.,* 2009: Mosaicking of the 1: 75 000 sheets of the Third Military Survey of the Habsburg Empire. *Acta. Geod. Geophys. Hu. 44:*115–120.

Nasci, R.S., Savage, H.M., White, D.J., Miller, J.R., Cropp, B.C., Godsey, M.S., Kerst, A.J., Bennett, P., Gottfried, K., and *Lanciotti, R.S.,* 2001: West Nile virus in overwintering Culex mosquitoes, New York City. *Emerg. Infect. Dis. 7:* 742.

Patz, J.A. and *Olson, S.H.,* 2006: Malaria risk and temperature: Influences from global climate change and local land use practices. *Proc. Natl. Acad. Sci. 103,* 5635–5636.

Piel, F.B., Patil, A.P., Howes, R.E., Nyangiri, O.A., Gething, P.W., Williams, T.N., and *Hay, S.I.,* 2010: Global distribution of the sickle cell gene and geographical confirmation of the malaria hypothesis. *Nat. Commun. 1,* 104.

Szénási, Z., Vass, A., Melles, M., Kucsera, I., Danka, J., Csohán, A., and *Krisztalovics, K.,* 2003: MaláriaMagyarországon: aktuális állapot és védekezési elvek. [Malaria in Hungary: origin, current state and principles of prevention]. *Orvosi hetilap 144,* 1011–1018.(In Hungarian)

Tóth S. and *Kenyeres Z.,* 2012: Revised checklist and distribution maps of mosquitoes (Diptera, Culicidae) of Hungary. *Eur Mosq Bull. 30,* 30–65.

Tóth, S., 2004: Magyarország csípőszúnyog-faunája (Diptera: Culicidae). [Mosquito Fauna of Hungary]. Natura Somogyiensis, Kaposvár. (In Hungarian)

Trájer, A.J., Bede-Fazekas, Á., Bobvos, J., and *Páldy, A.,* 2014: Seasonality and geographical occurrence of West Nile fever and distribution of Asian tiger mosquito. *Időjárás 118:* 19–40.

Vézilier, J., Nicot, A., Gandon, S., and *Rivero, A.,* 2012: Plasmodium infection decreases fecundity and increases survival of mosquitoes. *Proc. R. Soc. B. 279:* 4033–4041.

Wallace, J.R. and *Grimstad, P.R.,* 2002: A preliminary characterization of the physiological ecology of overwintering Anopheles mosquitoes in the midwestern USA. *J. Am. Mosq. Control. Assoc. 18,* 126–127.

World malaria report, 2005: In:World Health Organization and UNICEF. Website: http://www.unicef.fr/sites/default/files/documents/admin/unicef/929-2.pdf. Accessed April 30, 2015.

INSTRUCTIONS TO AUTHORS OF *IDŐJÁRÁS*

The purpose of the journal is to publish papers in any field of meteorology and atmosphere related scientific areas. These may be

- research papers on new results of scientific investigations,
- critical review articles summarizing the current state of art of a certain topic,
- short contributions dealing with a particular question.

Some issues contain "News" and "Book review", therefore, such contributions are also welcome. The papers must be in American English and should be checked by a native speaker if necessary.

Authors are requested to send their manuscripts to

Editor-in Chief of IDŐJÁRÁS
P.O. Box 38, H-1525 Budapest, Hungary
E-mail: journal.idojaras@met.hu

including all illustrations. MS Word format is preferred in electronic submission. Papers will then be reviewed normally by two independent referees, who remain unidentified for the author(s). The Editor-in-Chief will inform the author(s) whether or not the paper is acceptable for publication, and what modifications, if any, are necessary.

Please, follow the order given below when typing manuscripts.

Title page: should consist of the title, the name(s) of the author(s), their affiliation(s) including full postal and e-mail address(es). In case of more than one author, the corresponding author must be identified.

Abstract: should contain the purpose, the applied data and methods as well as the basic conclusion(s) of the paper.

Key-words: must be included (from 5 to 10) to help to classify the topic.

Text: has to be typed in single spacing on an A4 size paper using 14 pt Times New Roman font if possible. Use of S.I. units are expected, and the use of negative exponent is preferred to fractional sign. Mathematical formulae are expected to be as simple as possible and numbered in parentheses at the right margin.

All publications cited in the text should be presented in the *list of references*, arranged in alphabetical order. For an article: name(s) of author(s) in Italics, year, title of article, name of journal, volume, number (the latter two in Italics) and pages. E.g., *Nathan, K.K.,* 1986: A note on the relationship between photosynthetically active radiation and cloud amount. *Időjárás 90,* 10-13. For a book: name(s) of author(s), year, title of the book (all in Italics except the year), publisher and place of publication. E.g., *Junge, C.E.,* 1963: *Air Chemistry and Radioactivity.* Academic Press, New York and London. Reference in the text should contain the name(s) of the author(s) in Italics and year of publication. E.g., in the case of one author: *Miller* (1989); in the case of two authors: *Gamov* and *Cleveland* (1973); and if there are more than two authors: *Smith et al.* (1990). If the name of the author cannot be fitted into the text: *(Miller,* 1989); etc. When referring papers published in the same year by the same author, letters a, b, c, etc. should follow the year of publication.

Tables should be marked by Arabic numbers and printed in separate sheets with their numbers and legends given below them. Avoid too lengthy or complicated tables, or tables duplicating results given in other form in the manuscript (e.g., graphs).

Figures should also be marked with Arabic numbers and printed in black and white or color (under special arrangement) in separate sheets with their numbers and captions given below them. JPG, TIF, GIF, BMP or PNG formats should be used for electronic artwork submission.

More information for authors is available:
journal.idojaras@met.hu

Published by the Hungarian Meteorological Service

Budapest, Hungary

INDEX 26 361

HU ISSN 0324-6329